Aalto University
School of Chemical
Technology

School of Chemical Technology
Degree Programme of Chemical Technology

Tomi Heikkilä

Effect of viscosity on gas-liquid flow calculation in a dynamic process simulator

Master's thesis for the degree of Master of Science in Technology submitted for inspection, Espoo, 25th of February, 2014.

Supervisor Professor Ville Alopaeus

Instructors M.Sc. (Tech.) Olli Sorvari
D.Sc. (Tech.) Mikko Vermasvuori

Aalto University
School of Chemical
Technology

Aalto University, P.O. BOX 11000, 00076 AALTO
www.aalto.fi

Abstract of master's thesis

Author Tomi Heikkilä

Title of thesis Effect of viscosity on gas-liquid flow calculation in a dynamic process simulator

Department Chemical engineering

Professorship Processes and products **Code of professorship** Kem-42

Thesis supervisor Professor Ville Alopaeus

Thesis advisors / Thesis examiners M.Sc. (Tech.) Olli Sorvari, D.Sc. (Tech.) Mikko Vermasvuori

Date 25.02.2014 **Number of pages** 96+22 **Language** English

Abstract

Gas-liquid two-phase flow occurs in safety valve calculations in the process industry. In order to size the safety valves reliably, the pressure drop calculations of the two-phase flow needs to be accurate. Two-phase flow is affected by many variables such as the viscosity. The aim of this thesis is to implement reliable and accurate calculation methods for viscosity and pressure drop for two-phase flows in a dynamic process simulator, ProsDS. Furthermore, the effect of viscosity on two-phase flow is studied.

The literature part of this thesis consists of two main chapters. In the first chapter, the viscosity methods for gas and liquid phases are reviewed. In addition, the viscosity methods for petroleum fractions and crude oils are introduced. The second chapter focuses on the two-phase flow. Different variables related to two-phase calculations, flow patterns and pressure drop calculations methods are introduced. The effect of the viscosity on the two-phase flow is studied in the end of the second chapter.

The applied part is also divided into two sections. In the first part, the most accurate and practical viscosity methods of FLOWBAT simulator were integrated into ProsDS. The methods were verified using experimental values presented in the literature. In the second part, several two-phase pressure drop methods were compared to the experimental values from the literature containing gas-liquid flows with various viscosities. Pressure drop methods of Lockhart-Martinelli, Müller-Steinhagen-Heck and Bandel gave the most accurate results and they were implemented into ProsDS. The methods were tested in a safety valve inlet piping case. The results of the simulated case differed significantly from each other. The inconsistency of the results indicates that it is difficult to predict two-phase pressure drops reliably.

Keywords gas-liquid, two-phase, flow, pipe, viscosity, pressure drop

Aalto-yliopisto
Kemian tekniikan korkeakoulu

Aalto University, P.O. BOX 11000, 00076 AALTO
www.aalto.fi

Diplomityön tiivistelmä

Tekijä Tomi Heikkilä

Työn nimi Viskositeetin vaikutus kaasua ja nestettä sisältävän virtauksen laskentaan dynaamisessa prosessisimulaattorissa

Laitos Kemian tekniikka

Professuuri Prosessit ja tuotteet **Professuurikoodi** Kem-42

Työn valvoja Professori Ville Alopaeus

Työn ohjaaja(t)/Työn tarkastaja(t) DI Olli Sorvari, Tkt Mikko Vermasvuori

Päivämäärä 25.02.2014 **Sivumäärä** 96+22 **Kieli** Englanti

Tiivistelmä

Kaasua ja nestettä sisältävää kaksifaasivirtausta esiintyy prosessiteollisuuden varoventtiilitapauksissa. Varoventtiilien mitoituksen luotettavuuden parantamiseksi kaksifaasivirtauslaskentaa tulisi tarkentaa. Kaksifaasivirtaus riippuu monista muuttujista kuten esimerkiksi viskositeetistä. Tämän diplomityön tarkoituksena on implementoida tarkat ja luotettavat menetelmät viskositeetin ja kaksifaasivirtauksen painehäviön laskemiseen dynaamisessa prosessisimulaattorissa, ProsDS:ssa. Lisäksi työssä tutkitaan viskositeetin vaikutusta kaksifaasivirtaukseen.

Tämän työn kirjallisuusosa koostuu kahdesta pääluvusta. Ensimmäisessä luvussa vertaillaan erilaisia viskositeetin laskentamenetelmiä kaasuille ja nesteille. Lisäksi työssä tarkastellaan viskositeettimalleja öljyille. Toisessa luvussa keskitytään kaasua ja nestettä sisältävään kaksifaasivirtaukseen. Kappaleessa tuodaan esille kaksifaasilaskennan keskeiset muuttujat, eri virtaustyypit ja painehäviölaskentamenetelmät. Luvun lopuksi käsitellään viskositeetin vaikutusta kaksifaasivirtaukseen.

Soveltava osa on jaettu myös kahteen osaan. Ensimmäisessä osassa ProsDS:än toteutettiin FLOWBAT-simulaattorin tarkimmat ja käytännöllisimmät viskositeetin laskentamenetelmät. Menetelmien tarkkuutta arvioitiin kirjallisuudesta saatujen arvojen avulla. Toisessa osassa vertailtiin useita kaksifaasipainehäviölaskentamenetelmiä kirjallisuudesta saatuihin painehäviöihin. Painehäviömenetelmistä Lockhart-Martinelli, Müller-Steinhagen-Heck ja Bandel osoittautuivat tarkimmiksi ja ne implementointiin ProsDS:än. Menetelmiä testattiin simuloidussa varoventtiilin tuloputkitapauksessa. Simuloidun tapauksen tulokset erosivat toisistaan huomattavasti. Täten voidaan todeta, että kaksifaasivirtauksen painehäviötä on vaikea ennustaa luotettavasti.

Avainsanat kaasu-neste, virtaus, kaksifaasi, viskositeetti, painehäviö

Preface

This master's thesis was authored at the Technology and Process Competence Center of Neste Jacobs in Porvoo during the time period between the 15th of July 2013 and the 15th of January 2014. I had previously been working in Neste Jacobs as a summer employee in 2011 and 2012, which familiarized me with the software environment used in this thesis.

I would like to thank Professor Ville Alopaeus for supervising my thesis and giving me feedback. Professor Alopaeus also encouraged me to think outside of the box. I would also like to thank my instructors M.Sc. (Tech.) Olli Sorvari and D.Sc. (Tech.) Mikko Vermasvuori for giving me great guidance and ideas. Special thanks to M.Sc. (Tech) Jyri Lindholm for making this thesis possible.

I would want to thank my family, friends and colleagues for their support and company. Especially, I would like to express gratitude to my parents and my girlfriend for being present and having unending faith in me.

Porvoo, 25th of February, 2014

Tomi Heikkilä

Table of contents

Nomenclature

Symbols

$A_{A,i}$	Andrade constant for component i
$A_{B,i}$	Andrade constant for component i
A_G	Cross sectional area of the vapor phase
A_L	Cross sectional area of the liquid phase
API_G	API gravity
C	Lockhart-Martinelli parameter for different flows
$calc_i$	Calculated value
d	Diameter
d_{mol}	Molecular diameter
exp_i	Experimental value
F_P°	Correction factor of Lucas
F_Q°	Correction factor of Lucas
Fr_H	Froude number
G	Two-phase mass flux
G_G	Gas mass flux
G_{ij}	Liquid viscosity interaction parameter
g	Gravitational acceleration constant
H	Vertical height
j_G	Superficial velocity for gas phase
j_L	Superficial velocity for liquid phase
K	Correction factor for hydrogen-bonding effect
k	Boltzmann constant
k_{hyd}	Chung correction factor for hydrogen-bonding effect
M	Molar mass
m	Mass of the one molecule
N_A	Avogadro's number

P_C	Critical pressure
P_{cm}	Pseudocritical pressure
R	Ideal gas constant
r	Radius
Re	Reynolds number
R_S	Solution gas-oil ratio
SG	Specific gravity
S	Slip-ratio
T	Temperature
$T*$	Dimensionless temperature
T_C	Critical temperature
T_{cm}	Pseudocritical temperature
u_G	True average velocity for gas phase
u_L	True average velocity for liquid phase
v	Flow velocity
V_c	Critical volume
$\mathrm{We_L}$	Weber number
x	Vapor quality
X	Martinelli parameter
y_i	Mole fraction
Z_c	Critical compressibility

Greek symbols

Δp_G	Gas phase pressure drop
Δp_L	Liquid phase pressure drop
ϵ	Void fraction
ϵ_{min}	Minimum pair-potential energy
ϵ_r	Pipe roughness
η	Kinematic viscosity

η_i	Pure component viscosity
η_m	Mixture viscosity
η_{air}	Air viscosity
η_o	Saturaded oil viscosity
η_{od}	Dead oil viscosity
η_{water}	Water viscosity
θ	Angle from the horizontal plane
λ_{Baker}	Part of the x-coordinate in the Baker flow pattern map
μ_r	Reduced dipole moment
ξ	Reduced, inverse viscosity
ρ	Density
$\bar{\rho}$	Average Homogeneous density
ρ_{air}	Density of the air
ρ_{tp}	Two-phase density
ρ_{water}	Density of the water
σ	Surface tension
σ_c	Collision diameter
σ_h	Hard sphere diameter
Ω_V	Collision integral
Φ_G ,	Dimensionless multiplier term for gas pressure drop
Φ_L	Dimensionless multiplier term for liquid pressure drop
ϕ_{ij}	Interaction parameter
$\psi(x)$	Intermolecular potential function
ψ_{Baker}	Part of the y-coordinate in the Baker flow pattern map
ω	Acentric factor

Abbrevations

AAD	Average absolute deviation
API	American Petroleum Institute
EOS	Equation of state
RMSD	Root-mean-square deviation
UNIFAC	UNIQUAC functional-group activity coefficients
VLE	Vapor-liquid equilibrium

LITERATURE PART

1 Introduction

Viscosity is an essential characteristic property that is required for process engineering calculations such as the prediction of pressure drops in pipes. Viscosity describes the resistance of a fluid to shear stress. Viscosity is a function of temperature and pressure, but the change in the temperature or the pressure has different effects on gases and liquids. Viscosities can be expressed in two different forms: dynamic viscosity or kinematic viscosity. Dynamic viscosity is the tangential force per unit area required to move one horizontal plane with respect to the other at unit velocity when maintained a unit distance apart by the fluid. Kinematic viscosity is the ratio of the dynamic viscosity to the density. [1]

Gas viscosities can be predicted using theoretical methods, but liquid viscosities do not have a proper theoretical method for calculations, since the molecules of the liquid phase have intermolecular forces between each other such as repulsion and hydrogen bonding. There are plenty of viscosity calculation methods for gases and liquids in the literature. However, they often have three main drawbacks. Firstly, the application range and accuracy are restricted. Secondly, two or more correlations are frequently required for calculating viscosities of the gas and liquid phases. Thirdly, a separate density correlation is often needed for calculating fluid viscosity. [2]

A two-phase flow is specified as a gas-liquid flow in this thesis. Two-phase flow is present in many process engineering applications such as safety valve calculations. Reliable prediction of the two-phase pressure drop is important in the design of the relief device inlet piping. The pressure drop in the inlet pipe should not be greater

than three percent of the set pressure of the safety valve for two reasons. Firstly, it will ensure that the pressure in the vessel before the valve will not increase too much. Secondly, it will ensure that the valve will operate stably and will not chatter or flutter. [3]

Two-phase flow is generally more complicated physically than a single-phase flow due to the simultaneous motions of the vapor and the liquid phases. The single-phase flow is only affected by inertia, viscous and pressure forces. Two-phase flow is also affected by interfacial tension forces, liquid wetting characteristics of the tube wall and the different momentums of the liquid and the gas phases. [4]

Two-phase flow can be divided in different flow patterns depending on the pipe layout and a geometrical distribution of the liquid and vapor phases. Adverse flow pattern can cause spikes in the pressure drop values, which can be harmful for the system. Flow patterns can be predicted using flow regime maps. Flow regime maps are often based on the experimental data and they usually are accurate only for certain systems. The unwanted flow patterns and their transition zones can be avoided by using flow regime maps. [5]

The pressure drop of the two-phase flow can be calculated using various frictional pressure drop methods. All of the methods have their advantages and disadvantages. The accuracy for the two-phase pressure drop methods depend on many variables. Over thirty percent errors are common among the prediction of the two-phase pressure drops.

2 Viscosity

2.1 General

Gases can be divided into dilute gases and dense gases. Dilute gas is defined as gas condition in the range of temperature and pressure where the gas viscosity is independent of density. It generally means low pressures and high temperatures. Dense gases are defined to be dependable on the density at high pressures. [1]

This chapter considers the viscosity in three parts. The viscosity of dilute gases and their mixtures are treated at first. Secondly, the dense gases and liquid viscosities are handled together. The viscosity of petroleum fractions and crude oils are considered thirdly.

2.2 Evaluation methods

The viscosity calculation methods are mostly evaluated using average absolute deviation (AAD), which is shown in Equation (1). Another evaluation method is root-mean-square deviation (RMSD), which is shown in Equation (2).

$$\mathrm{AAD} = \frac{1}{n}\sum_{i=1}^{n}\frac{|calc_i - exp_i|}{exp_i}\cdot 100\ \% \tag{1}$$

Where $calc_i$ Calculated value

exp_i Experimental value

n Total number of values

$$RMSD = \sqrt{\frac{\sum_{t=1}^{n}(calc_i - \exp_i)^2}{n}} \tag{2}$$

2.3 Gas viscosity

2.3.1 **Theoretical methods**

Theoretical models for calculating gas viscosities are based on the kinetic gas theory. The kinetic gas model postulates that all molecules are non-attracting rigid spheres moving randomly. The molar density is the amount of molecules in a unit volume and the mass density is the mass in a unit volume. The average distance between molecules is presumed to be many times their diameter. In the equilibrium, molecules are in constant random motion and they have a mean velocity. [6, 7]

Maxwell showed that gas viscosity is independent of density and it depends on the square root of the absolute temperature. He obtained expression for the viscosity of the low density gases: [6]

$$\eta = \frac{2}{3\pi^{\frac{3}{2}}} \frac{\sqrt{mkT}}{d_{mol}^2} \tag{3}$$

Where m Mass of one molecule, kg

k Boltzmann constant, 1.381 * 10^{-23} $\frac{m^2 kg}{s^2 K}$

T Temperature, K

d_{mol} Molecular diameter, m

Hirchfelder et al. [8] assigned a value of 26.69 for the equation of Maxwell. Rayleigh [1] indicated that there are intermolecular forces between the atoms. Chapman and Enskog [9] extended the viscosity model and augmented the intermolecular potential energy parameter. The Chapman-Enskog model is shown in Equation (4).

$$\eta = \frac{26{,}69\sqrt{MT}}{\sigma_h^2 \Omega_V} \tag{4}$$

Where Ω_V Collision integral

M Molar mass, mol/kg

σ_h Hard sphere diameter, m

Equation (4) can be applied to monoatomic gases only. The Collision integral is temperature dependent. There is no attraction between the molecules if the collision integral is unity. Chapman-Enskog theory requires the collision parameter and the collision integral to be solved. The collision integral can be obtained from the complex function of a dimensionless temperature (T*), which depends upon the intermolecular potential chosen. In Figure 1 is shown the function for potential energy [ψ(r)] of interaction between two molecules separated by distance (r). [9]

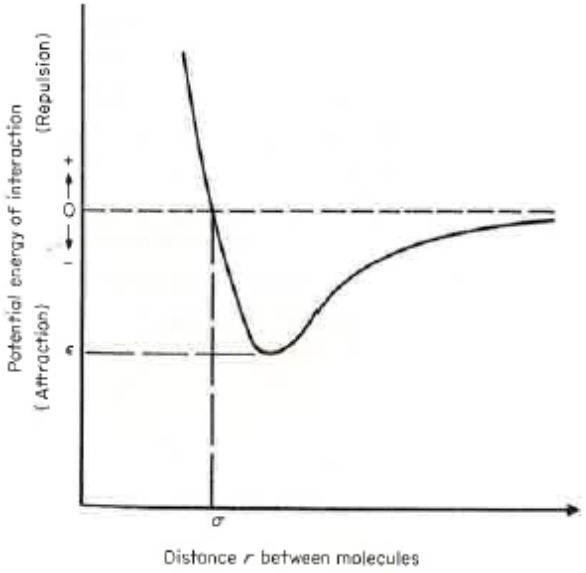

Figure 1. Intermolecular forces between two molecules.

At large separation distances the molecules attract each other and at small distances repulsion occurs, which can be seen from Figure 1. The minimum of the potential energy function curve is defined as the minimum of the pair-potential energy (ϵ). The dimensionless temperature (T*) is related to pair-potential energy, and it is defined for any potential curve in Equation (5). [9]

$$T^* = \frac{kT}{\epsilon_{min}} \tag{5}$$

Where T* Dimensionless temperature

ϵ_{min} Minimum pair-potential energy, J

The intermolecular potential function describes interaction between two molecules separated from each other. When only minimum pair-potential energy and a hard sphere diameter is used, it is called two-parameter potential. In order to know collision integral, one must solve intermolecular potential function. Many models have been proposed for the potential function, but Lennard-Jones 12-6 is the first and widely used model for ideal gas viscosity: [9]

$$\psi(r) = 4\epsilon\left[\left(\frac{\sigma_c}{r}\right)^{12} - \left(\frac{\sigma_c}{r}\right)^{6}\right] \tag{6}$$

Where $\psi(r)$ Intermolecular potential function, J

σ_c Collision diameter, m

r Radius, m

The collision diameter is defined to be a value, which causes the intermolecular potential function to be zero. When the equations (5) and (6) are used, the parameters for the collision diameter and the minimum pair-potential energy should be taken together from the same data source. [1] Several researchers have been investigated the collision integral. Neufeld et al. [10] proposed empirical equations for the collision integral, which contains up to 12 adjustable parameters. In the equation (7) is shown a reasonably accurate and convenient method for calculating the collision integral. The equation is valid under the dimensionless

temperature from 0.3 to 100. The max deviation of Equation (7) is 0.16 % and the average deviation is 0.064 %.

$$\Omega_V = \frac{A}{T^{*B}} + \frac{C}{e^{DT^*}} + \frac{E}{e^{FT^*}} \tag{7}$$

Where A = 1.16145, B = 0.14874, C = 0.52487, D = 0.77320, E = 2.16178 and F = 2.243787. [10]

The collision integral is a function of the dimensionless temperature and it can be applied to the Chapman-Enskog equation. Numerous investigators have tried to find the most accurate values for the collision diameter and the minimum pair-potential energy. There are many solutions for these parameters which give satisfying results for any given compound. For example, Svehla suggested parameters for n-butane, that e/k = 513.4 K and σ is 4.730 Å, whereas Flynn and Thodos proposed ϵ/k = 208 and σ = 5.869 Å. [7] Kim and Ross proposed following equation for the collision integral: [11]

$$\Omega_V = 1.604(T^*)^{-0.5} \tag{8}$$

Equation (8) is applicable at reduced temperature from 0.4 to 1.4. Kim and Ross reported the maximum error of 0.7 %. [11] By substituting Equation (8) into (4) viscosity can be presented as:

$$\eta = \frac{16.64 * T^* \sqrt{M}}{\sqrt{\frac{\epsilon}{k}}\sigma^2} \tag{9}$$

Parameters ϵ_{min}, k and σ are treated as one, because they cannot be described individually from the experimental viscosity data. It is difficult to describe the dynamics of the collisions between anisotropic molecules. Therefore, modified

theories and empirical correlations have generally been used for calculating the viscosity of the gases. [12]

2.3.2 **Semi-theoretical methods**

Semi-theoretical methods combine the theoretical models and experimental values [1]. Chung et al. [13, 14] modified the Chapman-Enskog theory to characterize the effects of molecular structure and polar effects. They introduced a new correction factor to account these effects, which made viscosity prediction with the Chapman-Enskog theory suitable for polyatomic, polar and hydrogen bonding dilute gases. The correction factor is shown in Equation (10).

$$F_c = 1 - 0.2756\,\omega + 0.059035\,\mu_r^4 + k_{hyd} \tag{10}$$

Where ω Acentric factor

μ_r Reduced dipole moment

k_{hyd} Correction factor for hydrogen-bonding effect

The parameter k can be found from the association parameters tables of Chung and others. Reduced dipole moment and parameters for ϵ/k and σ can be obtained from the critical values, which are shown in Equations (11),(12), and (13). [13, 14]

$$\mu_r = 131.3\,\frac{\mu}{\sqrt{V_C T_C}} \tag{11}$$

$$\sqrt{\frac{\epsilon}{k}} = \frac{T_C}{1.2593} \tag{12}$$

$$\sigma = 0.809\,V_C^{1/3} \tag{13}$$

Where T_C Critical temperature, K

V_C Critical volume, cm^3/mol

μ Dipole moment, Debyes

σ Surface tension, $\frac{N}{m}$

By substituting Equations (12) and (13) into (4) and multiplication by Fc results as:

$$\eta = 40.785 \frac{F_c \sqrt{MT}}{\mathrm{V_c}^{2/3} \Omega_V} \tag{14}$$

For Equation (14), Chung et al. reported an AAD of about 1.5 % for 40 substances including non-polar, polar and hydrogen-bonding. [13, 14] Poling et al. reported an AAD of 1.9 % using 29 substances [7].

2.3.3 **Empirical methods**

Many empirical models for calculating gas viscosities are based on corresponding states theory. The corresponding states theory was found by Van der Waals. According to corresponding states theory, all substances have the same relationship between pressure, volume and temperature if they are divided by their critical constants. The quantity of $N_A \sigma^3$ is assumed to be proportional to the critical volume, which is proportional to RTc/Pc. Thus, dimensionless viscosity with a reduced viscosity term can be defined as shown in Equations (15) and (16): [7]

$$\eta_r = \xi \eta = f(T_r) \tag{15}$$

$$\xi = \left[\frac{(RT_c) N_A^2}{M^3 P_c^4} \right]^{1/6} \tag{16}$$

Where R Ideal gas constant, 8.314 $\frac{J}{mol\ K}$

N_A Avogadro's number = 6,023 * 10^26

Pc Critical pressure, Pa

ξ Reduced, inverse viscosity, $\frac{m^2}{N*s}$

There are plenty of different versions for Equation (15) recommended by several authors. Stiel and Thodos [15] proposed empirical corresponding states equations

using dimensional analysis. They fitted equations for 52 non-polar gases. Yoon and Thodos [16] improved the method for polar gases with and without hydrogen bonding. The method is easy to apply. It only requires critical properties for temperature, pressure, molar mass and compressibility. Stiel and Thodos reported AAD of 1.8 % for non-polar gases using 50 components [15]. Yoon and Thodos tested their model with 11 hydrogen bonded type polar gases, and the AAD was found to be 1.5 %. For 41 non-hydrogen bonded polar gases, they reported an AAD of 2.6 %. [16]

Poling et al. [7] recommends the specific form for equation suggested by Lucas. The method includes correction factors for polarity and quantum effects. The reduced dipole moment is required to obtain correction factors. In Equations (17) and (18) are shown the method of Lucas and formula for the reduced dipole moment:

$$\eta\xi = \left(0.807T_r^{0.618} - 0.357e^{-0.449T_r} + 0.340e_r^{-4.058T_r} + 0.018\right) F_P^{\circ} F_Q^{\circ} \quad (17)$$

$$\mu_r = 52.46\frac{\mu^2 P_C}{T_c^2} \quad (18)$$

Where F_P°, F_Q° Correction factors of Lucas

The correction factors account for quantum effects, which depend on the reduced dipole moment. Correction factor are shown in Equations (19), (20) and (21).

$$F_P^{\circ} = 1;\ 0 \leq \mu_r < 0.022 \quad (19)$$

$$F_P^{\circ} = 1 + 30.5(0.292 - Z_c)^{1.72};\ 0.022 \leq \mu_r < 0.075 \quad (20)$$

$$F_P^{\circ} = 1 + 30.5(0.292 - Z_c)^{1.72}|0.96 + 0.1(T_r - 0.7)|;\ 0.0755 \leq \mu_r \quad (21)$$

Where Z_c Critical compressibility

The correction factor F_Q° is used only for quantum gases such as helium and hydrogen. The method of Lucas is easy to apply and it does not require many parameters, which can be seen from the equations (17) to (21). The model is reasonably accurate. Poling et al. reported the AAD of 3 % for the method of Lucas. The method is more accurate for polar than non-polar compounds. [7]

Reichenberg [7] developed a group contribution corresponding states method for organic compounds at low pressure. In addition to the group contributions, the method requires temperature, critical temperature and reduced dipole moment. Poling et al reported AAD of 1.9 % for 29 substances.

American Petroleum Institute (API) has developed correlation for the viscosity of pure compounds as a function of temperature. The correlation uses specific coefficients for every compound. There are over 300 coefficients for pure compounds listed in their databook. The correlation is applicable under the 0.6 reduced pressure. API reported the AAD for whole temperature range less than 5 %, but the general deviation is better than 2 %. [17]

2.3.4 **Methods for mixtures**

Viscosities of gas mixtures at low pressures can be estimated using two different approaches. Chapman and Enskog theory can be extended for the gas mixtures. There are plenty of different versions available, but many of them are very complicated. Four well-known extensions are Brokaw, Reichenberg, Wilkes, Herning and Zipperers. All of these methods require viscosity values for the pure components. The alternative way is to apply mixing rules in the models such as Chung et al, Stiel & Thodos and Lucas. [12] Most of the estimation methods are for low-pressure gas mixtures having deviation of 10 % from the experimental values [1].

Brokaw [18] extended the theory of Chapman and Enskog to polar and non-polar mixtures by applying several mixing rules to the pure component viscosities, molecular weights, reduced temperatures and dipole moments. Brokaw tested his model for five binary mixtures, including both polar and non-polar systems. According to his report, the method predicts viscosities within 1 % for 2.

The methods Wilke and Herning-Zipperer are simple and easy to apply. They both require only pure component viscosities and molecular weights. [19, 20] Wilke [19] compared values for 17 binary systems and reported AAD of less than 1 %. Several other investigators have also tested the method of Wilke and they obtained good results for non-polar components. The method of Herning and Zipperer predicts viscosities decently and it is simpler than the model of Wilke. Both of these methods predicted viscosities less accurately for the gas mixtures of the hydrogen systems. [7] Nonetheless, the method of Wilke is recommended by both API and Design Institute for Physical Properties (DIPPR) for calculating viscosities of gas mixtures at low pressure. [21] The method of Wilke is applicable under the reduced pressure of 0.6. It is shown in the equations (22) and (23). [19, 20]

$$\eta_m = \sum_{i=1}^{n} \frac{y_i \eta_i}{\sum_{j=1}^{n} y_j \phi_{ij}} \tag{22}$$

$$\phi_{ij} = \frac{\left[1 + \sqrt{\frac{\eta_j}{\eta_i}} \left(\frac{M_j}{M_i}\right)^{\frac{1}{4}}\right]^2}{\sqrt{8 * \left(1 + \frac{M_j}{M_i}\right)}} \tag{23}$$

Where η_i Pure component viscosity, Pa s

y_i Mole fraction

ϕ_{ij} Interaction parameter

Reichenberg [22] introduced another method for the gas mixtures. The method requires the temperature, composition, viscosity, critical temperature, critical pressure, molecular weight, and dipole moment for each compound. The model is quite complex, which results in greater accuracy.

The corresponding states method assumes that a mixture of compounds acts similarly to some pure components in the reduced state. The critical properties of the mixture are calculated using the critical properties of the pure components. The critical properties of the mixture and the functions of the compositions are called pseudocritical properties. The values of the pseudocritical properties are not expected to be equal to the true mixture critical properties. The corresponding states method estimates these pseudocritical and other mixture properties from the pure components properties, mole fractions of the mixture, combining and mixing rules. [7] In the equations (24) and (25) are shown how to calculate pseudocritical temperature and pseudocritical pressure. [7]

$$T_{cm} = \sum_{i=1}^{n} y_i T_{ci} \tag{24}$$

$$P_{cm} = RT_{cm} \frac{\sum_{i=1}^{n} y_i Z_{ci}}{\sum_{i=1}^{n} y_i V_{ci}} \tag{25}$$

Where T_{cm} Pseudocritical temperature, K

P_{cm} Pseudocritical pressure, Pa

Lucas [23] extended his method to mixture using mole fraction average mixing rules for polar and quantum corrections. The extended method is shown in the equations from (26) to (29). The subscript H denotes the component of the highest molecular weight and the L denotes the lowest molecular weight.

$$M_m = \sum_{i=1}^{n} y_i M_i \tag{26}$$

$$F_{Pm}^{\circ} = \sum_{i=1}^{n} y_i F_{Pi}^{\circ} \tag{27}$$

$$F_{Qm}^{\circ} = \sum_{i=1}^{n} y_i F_{Qi}^{\circ} \tag{28}$$

$$A = 1 - 0.01\left(\frac{M_H}{M_L}\right)^{0.87} \tag{29}$$

Lucas method is not interpolative, which means that it does not necessary give exact pure component viscosity when there is only one component present [7]. Lucas reported an AAD of 5 %, but there were no detailed results [23].

Chung et al. [13, 14] also proposed a method for calculating the viscosity of gas mixture with a correction factor for shape and polarity. Chung et al. method was tested for 40 dilute gas binary mixtures including nonpolar-nonpolar, nonpolar-polar, and polar-polar systems. The method estimated viscosities with an AAD of about 4 %, when binary interaction parameters were used.

Poling et al. [7] compared six different calculating methods for gas mixtures. They selected 10 binary gas mixtures including nonpolar-nonpolar, nonpolar-polar, and polar-polar systems. The results are shown in the Table 1. The method of Reichenberg is the most accurate model, but also the most complex one. Poling et. al recommend to use the method of Reichenberg, all of the required variables are available. The methods of Lucas and Chung are recommended if the critical values for all of the pure components are available.

Table 1. Comparison of the calculating methods for gas mixture viscosities. [7]

Method	**AAD**
Wilke	3.0 %
Herning-Zipperer	3.5 %
Brokaw	2.6 %
Reichenberg	1.7 %
Lucas	4.1 %
Chung et al.	3.5 %

2.3.5 **Effect of pressure**

For dilute gases, the density does not change significantly with pressure, thus the gas viscosity increases with the temperature only. At higher pressures, the density will increase rapidly which will result in an increase in viscosity. [1] The viscosity of nitrogen gas as a function of pressure is shown in Figure 2. The pressure has more effect near the critical temperature and pressure. [7]

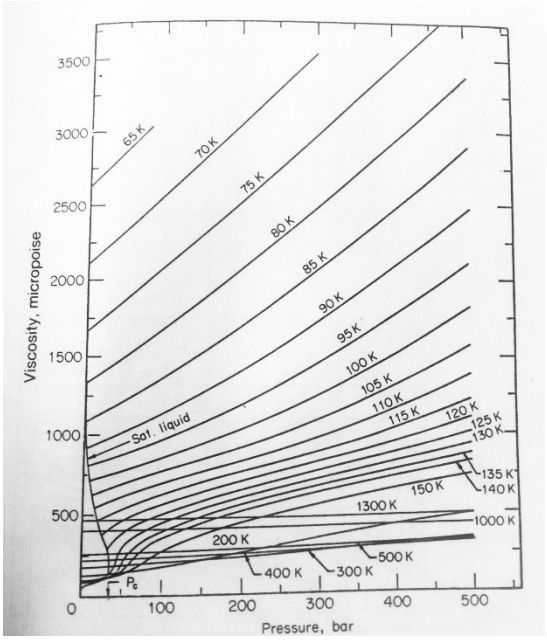

Figure 2. Viscosity of nitrogen as a function of pressure at different temperatures. [7]

The dense-gas theory of Enskog is well known method for predicting the effect of pressure for gas viscosities. The theory assumes that gas consists of dense hard

spheres. The system is described as a low density hard sphere system where all events occur faster due to the higher rates of collision. The method describes the effect of pressure with the ratio of dense gas to dilute gas, which is a function of pressure and temperature. The method is illustrated in Equation (30). However, there is no correlation for successive hard-sphere collisions. [7]

$$\frac{\eta}{\eta^o} = \mathrm{f}(\mathrm{P_r}, T_r) \tag{30}$$

Where η^o Dilute gas viscosity, Pa s

The method of Reichenberg describes the viscosity ratio using constant functions for reduced temperature. Average error for the method was reported to be only a few percent, except for ammonia. Lucas method is similar to the method of Reichenberg. It requires critical temperature, critical pressure, critical compressibility factor and dipole moment, in addition to temperature and pressure. Reid et al. [9] tested both methods for 5 non-polar and 1 polar hydrogen bonding fluids. They reported AADs of 4.2 % and 4.5 % for the methods of Reichenberg and Lucas.

Another way to predict the effect of pressure on the viscosity of gas is the residual viscosity. Residual viscosity is a subtraction between the viscosities of dense and dilute gases at the same temperature, whereas the Enskog theory uses the viscosity ratio between dense and dilute gases. Dilute-gas viscosity data can be searched from the experimental data or it can be calculated using viscosity methods for low pressure gases. Jossi, Stiel and Thodos proposed a simple method for calculating pressure effects for non-polar gases and Stiel and Thodos invented a model for polar gases. [24] The method for non-polar gases is shown in Equation (31):

$$[(\eta - \eta^{\circ})\xi + 1]^{0.25} = 1.0230 + 0.23364\rho_r + 0.58533\rho_r^2 - 0.40758\rho_r^3 + 0.093324\rho_r^4 \quad (31)$$

Where ρ_r Reduced gas viscosity

The method by Jossi, Stiel and Thodos can be applied in the range of reduced gas density from 0.1 to 3. The average error was reported to be 3.7 % when 9 different gas mixtures were tested. [25]

2.4 Liquid and dense gas viscosities

2.4.1 **Effect of temperature and pressure**

Liquid viscosities are affected by the change in pressure and temperature. Increasing the pressure also increases the viscosity, but in the other hand, the increased temperature under isobaric conditions decreases the liquid viscosity [7]. The effect of temperature on viscosities of n-decane and ethanol at atmospheric pressure is shown in Figure 3. The curve was regressed using experimental data points from the literature [26, 27]. In Figure 4 is shown the effect of pressure on some organic compounds at room temperature. In addition, liquid viscosities vary due to their polarity. Viscosities of polar liquids are generally higher than non-polar liquids. [7]

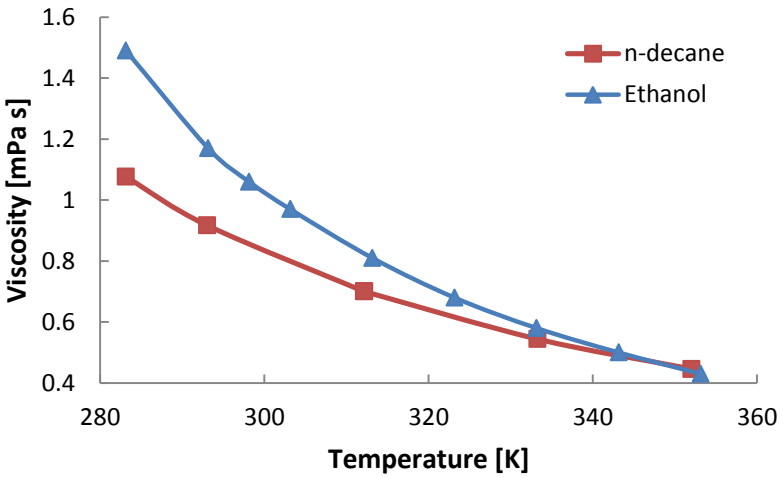

Figure 3. Effect of temperature on liquid viscosity at atmospheric pressure.

Viscosities for liquids are larger than gases at the same temperature, for example the viscosity of the liquid benzene is 36 times larger than the viscosity of the gas phase. Saturated vapor should have the same viscosity as saturated liquid at the critical point. [7]

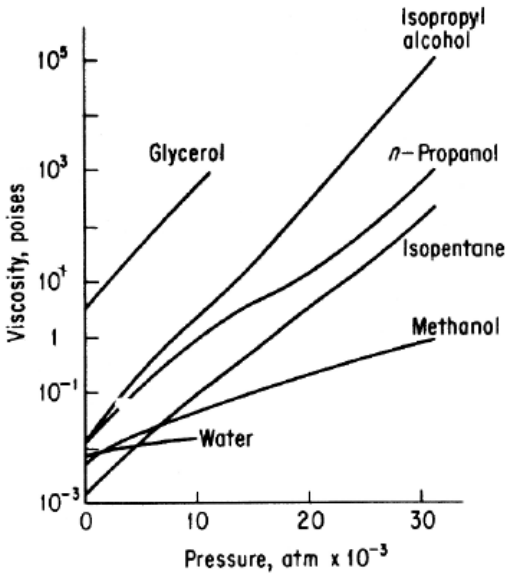

Figure 4. The effect of pressure on liquid viscosities of some organic compounds at room temperature. [24]

2.4.2 **Theoretical methods**

Theoretical models for estimating dense gas or liquid viscosities are based on statistical mechanics and they can be divided into distribution function theory or correlation function theory [12]. Kirkwood et al. [28] found an expression for viscosity relating momentum flux through velocity averages to the distribution function. They found that the friction coefficient is related to the intermolecular force field. There are plenty of different theoretical expressions for the friction coefficient, but they are not sufficiently accurate to calculate the viscosity [12]. In addition, theoretical models are not suitable for engineering applications due to their complexity and uncertainty.

2.4.3 **Semi-theoretical methods**

Semi-theoretical models for dense gases and liquids are based on principle of corresponding states or statistical mechanics models such as reaction rate, hard sphere and square well theory. Temperature and either density or specific volume is required for using these models. The viscosity is commonly required at a certain temperature and pressure. Therefore, a density prediction method is also needed in addition to the viscosity model. The density estimation method has to be accurate, because liquid viscosity is highly sensitive to the density. [12]

According to the principle of corresponding states, a dimensionless property of one substance is equal to that of reference substance, when both are evaluated at the same reduced conditions [12]. Ely and Hanley [29] proposed and extended corresponding states model, which uses methane as a reference fluid. The model requires correlations for a reference fluid viscosity and density. In addition, the method requires critical properties and acentric factor are required. Ely and Hanley selected methane for the reference fluid, because it had sufficiently reliable data available at the time. However, the drawback using methane as a reference fluid is the high freezing point (T_r = 0.48), which is much higher than the reduced temperatures for the other fluids in a liquid state. Ely and Hanley solved the

problem by extrapolating the density correlation for methane and added an empirical correction for non-correspondence. Monnery et al. [12] reported an AAD of 5 % to 10 % for n-paraffins, but for the isomeric paraffins and napthenes they reported AADs of 55 %. The overall AAD was 7 %.

Ely [29] modified the Ely-Hanley model to correct the correspondence between the reference fluid and pure high molar mass fluids. In addition, size and mass differences in mixtures were corrected. Ely changed the reference fluid from methane to propane, because it has the lowest triple point among the paraffins. The triple point is defined as the temperature and pressure at where the vapor, liquid and solid phases of a substance exist in equilibrium. Ely also developed more simple shape factor correlations. Estimated viscosities with the new model were similar with the results of earlier proposed models.

Many investigators have tried to improve the method Ely-Hanley by creating empirical modifications to the shape factor. Hwang and Whiting [30] made an improved method for branched alkanes, naphtenes, aromatics and various polar and associating compounds. They tested the method for 38 polar, hydrogen bonding and non-polar substances and reported an AAD of 5.3 % while using the same subtances they reported an AAD of 17.6 % for the method of Ely-Hanley. Monnery et al. [12] estimated viscosities for 46 hydrocarbons with an AAD of about 6 %.

Letsou and Stiel [31] developed a method for high temperature saturated liquids at the reduced temperature range from 0.7 to 0.92. They tested method for 10 hydrocarbons with an AAD of about 3 %. Reid et al. [9] reported deviations from 15 % to 20 % for other compounds than hydrocarbons.

Teja and Rice [32] modified three-parameter corresponding method of Lee-Kessler. The method is based on the use of two reference fluids, one spherical and the other

non-spherical. They tested the method for six non-polar mixtures and reported an AAD of 0.7 %. Okeson and Rowley [33] extended Lee-Kesler method to four-parameter corresponding method involving three reference fluids such as methane, n-octane and water. They reported an AAD of 7.9 % for 28 hydrocarbons.

The well-known theory for liquid viscosity is reaction rate theory by Eyring and his co-worker in 1936 [34]. Monnery et al. [12] describes a reaction theory that the volume in the gas is sparsely populated by molecules, whereas the volume of the liquid is densely populated by molecules. Viscous flow is considered as a reaction causing the molecules to acquire the activation energy.

There are many applications for the theory of Eyring. McAllister made an assumption that the free energy of activation of flow was additive and the probability of the interactions were proportional to mole fractions. Kalidas and Laddha extended the model of McAllister to a ternary system. They reported a maximum deviation of 1.8 % from experimental data after they had fitted the binary and ternary parameters to the experimental data. Most of the applications for the theory of Eyring are not suitable for practical use, because they require parameter fitting from the experimental data. [12]

2.4.4 **Empirical methods**

The most popular method for estimating liquid viscosity is Andrade equation, which was first proposed by de Guzman in 1913. The equation describes liquid viscosity with a function of temperature: [23]

$$\ln \eta_i = A_{A,i} + \frac{A_{B,i}}{T} \tag{32}$$

Where η_i Viscosity, cP

T Temperature, K

$A_{A,i}$, $A_{B,i}$ Empirical constant for component i

The equation is applicable under the normal boiling point temperature. Andrade equation does not include the effect of pressure, which has led to several modifications of the equation. A third parameter, C, was added to obtain Vogel equation, which is shown in Equation (33). [23] Empirically determined constants A, B and C for different substances have been published by many authors [1, 7]. Plenty of attempts have been made to predict the constants, but none of them have succeeded. [1]

$$\ln \eta_i = A_i + \frac{B_i}{T + C_i} \tag{33}$$

Allan and Teja [23] calculated the constants from the Vogel equation (33) as a function of the carbon number for pure n-alkanes from C_2 to C_{20}. The method uses the effective carbon number for the substance of interest, which is obtained from the one value of liquid viscosity. They reported an AAD of 2.3 %. The method was extended for mixtures and it was reported an AAD of 5.3 %. However, the method cannot be used for substances with an effective carbon number above 22.

Prezezdziecki and Sridhar [35] developed an empirical method, which was originally based on the free volume viscosity expression proposed by Batchinski. The method includes two variables, which are represents free volume and absorption of energy during molecular collision. Przezdziecki and Sridhar regressed those parameters using experimental data for 27 compounds. They reported and AAD of 8,7 % for low temperature liquid viscosities. Reid et al. [9] tested the method and reported large errors for alcohols. According to them, the method underestimates the viscosities of pure liquids and they did not recommended the method.

Orbey and Sandler [36] proposed a simple empirical method for hydrocarbons and their mixtures. The method is applicable over a wide range of temperatures and pressures. It requires the normal boiling point and two parameters from the

experimental data. The method was tested for 50 hydrocarbons with regressed parameters and it correlated the data with an AAD of 1.3 %. Orbey and Sandler reported an AAD less than 3 % using generalized parameters for alkenes from C_3 to C_{20}, expect C_5, C_6 and C_{14}, which had AADs below 10 %. The method predicted viscosities for alkane mixtures with an AAD of 2.4 %. [36]

There are also group contribution techniques for estimating liquid viscosity. The methods are easy to apply but they require tables for the group contributions. Orrick and Erbar cited by Poling et al. [7] proposed a method based on Andrade equation for low-temperature (T_r = 0.75) liquids. Two constants are determined using group contributions from their table. The method also requires input variables for the temperature, molecular weight and liquid density at 20°C. Orrick and Erbar tested method for 188 organic liquids and reported an AAD of 15 %. However, the deviation range was wide. Sastri and Rao [37] proposed a different group contribution method for liquids below their boiling points. The method assumes that the temperature dependency of density is related to the temperature dependency of vapor pressure. Poling et al. [7] recommend that neither of these two methods to be used for highly branched structures or for inorganic liquids. In addition, the method of Orrick-Erbar cannot be used for sulfur compounds.

Another similar approach to the Andrade equation is the Walther or American Society for Testing and Materials correlation (ASTM), which is shown in the equation (34). The equation requires two experimental parameters for each component. [23]

$$\ln(\eta + 0.8) = 10^{b_1} T^{b_2} \tag{34}$$

Methora [38] changed the Walther equation to one-parameter equation by fitting experimental data for 273 pure heavy hydrocarbons from API research Project 42. The unknown parameter is expressed in terms of hydrocarbon molar mass, normal

boiling point, critical temperature and acentric factor. The method is shown in Equation (35). Methora reported an AAD range of 5 % to 15 %.

$$\ln(\eta + 0.8) = 100(0.1\, T^{b}) \tag{35}$$

2.4.5 Equation of state based methods

Viscosity can also be estimated using the equations of state (EOS). The approach is based on the similarity between the P-T-V and P-n-T surfaces, which can be resulted in an explicit function of the temperature and the pressure [39]. According to Elsharkawy and others, there are three advantages of the EOS based models. At first, one single model can estimate both viscosities for gases and liquids near the critical region. Secondly, it can correlate high and low-pressure data without having density involved. Thirdly, it can improve the thermodynamic consistency in process simulation while using only a single EOS. [2]

Lawal [39] used a cubic equation of state, where viscosity replaces the volume. The method has four constants and two temperature dependent variables. Lawal reported an AAD of 5.9 % for pure components, and an AAD of 3.5 % for the mixtures. Heckenberger and Stephan [40] used an EOS method and reported an AAD of 5 % for alkanes up to octane, ethylene and propylene. However, the maximum errors for some organic compounds were 32.9 %.

Quinones-Cisneros et al. [41] developed a new friction theory to calculate the viscosity of the hydrocarbon fluids using EOS. The method separates total viscosity into a dilute gas term and a friction term in order to use Van der Waals fluid theory. The method is applicable for n-alkanes from methane to n-decane. In addition, method can be used for hydrocarbon mixtures. Quinones-Cisneros et al. tested the method for hydrocarbons and their mixtures. They reported an average AAD for pure hydrocarbons such as methane to be about 2 %. The maximum AAD was found to be 3.8 % for n-Pentane while using Soave-Redlich-Kwong -thermodynamic model.

For binary hydrocarbon mixtures, AAD was found to be around 3 %. A year later, Quinones-Cisneros et al. [42] proposed a simplified version of the friction theory, which requires only one parameter to calculate the viscosity. They reported an overall AAD of 2.6 %. For hydrocarbon mixtures they reported an AAD to be less than 5 % in the most cases. The drawback of the friction theory is that it requires database parameters for pure hydrocarbons.

2.4.6 **Methods for liquid mixtures**

Liquid viscosities are very sensitive to the structure of the constituent molecules below the reduced temperature of 0.7. Therefore, only slight association effects between components may significantly affect the viscosity of liquid mixtures. [7] The liquid viscosity can be calculated either from the pure components using a mixing rule or from the correlated mixture and viscosity equations. The logarithm viscosity equation for liquid mixtures is shown in Equation (36). [23]

$$\ln \eta_m = \sum y_i \ln n_i \tag{36}$$

Where η_m Mixture viscosity, Pa s

n_i Pure component viscosity, Pa s

Irving presented a review for various mixture equations and their accuracy using 318 data sets of non-polar and polar and aqueous mixtures. According to Irving, the most effective methods for estimating viscosity are parabolic type equations with an interaction parameter such as Grunberg-Nissan equation: [43]

$$\ln \eta_m = \sum x_i \ln \eta_i + \sum \sum x_i x_j G_{ij} \tag{37}$$

Where G_{ij} Liquid viscosity interaction parameter

For the Grunberg-Nissan equation, Irving reported RMSD of 2.3 % for non-polar mixtures, 3.0 for non-polar and polar mixtures, 8.9 % for polar mixtures and 24.0 % for aqueous mixtures. The accuracy of the method depends on the accuracy of the interaction parameter, which is a temperature dependent variable. Isdale optimized the values of the interaction parameter using over 2000 experimental mixture data points. He reported an overall RMSD of 1.6 % for mixtures. Isdale has also proposed a group contribution method for binary interaction parameters in the temperature of 298 Kelvin. [43]

Cao et al. [44] proposed a model called UNIMOD for both viscosity and activity coefficients of liquid mixtures. It is based on the theory of Eyring. UNIMOD is a complex model, which requires the viscosities of pure liquids and plenty of other parameters such as interaction potential energy parameters. Overall, UNIMOD predicts viscosity accurately if all the required data is available. Cao reported a MRS deviation of 0.83 % for binary systems and about 3.3 % for multicomponent systems. Cao et al. [45] also proposed a group contribution method for liquid mixtures. It uses UNIQUAC functional-group activity coefficients (UNIFAC) and vapor-liquid equilibrium (VLE) parameters. They reported an AAD of 4.4 % for 47 binary systems and 2.7 % for 7 ternary systems.

2.5 Viscosity of petroleum fractions and crude oils

2.5.1 **Fundamentals**

Petroleum is a complex mixture. Its physical and chemical properties, such as temperature dependence, vary significantly depending on the composition of the chemicals. [2] Therefore, viscosity correlations are specific only to certain pressure and temperature regimes due to differences in the oil nature and compositions. Typical viscosity curve of the crude oil at reservoir temperature as a function of pressure is shown in Figure 5. [46]

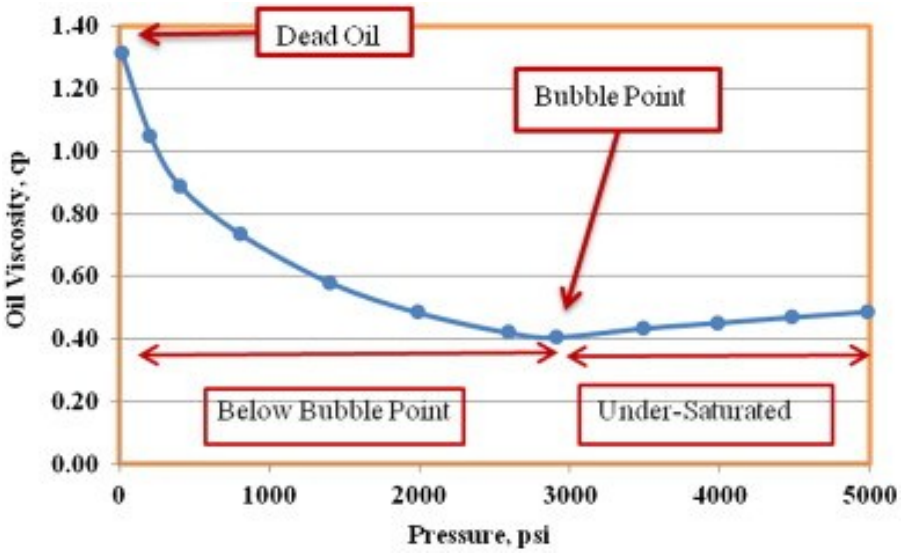

Figure 5. The viscosity curve of the crude oil as a function of pressure [47].

Crude oil viscosities can be classified into three categories: dead oil, saturated oil and unsaturated oil viscosities. All of them are specified for certain pressures, which can be seen from Figure 5. Dead oil viscosity does not have gas in the solution and it is defined at atmospheric pressure and system temperature. Saturated oil viscosity ,also called bubble-point viscosity, is defined at any pressure less than or equal to the bubble-point pressure. Under-saturated oil viscosity is defined as the viscosity of the crude oil at pressure above the bubble-point and reservoir temperature. [46]

Viscosities of the petroleum fractions and crude oil can be calculated using certain liquid viscosity methods. They may not be accurate, thus there are methods for calculating specific crude oil viscosities.

2.5.2 **Empirical methods**

Empirical methods are often used for prediction viscosity of the crude oils. The methods are based on properties such as specific gravities, saturation pressure and reservoir temperature. The correlations are often specified for certain oil areas, which make the methods accurate, but impractical. [2]

The gravity of a crude oil is defined as an index of the weight of a measured volume of the product. Two generally used scales are specific gravity and API gravity. Specific gravity is defined as the density ratio between the material and distilled water at the same temperature. Standard conditions for petroleum industry are specified to the temperature of 15.5°C and pressure of 1 atm. The API gravity of Crude oil is based on an arbitrary hydrometer scale, which is related to the specific gravity as shown in equation (38). [21]

$$API_G = \frac{141.5}{SG} - 131.5 \tag{38}$$

Where API_G API gravity

SG Specific gravity at 15.5°C

Dead oil viscosities can be calculated using API gravity and temperature. Beggs and Robinson [48] developed a correlation for dead and saturated oil viscosities using 600 oil systems including over 2500 data points. The dead oil viscosity correlation is shown in the equations (39) and (40). The other dead oil estimation methods are similar to Beggs and Robinson. Beal [49] developed a graphical correlation using total of 753 values for dead-oil viscosity at the temperature of 37°C and above. Glaso [50] proposed a model using the temperature range from 10°C to 150°C and experimental measurements from 26 crude oil samples. Labedi [51] developed correlation for light crude oils from Libyan reservoirs.

$$\eta_{od} = 10^A - 1 \tag{39}$$

$$A = 10^{3.0324 - 0.02023 * API_G} * T^{-1.163} \tag{40}$$

Where η_{od} Dead oil viscosity, Cp

T Temperature, R

There have been many comparisons between the viscosity correlations of the dead oil. Edreder and Rahuma [52] compared six dead oil viscosity correlations using six different oils such as Libyan crude oils and their own collected experimental data. The viscosity calculation results of Edreder and Rahuma are shown in Table 2. Beggs-Robinson method had the lowest AAD of 9.58 %. Elsharkawy and Alikhan reviewed 6 dead crude oil models for Middle East crudes and reported the second lowest AAD of 21.2 % for the Beggs-Robinson method.

Table 2 Comparison of the dead oil viscosity methods by Edrerer and Rahuma [52].

Model	**AAD**
Beal	21.00 %
Beggs-Robinson	9.58 %
Glaso	26.89 %
Egbogah	11.22 %
Labedi	17.35 %
Petrosky	17.86 %

Saturated oil exists, when the pressure is less than or equal to the bubble-point pressure. A slight decrease in pressure will release a bit of gas. Thus, the bubble-point pressure is the situation at which the first release of gas occurs. The quantity of dissolved gas in oil at reservoir conditions is defined as a solution gas-oil ratio. The estimation of the crude oil viscosity at bubble-point pressure or below than that includes two steps. At first, the viscosity of the crude oil should be calculated without dissolved gas at the reservoir temperature, which is the same as calculating the dead oil viscosity. The second step is to adjust the viscosity to account for the effect of the gas solubility at the pressure of interest. [46] Accuracy of the correlations for saturated crude oil viscosities is greatly dependent on the estimation of the gas-oil ratio [2]. There are many proposed correlations for the saturated oil viscosity. Most of the correlations have introduced the viscosity of the saturated oil as a function of both dead oil viscosity and solution gas-oil ratio while

other correlations use a function of dead oil viscosity and saturation pressure. [53] In the equations (41) and (42) are shown the saturated viscosity oil correlation by Beggs and Robinson.

$$\eta_o = 10.715 * (R_S + 100)^{-0.515} {\eta_{od}}^B \quad (41)$$

$$B = 5.44 * (R_S + 150)^{-0.338} \quad (42)$$

Where η_o Saturaded oil viscosity, Cp

R_S Solution gas-oil ratio, scf/STB

There are also plenty of correlations for under-saturated oil viscosity. The solution gas oil ratio is constant for under-saturated oils. Thus, the pressure is the main parameter, which influences on the oil viscosity. Under-saturated oil viscosity is often correlated as a function of bubble point oil viscosity, bubble point pressure and pressure. Some correlations involve also API gravities and dead oil viscosities. [2]

Dutt et al. [54] used a different approach for calculating viscosity for petroleum crude oil fractions. They proposed a method that calculates the kinematic viscosity, which requires temperature, normal boiling point temperature and density. They tested the kinematic viscosity of 15 crude oils and their fractions. They reported an AAD of 6 %. Viswanath et al. [1] tested the method of Dutt and others for 100 pure components. He reported an AAD of 14.6 %.

2.5.3 **Corresponding state methods**

Oil viscosities can also be calculated using corresponding states models. They require more parameters such as fluid composition, pour point temperature, molar mass, normal boiling point, acentric factor and critical temperature. Corresponding states models involve numerous computations and they do not predict viscosity of

the crude oil accurately. [55] The presented corresponding states methods are developed for the crude oils, but they can also be used for pure components. [56]

Baltatu [57] modified the method of Ely-Hanley to predict viscosity for petroleum fractions. Baltatu reported an overall AAD of 6.38 % for several oil producing areas including American crude oils, Arabia, the Persian Gulf and North Africa. The maximum deviations were from 18.7 % to 32.7 %.

Pedersen et al. [58] proposed also a method similar to method of Ely-Hanley for estimating hydrocarbon and crude oil viscosities. It uses methane as a reference fluid. The method requires critical temperatures, pressures and also molar masses for each component. In addition, the rotational coupling coefficient is also needed. Viscosities for the crude oils can be calculated using average molar mass. Pedersen et al. reported their method to predict viscosities within 5 % of their experimental data for crude oils. Pedersen and Fredenslund [59] extended the method of Pedersen et al. for mixtures below the freezing point of methane. However, the disadvantage of the method is that it does not predict viscosities accurately for systems, which has components with different sizes and shapes.

Aasberg-Petersen et al. [60] introduced their own method using two reference components, methane and decane, to overcome this problem. The model is applicable over large pressure ranges (1 - 500 bar) and above the reduced temperature of 0.476. Aasberg-Petersen et al. reported an AAD of 6.4 % for six oil mixtures from the North Sea. Elsharkawy et al. [2] compared the corresponding states methods of Pedersen and Aasberg-Petersen for Kuwaiti crudes. They reported an AAD of 40 % for Pedersen and 50 % for Aasberg-Petersen.

2.5.4 **Equation of state based methods**

Equation of state based models have also been studied for crude oils. Guo et al. [2] developed a model using EOS. They reported an AAD of 15.07 % for 17 oil samples.

By comparison to the method of Pedersen and Fredenslund, they reported an AAD of 17.40 % [61]. Elsharkawy and Alikhan proposed an EOS method using Middle East crudes. The method was tested with four empirical models for 49 Kuwaiti crudes. The empirical models were Beggs & Robinson, Labedi and Kartoatmodjo and Schmidt. Elisharkawy and Alikhan model was reported the lowest overall AAD of 21 %. [2]

2.6 Summary of the viscosity methods

Various viscosity methods were presented in this chapter. For gas viscosity, the method of Chung showed good results for both pure and mixture gas viscosities. However, it requires the association factor for each component, which makes it impractical. The same applies for the method of Lucas, which requires the dipole moment. The contribution method of Reichenberg is accurate, but it requires the group contributions to be inputted for every component. The corresponding methods of Thodos and others are simple to use and accurate enough to predict pure gas viscosities. For gas mixtures, the method of Wilke was the best and most recommended. The method of Brokaw was the most accurate, but also the most complicated. The method of Herning-Zipperer provided good accuracy with convenient equations.

There was no liquid viscosity method, which could be used in all conditions. Most of the methods require some database parameters to be inputted. The method of Andrade is well-known and the empirical parameters are available for almost all of the substances. However, it does not take into account the effect of pressure. The method of Grunberg-Nissan was found to be the best method for liquid mixtures. The drawback of the method is that it requires different interaction parameters for every component. The logarithm viscosity equation is very convenient, but it can be inaccurate for mixtures containing polar components.

The Friction theory was the most accurate method for hydrocarbon mixtures, but it also requires database parameters for each hydrocarbon component. The method of Petersen is also accurate for hydrocarbons and it does not require empirical data. Method of Petersen can also be applied for crude oils.

The crude oil viscosities can be calculated using different empirical methods, but they are often specified for certain crude oils only. Therefore, they can be inaccurate for other crude oils making them not applicable for general use.

3 Two-phase flow

3.1 General

Firstly, this chapter introduces the variables, which are used in two-phase flow calculations. Secondly, different flow patterns and flow regime maps are treated in horizontal and vertical pipes. Thirdly, calculation methods for two-phase pressure drops in horizontal pipes are reviewed. The effect of viscosity on the two-phase flow is considered in the end of the chapter.

3.2 Definitions of the variables in two-phase flow

3.2.1 **Flow quality**

Vapor quality is used to describe the composition of the flow. Vapor quality is the gas mass fraction of the total mass flux, where mass flux is the rate of mass flow per unit area:

$$x = \frac{G_G}{G} \tag{43}$$

Where x Vapor quality

G_G Gas mass flux, $\frac{kg}{s\ m^2}$

G Total mass flux, $\frac{kg}{s\ m^2}$

Void fraction and liquid holdup are common terms related to two-phase flow. Void fraction is defined as the ratio of the cross-sectional area of the gas phase to the cross-sectional area of the whole area in that segment, whereas the liquid holdup is defined as the ratio of the liquid volume in a pipe segment to the total volume of that pipe segment. The void fraction is illustrated in Figure 6. It is used to determine the mean velocities of the liquid and the vapor. In addition, it also influences on the flow pattern transitions, pressure drop calculations and heat transfer. There are

plenty of different correlations for the void fraction. The void fraction is a dimensionless variable and its general definition is shown in Equation (44). [62]

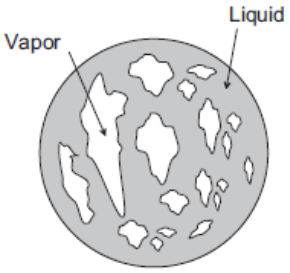

Figure 6. Cross-sectional void fraction. [62]

$$\epsilon = \frac{A_G}{A_G + A_L} \tag{44}$$

Where A_G Area of the gas phase, m^2

A_L Area of the liquid phase, m^2

3.2.2 **Velocity**

True average velocities, also called actual velocities, are the velocities which the phases actually travel. True average velocity is defined as volumetric flow rate of the phase divided by the cross-sectional area of that phase in the flow. [62]

$$u_G = \frac{\dot{Q}_G}{A_G} = \frac{G}{\rho_G}\frac{x}{\epsilon} \tag{45}$$

$$u_L = \frac{\dot{Q}_L}{A_L} = \frac{G}{\rho_L}\frac{(1-x)}{(1-\epsilon)} \tag{46}$$

Where u_G,u_L True average velocities for gas and liquid phases, $\frac{m}{s}$

Slip ratio is defined as the ratio of the true average velocities between the gas and liquid phase. Slip ratio is shown in Equation (47). No-slip denotes that the true average velocities of the both phases are the same.

$$S = \frac{u_G}{u_L} \tag{47}$$

Superficial velocities are often used for determining the flow patterns. Superficial gas velocity is defined as gas velocity without any liquid present and superficial liquid velocity in similar manner. Superficial velocities for both gas and liquid phases are shown in the equations (48) and (47). [62]

$$j_G = \frac{G\ x}{\rho_G} \tag{48}$$

$$j_L = \frac{G\ (1-x)}{\rho_L} \tag{49}$$

Where j_G, j_L Superficial velocities for gas and liquid phases, $\frac{m}{s}$

3.2.3 **Reynolds number**

Reynolds number is a dimensionless variable that describes the ratio of inertial forces to the viscous forces [62]. The expression for Reynolds number is shown in Equation (50). Reynolds is used to determine whether the flow is laminar or turbulent. Generally, laminar flow exists at Reynolds number below 2000 and turbulent flow at Reynolds number over 4000, but there are different definitions at specified conditions. The zone between the laminar and turbulent flow is called transition zone, where the flow may be either laminar or turbulent. In two-phase flow calculations, Reynolds number can be calculated for both phases using their physical properties.

$$Re = \frac{\rho D v}{\eta} \tag{50}$$

Where ρ Density, $\frac{kg}{m^3}$

D Diameter, m

v Flow velocity, $\frac{m}{s}$

η Viscosity, Pa s

3.2.4 **Friction factor**

Friction factor is a dimensionless measure of the resistance to flow by a pipe. Friction factors are divided into two types: Darcy and Fanning friction factors. Darcy friction factor is four times larger than the Fanning friction factor. The selection of the friction factor type depends on the pressure drop calculation method. There are plenty of correlations for the friction factor. Many of them are valid only for certain conditions such as laminar or turbulent flows. [63] A couple of common correlations are introduced in this subchapter.

Blasius friction factor correlation is said to be accurate for turbulent flows in smooth pipes, where the Reynolds number is between 4000 and 10000. Blasius correlation is shown in Equation (59). [63]

$$f_f = \frac{0.079}{Re^{0.25}} \tag{51}$$

Where f_f Fanning friction factor

Hagen-Poiseuille friction factor correlation is accurate for laminar flows and it is often used together with Blasius correlation: [63]

$$f_f = \frac{16}{Re} \tag{52}$$

Churchill friction factor correlation is applicable for laminar, transition and turbulent flow. The correlation can also be used for smooth and rough pipes, because it takes

into account the pipe roughness. Churchill model is shown in the equations (53), (54) and (55). [63]

$$f_f = 8 * \left[\left(\frac{8}{Re} \right)^{12} + \left(\frac{1}{A+B} \right)^{1.5} \right]^{\frac{1}{12}} \quad (53)$$

$$A = \left\{ 2.457 \ln \left[\left(\frac{7}{Re} \right)^{0.9} + \left(0.27 \frac{\epsilon_r}{d} \right)^{-1} \right] \right\}^{16} \quad (54)$$

$$B = \left(\frac{37530}{Re} \right)^{16} \quad (55)$$

Where ϵ_r Pipe roughness, m

D Pipe diameter, m

3.3 Flow patterns

3.3.1 **Horizontal pipe**

Flow pattern, also called a flow regime, is defined as a geometrical distribution of the liquid and vapor phases [5]. Two-phase flow patterns for co-current flow in horizontal tubes can be divided into eight regions, which are shown in Figure 7. Two-phase flow in a horizontal pipe is affected by the gravity, which influences by stratifying the liquid to the bottom of the tube and the gas to the top [5].

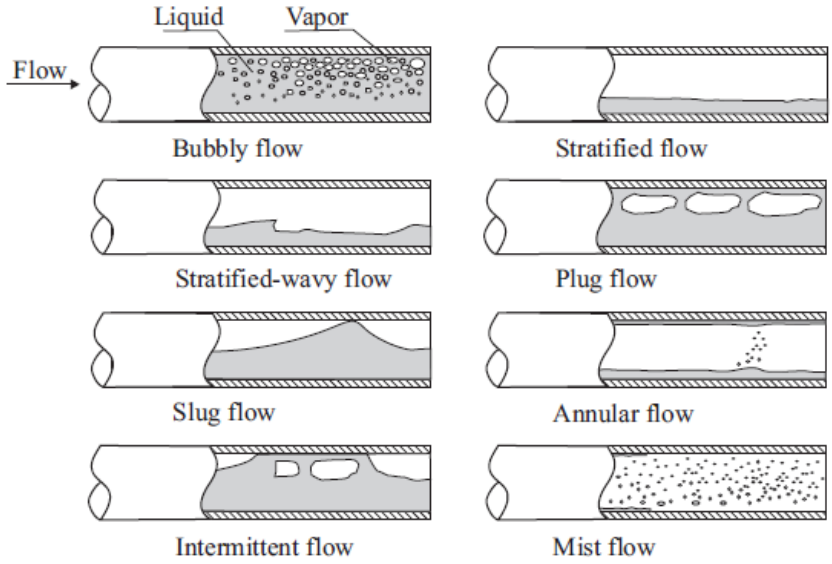

Figure 7. Different flow patterns of the two-phase horizontal flow. [62]

Bubbly flow consists of the gas bubbles, which are dispersed in the liquid. Most of the bubbles are located in the upper half of the pipe due to their buoyancy. Nonetheless, the bubbles will disperse uniformly when the shear forces are dominant. The bubbly flow generally occurs only at high mass flow rates. [64]

Stratified flow is the complete separation of the two-phase flow, which occurs at low liquid and gas velocities. Naturally, the gas phase is located in the upper layer and the liquid phase in the bottom layer due to the gravity. There is a clear interface between the two layers. Increasing the gas velocity will form waves on the interface which travel in the direction of the flow. This is called stratified-wavy flow. The size of the waves depends on the relative velocity of two phases. The waves tend to wet the walls of the pipe and they do not reach the top of the tube. [64]

Intermittent flow occurs when the waves wash the top of the pipe due to increased gas velocity. Amplitude of the wave changes intermittently keeping the top of the pipe wetted all the time. Intermittent flow consists of the plug and slug flow regimes. Plug flow has liquid plugs which are separated by elongated gas bubbles. There is a continuous liquid flow beneath the elongated bubbles. Slug flow occurs at

higher gas velocities when the diameters of the elongated bubbles become the size equal to the diameter of the pipe. [64]

Annular flow pattern occurs at even higher flow rates than intermittent slug flow. The liquid forms a continuous annular film around the circle of the pipe. There is an interface between the phases which may be interrupted by the small waves and droplets at the gas phase. High gas fractions may dry the top of the pipe changing the flow pattern to stratified-wavy flow. Annular flow is sometimes grouped with the mist flow. Mist flow will take place at even higher gas flow rates. All the liquid may be stripped from the wall and entrained as small droplets in the continuous gas phase. [64]

3.3.2 **Vertical pipe**

In vertical flow, axial symmetry exists and flow patterns are more stable. In addition, vertical pipe flow is not affected by gravity in the same way as in a horizontal pipe. Co-current upflow of gas and liquid in a vertical pipe can be categorized into several flow patterns. Bubbly flow occurs when bubbles of different sizes and shapes are observable as the gas is dispersed in the continuous liquid phase. Slug flow develops when increasing gas void fraction forms bubbles with a characteristic shape of a bullet. The bubbles are commonly referred to as Taylor bubbles and they are similar in dimension to the pipe diameter. Churn flow forms as the flow velocity increases. The flow becomes unstable with the fluid and it travels up and down, but with the net upward flow. The instability is caused by the relative parity of the gravity and shear forces acting in opposing directions on the liquid film of Taylor bubbles. Churn flow may not develop at all with small diameter pipes. Annular flow occurs when the interfacial shear of the high velocity gas on the liquid film becomes dominant over gravity. The liquid flows as a thin film on the walls and gas in the center of the pipe. The liquid may be entrained in the gas core as small droplets. Increasing the flow rate may cause the entrained droplets form transient structures such as the clouds of liquid in the central gas core. [65]

3.4 Flow regime maps

3.4.1 **Horizontal pipe**

Flow pattern maps also known as flow regime maps are used to predict flow patterns. A flow regime map is a diagram displaying the transitions boundaries between the flow patterns. It is typically plotted using dimensionless parameters to represent the liquid and gas velocities. Flow regime maps can be classified into empirical and theoretical or semi-theoretical maps. Empirical maps are fitted to the observed flow regime maps while the transitions of the theoretical and semi-theoretical maps are predicted from physical properties. Theoretical and semi-theoretical maps generally consist of two flow parameters such as superficial gas and liquid velocities. The parameters define a coordinate system, where the different flow patterns are charted. Unfortunately, most of the flow pattern maps are only valid for specific systems such as air-water. [66]

The Baker map is a well-known empirical flow pattern map for horizontal flow. It is based on the observations of gaseous and condensate petroleum products. The variables of the map scale for different conditions. The map requires mass velocities and densities for the liquid and the vapor phase. In addition, these properties are also required for the water, because it is used as a reference fluid. Two parameters are introduced taking into account the physical properties of both phases. The parameters are shown in the equations (56) and (57), where the subscripts G and L stand for gas and liquid phases. The map is presented in Figure 8. [67] According to Rounhani and Sohal, it does not predict the flow regimes accurately [68].

$$\lambda_{Baker} = \sqrt{\frac{\rho_G \, \rho_L}{\rho_{Air} \, \rho_{Water}}} \tag{56}$$

$$\psi_{Baker} = \frac{\sigma_{Water}}{\sigma} \left[\frac{\eta_L}{\eta_{Water}} \left(\frac{\rho_{Water}}{\rho_L} \right)^2 \right]^3 \tag{57}$$

Where λ_{Baker} Part of the x-coordinate in the Baker flow pattern map

ψ_{Baker} Part of the y-coordinate in the Baker flow pattern map

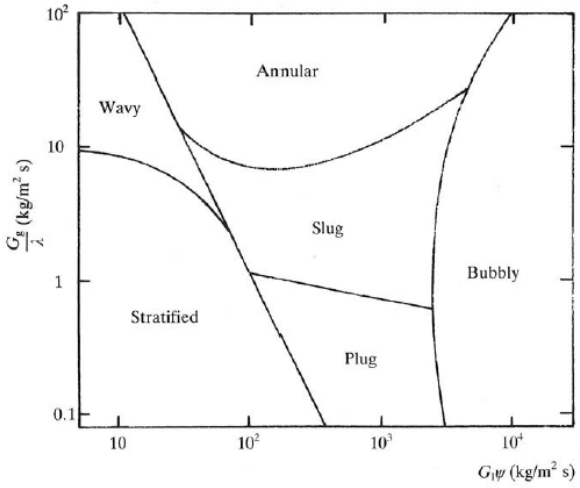

Figure 8. The flow pattern map of Baker [67].

Mandhane et al. [69] developed a similar flow patter map using a larger database containing 5935 observations. Mandhane map requires only superficial gas velocity and liquid velocity, which makes the map easy to use. According to Mandhane et al, the pattern map predicted correctly the flow regime for 68 % of the data points whereas the accuracy for Baker map was 42 %.

Taitel and Dukler [70] developed a flow pattern map on a semi-theoretical basis for horizontal pipes. It is also valid for up to inclination of 10 degrees. The pattern uses momentum balance and it considers stratified flow as initial guess. A stability analysis is used to determine if the stratified flow regime is stable under the prevailing conditions. Taitel and Dukler pattern map is only suitable for small diameter pipes [65]. The map was originally developed for adiabatic flow, but it has also been used successfully for diabatic flows [65].

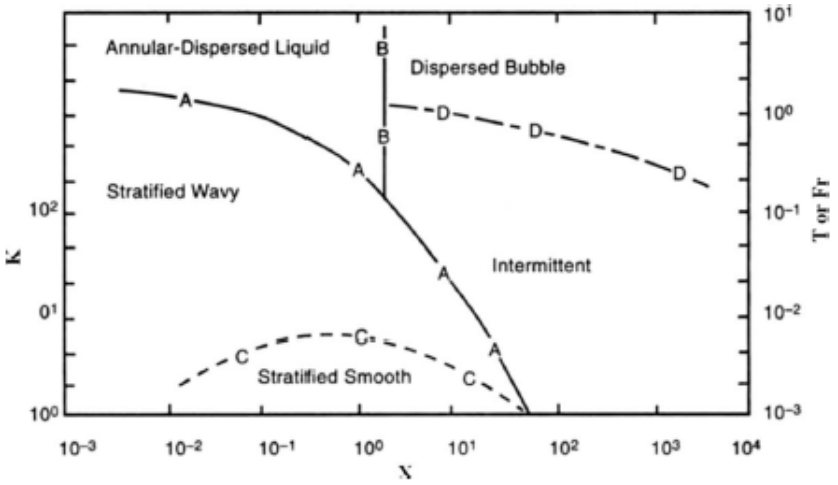

Figure 9. The flow pattern map of Taitel and Dukler for horizontal pipes. [70]

Previous flow pattern maps were mostly predicting adiabatic two-phase flow regimes. Kattan et al. [71] proposed a diabatic flow regime map, which is originally based on a modified Tailtel-Dukler flow pattern map. The map is designed for evaporation flows including influences of the heat flux. The flow pattern map of Kattan et al. consists of five flow regimes: stratified, stratified-wavy, intermittent, annular and mist flows. At first the flow pattern map of Kattan was modified by Thome and El Hajal to make it more practical [72]. Wojtan et al. [73] improved the map of Thome and El Hajal. They subdivided stratified-wavy region into three subzones: slug, and slug/stratified-wavy and stratified-wavy. They also introduced new dryout regime. The dryout regime is encountered when the heated wall becomes dry before complete evaporation. The flow pattern map does not cover bubble flow. The flow pattern map of Wojtan et al. for chlorodifluoromethane with two different heat flux values is shown in Figure 10, where S = stratified flow, SW = stratified-wavy flow, I = intermittent flow, A = annular flow, M = mist flow and D represents dryout flow regime. From the figure can be seen the effect of heat flux for dryout regime transitions.

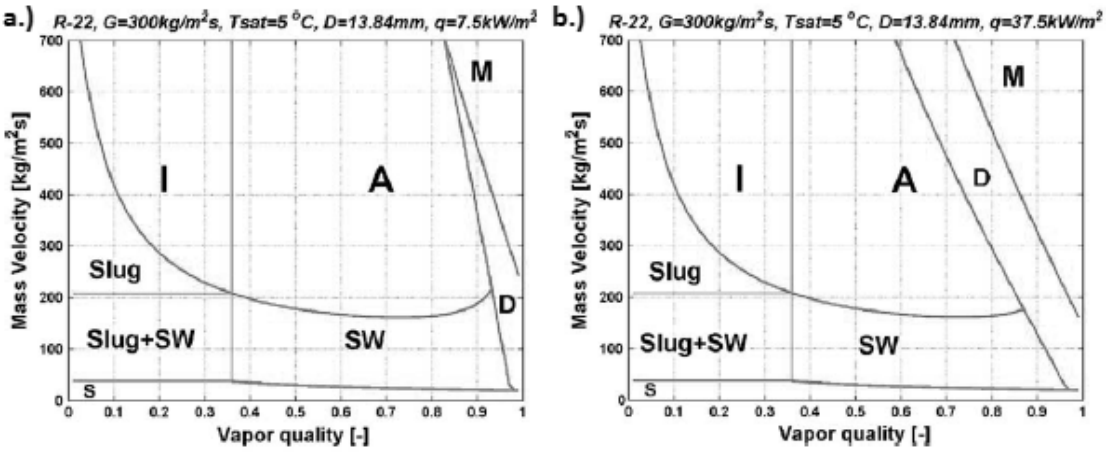

Figure 10. The flow pattern map of Wojtan and others for chlorodifluoromethane with two different initial heat fluxes.

3.4.2 **Vertical pipe**

Hewitt and Roberts [74] proposed a well-known flow regime map for vertical pipes using low pressure air-water and high pressure steam-water mixtures. The map uses superficial momentum fluxes of the gas and liquid. The flow regime map of Hewitt and Roberts is presented in Figure 11.

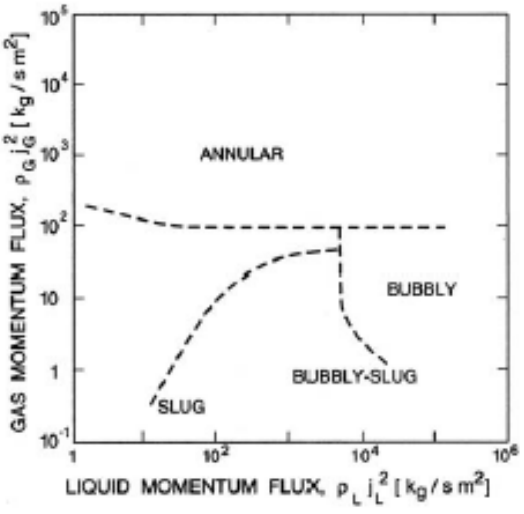

Figure 11. The flow regime map of Hewitt and Roberts for vertical pipes. [74]

3.5 Pressure drop calculation

Two-phase flow pressure drop can be modeled using homogeneous or separated flow. A homogeneous flow model is a simple concept, which assumes equal velocities for the both phases and the slip ratio to be unity. The flow is described as a pseudo fluid, which is characterized by the suitably averaged properties of the liquid and vapor phase. Single phase flow equations can be used for calculating the pressure drop. A separated flow model considers the two phases to be separated into two streams, each flowing in its own area.

3.5.1 **Total pressure drop**

The pressure drop is defined as the change of fluid pressure occurring as a two-phase flow passes through the system. The total pressure drop is the sum of the static head pressure drop, momentum pressure drop and the frictional pressure drop:

$$\Delta p_{total} = \Delta p_{static} + \Delta p_{momentum} + \Delta p_{friction} \tag{58}$$

The static pressure drop for a homogeneous two-phase flow is:

$$\Delta p_{static} = \rho_{tp}\, g\, H \sin\theta \tag{59}$$

$$\rho_{tp} = \rho_L(1-\epsilon) + \rho_G\epsilon \tag{60}$$

Where ρ_{tp} Two-phase density, $\frac{kg}{m^3}$

g Gravitational acceleration constant, 9.81 $\frac{m}{s^2}$

H Vertical height, m

θ Angle from the horizontal plane, rad

The static pressure drop occurs only in inclined or vertical flows, which deviates from the horizontal plane. The momentum pressure drop is described as the kinetic

energy of the flow and it is shown in equation (61). There is no momentum pressure drop in adiabatic flows. [64]

$$\Delta p_{momentum} = G^2 \left\{ \left[\frac{(1-x)^2}{\rho_L (1-\epsilon)} + \frac{x^2}{\rho_G \epsilon} \right]_{out} - \left[\frac{(1-x)^2}{\rho_L (1-\epsilon)} + \frac{x^2}{\rho_G \epsilon} \right]_{in} \right\} \quad (61)$$

3.5.2 **Frictional pressure drop**

Frictional pressure drop calculation is the most important and difficult part in the calculations of the two-phase flow. There are plenty of different approaches for calculating the frictional pressure drop. Frictional pressure drop methods are often referred to as pressure drop methods. They can be divided into empirical, analytical and phenomenological methods. All the approaches have their advantages and disadvantages. Empirical methods are the most used for modeling a two-phase flow. They require minimum knowledge of the flow characteristics. Therefore, they are easy to apply and they can offer satisfied results in the range of the available database. The empirical methods have few disadvantages. They are limited by their database and their suitability for general use. In addition, they do not recognize different flow regime types. [75]

Analytical pressure drop methods are general methods, which do not require any empirical information. They use complex mathematical models. Iterative and numerical procedures are overdriving and time consuming, thus the analytical models are not treated in this chapter. [75]

Phenomenological methods are based on a theoretical approach of the flow characteristics, but they also require some empirical information such as a flow regime map. [75] In this thesis, phenomenological methods are defined as pressure drop calculation methods which take into account the different flow patterns. There is no general flow pattern based model available yet for all of the flow patterns.

According to Quiben and Thome [66], knowing the right flow pattern is important when calculating the pressure drop especially at low flow rates and at high vapor qualities. The most common empirical methods, which do not take into account different flow patterns, may cause over 50 % errors for particular flow regimes. In addition, these methods have several other disadvantages. Firstly, they do not account explicitly for the influence of interfacial waves. Secondly, they do not account the upper dry perimeter of stratified flows. Thirdly, they use a local void fraction instead of the actual velocities of the vapor and liquid phases. Fourthly, they represent annular film flows as tubular flow. Fifthly, they do not capture the peak in the pressure gradient at high vapor qualities. Finally, they do not work at conditions when there is only one phase present.

3.6 Pressure drop methods

3.6.1 **Lockhart-Martinelli**

Lockhart-Martinelli is one of the most known empirical pressure drop calculation methods for two-phase flow. It is based on experimental data of various sources. The experimental data consist of air flow with different liquids flows such as water, benzene and diesel. The diameter ranged from 1.5 mm to 25 mm and the pressure range from 110 kPa to 360 kPa. [76]

Lockhart and Martinelli [76] divided two-phase flow into four flow regimes depending on the turbulence of the gas or the liquid flow. Four different flow regimes, their Reynolds numbers and their correction terms are listed in
Table 3. The method of Lockhart-Martinelli is based on two assumptions. At first, the static pressure drop for liquid and gaseous phases must be equal regardless of the flow pattern. Secondly, the volume occupied by both liquid and the gas phase at any position must be equal to the total volume of the pipe. Therefore, the flow pattern does not change along the pipe. The method of Lockhart-Martinelli was

recommended by Whalley [77] when the viscosity ratio between liquid and gas phases is over 1000 and the mass flow rate is below 100 $\frac{kg}{m^2 s}$.

Table 3. Flow regimes in the method of Lockhart-Martinelli.

Liquid phase	Gas phase	Re_L	Re_G	C
Turbulent	Turbulent	> 2000	> 2000	20
Turbulent	Laminar	> 2000	< 1000	12
Laminar	Turbulent	< 1000	> 2000	10
Laminar	Laminar	< 1000	< 1000	5

The method of Lochart-Martinelli calculates frictional pressure drop using multiplier term for the pressure drop of the liquid or the gas phase, which would exist if either of the fluids were flowing alone in the pipe: [76]

$$\Delta p_{friction} = \Phi_G^2 \Delta p_G \tag{62}$$

$$\Delta p_{friction} = \Phi_L^2 \Delta p_L \tag{63}$$

Where Φ_G , Φ_L Dimensionless multiplier term for gas and liquid phases

Δp_G, Δp_L Single-phase pressure drop for gas and liquid phases

Single-phase pressure drops are calculated as:

$$\Delta p_G = -\frac{2 f_G x^2 G^2}{D \rho_G} \tag{64}$$

$$\Delta p_L = -\frac{2 f_L (1-x)^2 G^2}{D \rho_L} \tag{65}$$

Where f_G, f_L Single-phase friction factor term for gas or liquid phase

G Mass flux flow, $\frac{kg}{m^s\, s}$

D Inner diameter of the pipe, m

ρ_G Gas density, $\frac{kg}{m^3}$

Lockhart and Martinelli [76] proposed that the single-phase friction factors are calculated as:

$$f_G = \frac{0{,}079}{Re_G^{0.25}} \tag{66}$$

$$f_L = \frac{0{,}079}{Re_L^{0.25}} \tag{67}$$

Where the Reynolds numbers for both phases are calculated using vapor quality:

$$Re_G = \frac{xGD}{\eta_G} \tag{68}$$

$$Re_L = \frac{(1-x)GD}{\eta_V} \tag{69}$$

Lockhart and Martinelli [76] proposed a graphical correlation for determining the pressure drop multiplier term for four flow regimes using experimental data. They introduced a so-called Martinelli-parameter, which is the ratio between the single-phase pressure gradients:

$$\mathrm{X} = \sqrt{\frac{\Delta p_L}{\Delta p_G}} \tag{70}$$

Where X Martinelli parameter

Lockhart and Martinelli [76] derived multiplier equations from the graphical correlation for each flow regimes using correction term C, which are shown in Table 3. Multiplier terms for each phase are shown in the equations (71) and (72).

$$\Phi_L^2 = 1 + \frac{C}{X} + X^2 \quad (71)$$

$$\Phi_G^2 = 1 + \mathrm{CX} + X^2 \quad (72)$$

Where C Lockhart-Martinelli parameter for different flows

3.6.2 **Friedel**

Friedel [78] obtained correlation by optimizing the two-phase multiplier using a large database of two-phase drop measurements. The method is simple and applicable to all vapor qualities. In addition to the horizontal flow, the method is applicable to vertical upflow aslwell. Whalley [77] recommended not use the method when the viscosity ratio between liquid and gas phases is above 1000.

The method of Friedel uses its own multiplier term and the pressure drop of the pure liquid. The pressure drop of the pure liquid is different than the single-phase pressure drop term. It assumes whole two-phase flow to be liquid, whereas single-phase pressure drop term only calculates the pressure drop for the liquid, which is actually flowing in the pipe. The method of Friedel for calculating the frictional pressure and his multiplier term are shown in the equations (73) and (74).

$$\Delta p_{friction} = \Phi_{fri}^2 \Delta p_{L0} \quad (73)$$

Where Φ_{fri} Multiplier term of Friedel

Δp_{L0} Pure liquid pressure drop, $\frac{Pa}{m}$

$$\Phi_{fri}^2 = \mathrm{E} + \frac{3.24 * \mathrm{F} * \mathrm{H}}{Fr_H^{0,045} We_L^{0,035}} \quad (74)$$

Where the calculations of the terms E, F, H, $\mathrm{Fr_H}$ (Froude number), and $\mathrm{We_L}$ (Weber number) are shown in the equations from (75) to (79).

$$\mathrm{E} = (1-x)^2 + x^2 \frac{\rho_L f_{Go}}{\rho_G f_{Lo}} \tag{75}$$

$$\mathrm{F} = x^{0.78}(1-x)^{0.224} \tag{76}$$

$$\mathrm{H} = \left(\frac{\rho_L}{\rho_G}\right)^{0.91} \left(\frac{\eta_G}{\eta_L}\right)^{0.19} \left(1 - \frac{\eta_G}{\eta_L}\right)^{0.7} \tag{77}$$

$$Fr_H = \frac{G^2}{gD\bar{\rho}^2} \tag{78}$$

$$We = \frac{G^2 D}{\bar{\rho}\sigma} \tag{79}$$

$$\bar{\rho} = \left(\frac{x}{\rho_V} + \frac{(1-x)}{\rho_L}\right)^{-1} \tag{80}$$

Where σ Surface tension, $\frac{N}{m}$

$\bar{\rho}$ Average homogeneous density, $\frac{kg}{m^3}$

The pressure drop of the pure liquid can be calculated as:

$$\Delta p_{L0} = \frac{2 f_{Lo} G^2}{D \rho_L} \tag{81}$$

3.6.3 **Müller-Steinhagen and Heck**

Müller-Steinhagen and Heck [79] proposed a simple empirical pressure gradient correlation, which uses an empirical extrapolation between all liquid flow and all vapor flow. The method was developed using a large data bank containing over 9300 measurements of frictional pressure drops. The method of Müller-Steinhagen and Heck is applicable with all vapor qualitities.

$$\Delta p_{friction} = F(1-x)^{1/3} + Bx^3 \tag{82}$$

Where the F term is calculated as:

$$F = A + 2(B - A)x \tag{83}$$

Where A and B are the pure liquid pressure drop and pure vapor pressure drop. Pure liquid pressure drop was shown in Equation (75) and pure vapor pressure drop is defined as:

$$\Delta p_{G0} = \frac{2 f_{G0} G^2}{D \rho_G} \tag{84}$$

3.6.4 **Beggs and Brill**

Beggs and Brill [80] developed a phenomenological two-phase pressure drop calculating method based on their experimental data for air-water flows in 25 mm and 38 mm pipes. In addition to the horizontal flow, the method also allows a vertical, inclined upward and downfall flows. The method recognizes four different flow patterns for the horizontal flow, which are segregated, intermittent, distributed and transitional flows. Segregated flow pattern includes stratified, wavy and annular flows. Plug and slug flow patterns are under intermittent flow, where at least one of the two phases must be discontinuous. Distributed flow pattern consists of bubble and mist flows, where the liquid phase is continuous and gas phase is discontinuous.

3.6.5 **Bandel**

Bandel [81] divided two-phase pressure drop calculations into three flow regimes: annular, stratified and the transitional flow regime. He proposed an iterative phenomenological method to calculate the frictional pressure drop for annular and the stratified flow regimes. The pressure drop of the transitional flow regime is interpolated from the calculated ones. The method of Bandel is shown in Appendix A.

3.6.6 **Moreno-Quibén and Thome**

Moreno-Quibén and Thome [75] proposed a diabatic phenomenological two-phase frictional pressure drop method, which uses the flow pattern map of Wojtan for adiabatic and evaporating flows in horizontal plain tubes. The method covers every flow regime from the map. Therefore, it does neither recognize nor calculate the bubbly flow regime. Moreno-Quibén and Thome tested their method mainly for refrigerants such as chlorodifluoromethane and tetrafluoroethane. Even though, the method is designed for evaporating adiabatic flow, they showed that both diabatic and adiabatic frictional pressure drop values are quite close to each other. In addition they showed that the boiling process itself does not affect to the frictional pressure drop. [82]

3.7 Comparison of the pressure drop methods

In 1986, Müller-Steinhagen and Heck [79] compared 15 different two-phase pressure drop calculation methods using over 9000 data sets. The method of Bandel was the most accurate with an AAD of 32.6 %. It predicted 60 % of the values within ±30 % of the measured data. Thus, it can be concluded that the prediction of the two-phase pressure drop is moderately inaccurate.

In 1999, Tribbe and Müller-Steinhagen [75] evaluated the phenomenological models for predicting the pressure drop gradient in horizontal pipes. Their databank included almost 7000 experimentally derived data points of pressure drops. Databank consists of six different fluid systems: air-water, stream-water, air-oil, air-aqueous CMC solutions, refrigerants and cryogenics. They used the Gaussian probability density function and distribution of logarithmic ratios to compare different methods. Tribbe and Müller-Steinhagen generated two composite methods using a number of phenomenological models and modifying the flow pattern maps. The pressure drop predictions of the empirical methods were much more accurate for air-water data, but significantly less accurate for the other fluid systems. The method of Bandel was the most accurate from the individual methods.

Other phenomenological methods did not perform as well as the empirical methods. However, the two generated composite models performed well reducing the standard deviation of the overall distribution by 10 % compared to the method of Bandel.

Shannak [83] investigated air-water frictional pressure drop for horizontal and vertical orientation. He compared the methods using the databank collected by Friedel, which has over 16 000 measured data points for different orientations and systems such as air-water, refrigents, air-oil and plenty of other systems. He proposed his own method, which had the smallest AAD of 35 %. The comparison of the empirical pressure drop methods by Shannak is shown in Table 4. The methods of Shannak and Friedel had the lowest AAD. However, both of the methods are based on the test data. The method of Müller-Steinhagen and Heck performed well even though it is not based on the test data.

Table 4. Comparison of the empirical frictional pressure drop calculation methods. [83]

Correlation	Standard deviation	AAD
Shannak (2008)	35 %	25 %
Friedel (1979)	40 %	30 %
Müller-Steinhagen and Heck (1986)	50 %	34 %
Lockhart and Martinelli (1949)	86 %	73 %
Martinelli and Nelson (1948)	76 %	60 %
Homogeneous model	100 %	82 %

Empirical methods for calculating two-phase pressure gradients of the refrigerants in horizontal tubes were studied by Didi, Kattan and Thome. Over 1500 experiment points for five different refrigerants were used. Müller-Steinhagen and Heck - method was the best for annular flows while the method of Grönnerud the most

accurately predicted intermittent and stratified-wavy flows. However, the statistical deviations between the predicted and the experimental values were large. [84]

Moreno-Quibén and Thome [75] compared their own frictional pressure drop calculation method for horizontal two-phase evaporating flow with three other existing methods: Friedel, Grönnerud, Müller-Steinhagen and Heck. The comparison was made using 2500 experimental values for three different refrigerants. Their own method predicted 82 % of the data points within ± 30 % and 65 % of the data points within ± 20 %. Müller-Steinhagen and Heck was the second most accurate method. It predicted 76 % of the data points within ± 30 % and 50 % of the data points within ± 20 %.

3.8 Effect of viscosity

In the 70s, Weisman et al. [85] investigated the effects of fluid properties for two-phase flow. They concluded that the flow pattern is only slightly affected by the viscosity. However, they used only viscosities up to 0.15 Pa s, which can be considered as fairly low liquid viscosity.

Matsubara and Naito [4] studied the effect of liquid viscosity on two-phase flow patterns using liquid viscosity range from 0.001 to 11 Pa s. The model of Taitel and Dukler was used for predicting flow patterns. It predicted the flow patterns well up to 0.1 Pa s, but higher viscosities caused difference between the model and experimental results. The model over predicted the effect of viscosity and it could not predict the stratified flow regime at high viscosities. Matsubara and Naito recommended using a different approach for high viscosity cases.

Foletti et al. [86] compared experimental air-water and air-oil flows with the flow pattern maps such as Mandhane, Baker and Pelatas & Aziz. The flow pattern map of Mandhane predicted plug and slug flow regimes fairly good for air-oil flows. It is remarkable that the map of Mandhane does not distinguish bubbly and plug flows

from each other. The high viscosity flow pattern experiments were done by using oil with viscosity of 0.896 Pa s. Foletti et al. reported a poor agreement between all of the tested flow pattern maps and the experimental observations for air-oil flows. For example, the flow pattern map of Mandhane predicted almost all of the data points to the stratified flow regime. According to Foletti et al., the current flow pattern maps are not able to predict the high viscous two-phase flows properly.

Zhao et al. [87] investigated the effects of liquid viscosity on flow pattern, liquid holdup and pressure gradient using liquid viscosity from 1.0 Pa s to 7.5 Pa s. Their experimental results were compared to the method of Beggs and Brill. Comparison between the experimental values and the flow patterns of the Beggs and Brill at two different viscosities is shown in Figure 12. The method of Beggs and Brill predicted the flow patterns correctly at liquid viscosity of 1.0 Pa s. The difference between the method and the experimental results started to grow as the viscosity increased. Nonetheless, the predictions of the method were acceptable up to the viscosity of 3.5 Pa s. At higher viscosities, the discrepancies become significant. The predicted pressure drop acted in similar manner. The liquid holdup correlation of Beggs and Brill neglects the viscosity. Therefore, it gave invalid results for high viscosity flows.

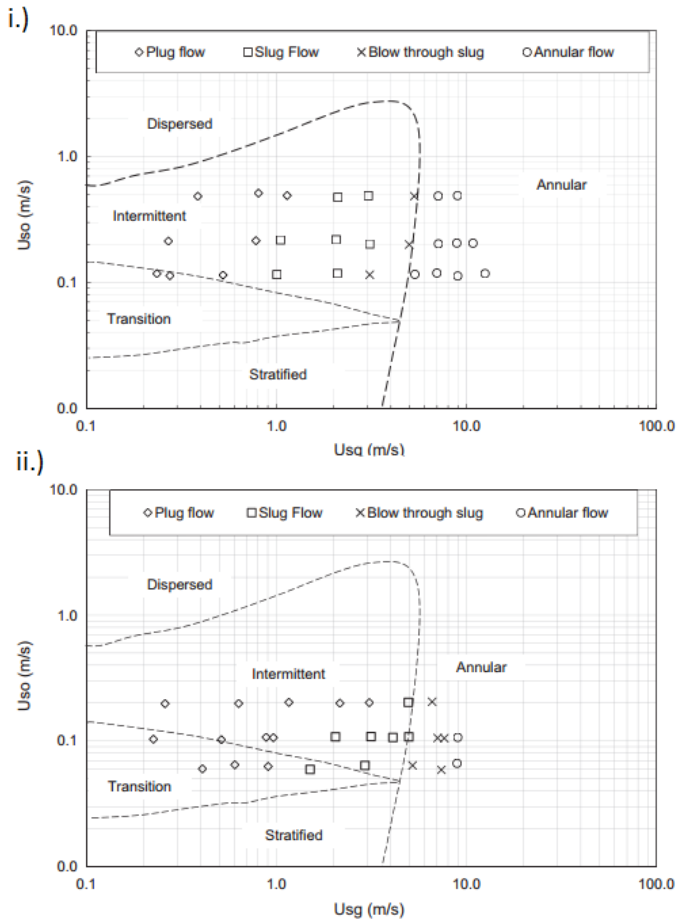

Figure 12. The comparison between the Beggs and Brill correlation and the experimental values at different liquid viscosities i.) 1.0 Pa s and ii.) 5.0 Pa s.

Szalinski et al. [88] compared air-water and air-silicone oil two-phase flows in a vertical pipe. The viscosity of the silicone oil was 0.0053 Pa s. According to them, flow pattern transition regions depend on the subjective assessment of the observer. Thus, they defined the different flow patterns using the size of the largest bubbles observed during the measurements. They used different methods for the slug to annular transition, because those could not be predicted based on only the size of the bubbles. They concluded that the viscosity affects the size of the bubbles at similar superficial velocities. The air-water flow had larger bubbles due to the lower viscosity of the water, which means that the flow pattern transition takes place at lower superficial velocities of the gas and liquid phases compared to the air-oil flow. However, it did not apply to the transition boundary between the churn

and annular flows, which they found to occur at lower gas velocities for the oil than for the water.

Da Hlaing et al. [89] studied the effect of viscosity in a vertical pipe for air-water and air-glycerol solution systems. According to them, the pressure drop decreases with the increasing Reynolds number in the bubble, slug and slug-churn flow regimes. On the contrary, the pressure gradient increases with the increasing Reynolds number in the annular and mist flow regimes. Reynolds number is affected by the viscosity, where the increased viscosity decreases the Reynolds number. The viscosity affects more in slug and slug-church flow regimes when the flow is laminar. Churn, annular and mist flows are affected less by the viscosity, because the flow is turbulent. Da Hlaing and others could not predict transitions from slug to churn flows and from churn to annular flows accurately.

APPLIED PART

4 Objectives of the applied part

The purpose of the applied part was to improve two-phase calculations of the dynamic process simulator, ProsDS, and study the effect of viscosity on two-phase flow. ProsDS did not have any viscosity calculating methods. The most reliable and practical viscosity methods from FLOWBAT simulator were applied to ProsDS. The chosen methods were compared against the experimental viscosity data presented in the literature. The effect of viscosity on two-phase flow was studied using experimental two-phase pressure drop data from the literature, which contained gas-liquid mixtures with different viscosities. Different frictional pressure drop methods were compared against the experimental data. The best performed pressure drop methods were encoded into ProsDS.

5 Implementation of the viscosity methods

5.1 Software environment

Neste Jacobs has its own dynamic process simulator, ProsDS. It is part of the NAPCON Suite concept, which offers automation and simulation solutions to the customers. ProsDS is developed for chemical engineering and it is used for wide range of applications from individual unit processes to complex simulation cases. One of the main usages of ProsDS is training simulators. Operators can train different situations, which are reflections of the real world cases. ProsDS is programmed using FORTRAN and LISP languages.

FLOWBAT is a steady state simulation program for chemical processes. It is developed together with Neste Jacobs and Aalto University School of Chemical Technology. Some of the FLOWBAT features are integrated into ProsDS, such as the component database, which consists of physical properties for 3000 components. FLOWBAT is also encoded with FORTRAN.

5.2 Selected methods from FLOWBAT

The plan was to select the most reliable and practical viscosity methods from FLOWBAT and integrate them into ProsDS. FLOWBAT has many methods for calculating gas and liquid viscosities. All of the methods were reviewed in the literature part, but some of them are not practical for a common simulator use.

FLOWBAT has two methods for calculating pure gas viscosity: Thodos and Petersen. Thodos can be applied for both polar and non-polar gases while the method of Petersen is only valid for hydrocarbons. Despite the fact that the method of Lucas was recommended for calculating pure gas viscosity in the literature part, the method of Thodos was chosen to encode in ProsDS. The method of Thodos was shown to be accurate enough in the literature part. In addition, the method of Lucas

requires dipole moment, which is difficult to predict. The dipole moment correlation increases inaccuracy, which in turn increases the inaccuracy of the viscosity method of Lucas. Therefore, more accurate results cannot be obtained using method of Lucas.

The method of Petersen can calculate the viscosities of pure and mixture hydrocarbons for both gas and liquid phases. It also takes into account the pressure changes of the system. Therefore, the method was selected to ProsDS. The method of Petersen can be used only for hydrocarbons. Thus, other viscosity methods are also required.

Herning-Zipperer and Petersen are the two methods for calculating the viscosity of the gas mixtures in FLOWBAT. The method of Herning and Zipperer was selected to ProsDS, because it is almost as accurate as the method of Wilson, which was recommended in the literature part.

There are five methods for calculating liquid viscosity in FLOWBAT, which are:

- Andrade
- Letsou and Stiel
- Prezezdziecki
- Yaws
- Visvanath and Natarajan

Andrade, Yaws, Visvanath and Natarajan methods are quite similar and they all require database values for each component. They do not take into account the effect of pressure. The method of Andrade is accurate and it has the largest database. It is also valid from the melting point to the boiling point of the component. Therefore, the method of Andrade is chosen for ProsDS.

The method of Letsou and Stiel was also selected to ProsDS, because it can be used for saturated liquid and it is good for high temperature processes. The method of Prezezdziecki was not recommended in the literature part, because it underestimates the viscosities of the pure liquids. Therefore it was not chosen for ProsDS.

FLOWBAT has three methods for calculating the viscosity of the liquid mixture: UNIMOD, Logarithm mixture equation and Petersen. UNIMOD-method requires UNIFAC-parameters, which are not available for all of the components. Thus, UNIMOD was not chosen for ProsDS. Logarithm mixture equation was selected to ProsDS, because it is practical and accurate enough for non-polar mixtures. The drawback of the equation is that it does not consider any interactions between the molecules, which may lead to inaccurate viscosities for polar mixtures. In order to improve the accuracy of the liquid mixture viscosities, The Grungberg-Nissan equation should be applied. However, it is not practical requiring the values for every interaction parameter for different mixtures. All of the selected methods for ProsDS in order to calculate viscosities are shown in Table 5.

Table 5. Selected viscosity methods for ProDS.

	Pure component	Mixture
Gas	Thodos	Herning and Zipperer
	Petersen	Petersen
Liquid	Andrade	Logarithm mixture function
	Letsou and Stiel	Logarithm mixture function
	Petersen	Petersen

5.3 ProsDS Implementation

5.3.1 **Structure**

Microsoft Visual Studio 2013 was used for coding. The viscosity methods could be called directly from ProsDS due to the FLOWBAT integration. Viscosity methods were encoded in a way, so that they require only one parameter for choosing the model for both liquid and gas phases. There are total of six different combinations for calculating the viscosity, which are shown in Table 6.

Table 6. Different combinations of the viscosity methods.

Viscosity calculating method		
Gas	Liquid	Number
Thodos	Andrade	1
	Letsou	2
	Petersen	3
Petersen	Andrade	4
	Letsou	5
	Petersen	6

5.3.2 **Testing and verifying**

Viscosity methods were tested and compared against the experimental values from the literature. Only a small database was used in order to ensure that the methods are working correctly and to give indications of their accuracy level. Total of 108 experimental data points were used for four different systems. The components and conditions of the database are shown in Table 7. The database consists of a large pressure range in order to see its effect on the viscosity, and whether the pressure correction is obligatory in viscosity methods.

Table 7. Contents of the experimental data.

Component	Phase	T [K]	P [MPa]	Data points	Error	Ref.
Propane	Gas	280 - 600	0.1 - 30.0	36	1 %	[90]
Methane-Propane	Gas	310 - 410	0.1 - 13.8	40	0.05 %	[91]
Octane	Liquid	298 - 373	0.1 - 160.7	16	0.01 %	[92]
Pentane-Octane-Decane	Liquid	298 - 373	0.1 - 21.7	22	0.01 %	[93]

An AAD was used for the evaluation of the different viscosity methods. The methods of Thodos and Petersen were tested using experimental values for the viscosity of pure propane. The results are presented in Figure 13. From the figure can be seen that the method of Thodos is very accurate for pure non-polar gases such as Propane. Most of the deviations were achieved near the critical conditions, where the deviations were around 20 %. The method of Petersen is accurate under atmosphere conditions. However, at high pressure conditions AADs were about 20 %, which generally means around 5 $\frac{\mu Pa}{s}$ deviations between the calculated and the real gas viscosities.

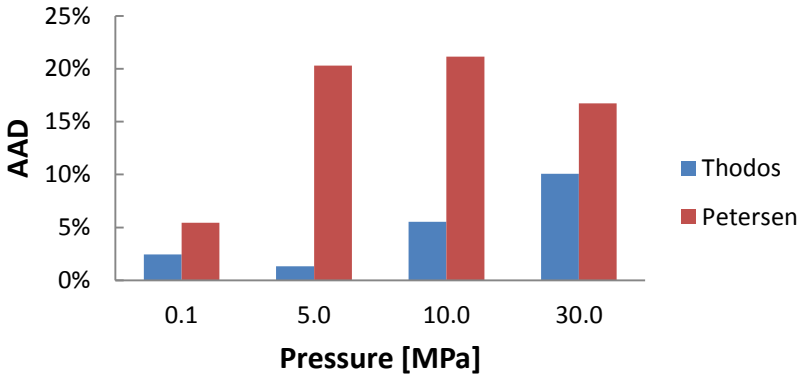

Figure 13. Comparison of the viscosity methods for pure propane gas at different pressures.

The methods of Herning-Zipperer and Petersen were selected for the gas mixtures. They were compared against methane-propane mixture at different pressures. The results are shown in Figure 14. In FLOWBAT, the method of Thodos is used together

with the method of Herning and Zipperer. The method of Herning and Ziperrer is designed for low pressure gas mixtures. The FLOWBAT does not take into account the effect of pressure and all the calculations are made in atmospheric conditions. Therefore, the AAD for Herning and Zipperer -method increases linearly with the pressure, which can be seen from Figure 14. An overall AAD for the method remained low. The method of Petersen calculates the pressure differences, but the AAD remained higher at almost each pressure compared to the method of Herning-Zipperer. However, the accuracy of Petersen is moderately good and it can be used for calculating the viscosity of the hydrocarbon gas mixtures.

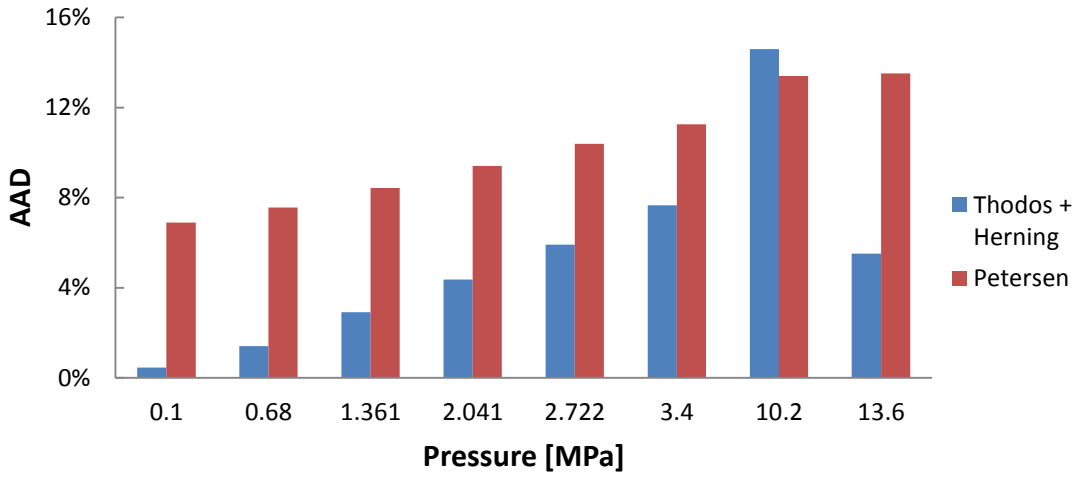

Figure 14. Comparison of the viscosity methods for methane-propane gas mixture at different pressures.

The comparison of the calculating methods for pure liquid viscosity is shown in Figure 15. The methods of Andrade and Letsou-Stiel do not take into account the effect of pressure. Therefore the errors increase almost linearly with pressure. The method of Andrade showed superb accuracy at atmospheric conditions due to its two empirical data parameters, which are specified at these conditions. The AAD is less than 1 % at atmospheric pressure. The method of Letsou and Stiel showed poor accuracy. The method should be used carefully, only at high temperatures near the critical conditions. The method Petersen is accurate at all pressures. It was the only

method that calculated the viscosity at 160 MPa and the AAD was below 5 %. The highest AAD of 7 % was observed at atmospheric pressure. An AAD of 7 % for the viscosity of liquid octane means only 0.03 Pa/s difference in viscosity, which can be considered as a fairly small deviation.

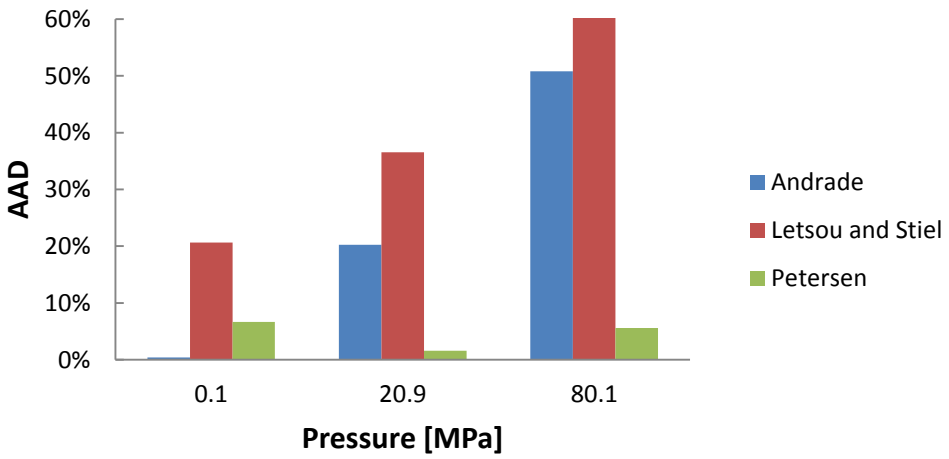

Figure 15. Comparison of the viscosity calculating methods for pure liquid octane at different pressures.

Methods for liquid mixture viscosities were tested using viscosity values for pentane-octane-decane mixture. The methods of Andrade with mixture logarithm function and Petersen were tested. The results of the comparison are shown in Figure 16. Both methods give satisfying results for atmospheric conditions. The deviation of the Andrade method increases almost linearly with the pressure due to the lack of pressure correction in the method of Andrade. The method of Petersen is accurate at any pressure. It is reasonably to notate that the mixture is non-polar and consist of only hydrocarbons. The method of Petersen is only valid for pure hydrocarbons and their mixtures. The methods of Andrade and mixture logarithm function give accurate values for non-polar systems, because the interaction parameters are not needed.

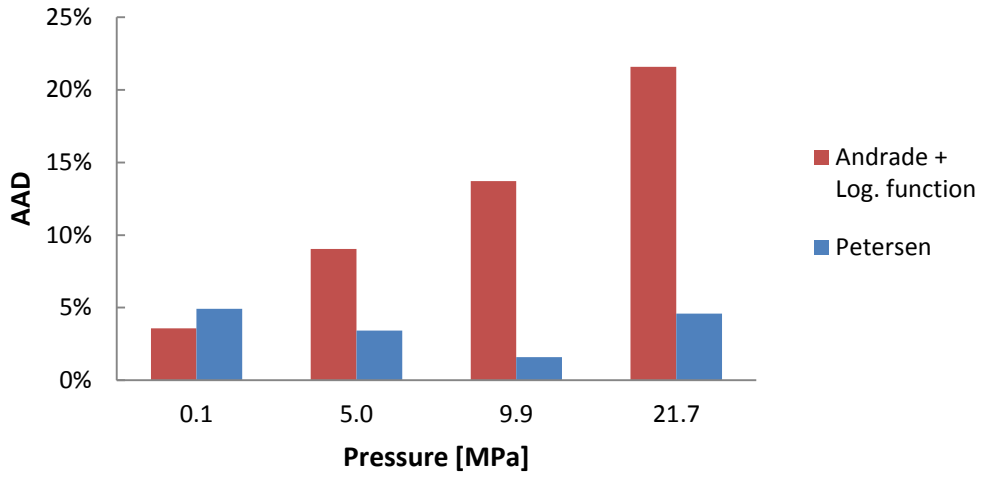

Figure 16. Comparison of the viscosity calculating methods for liquid Pentane-Octane-Decane mixture at different pressures.

6 Improving the two-phase calculations in ProsDS

6.1 Procedure

The main purpose was to improve two-phase flow calculations in ProsDS. The selected pressure drop methods were tested for a gas-liquid horizontal flow using experimental data presented in the literature. The effect of the viscosity was also investigated. However, the two-phase pressure drop is greatly influenced by many other variables such as flow-pattern, void fraction, friction factor correlation and density, which made the observations more complex. Six different pressure drop calculation methods were selected for the calculation of the two-phase pressure drop. The selected pressure drop methods and their features are shown in Table 8. The pressure drop methods were tested against experimental data presented in the literature using Microsoft Excel. The best performed methods were chosen and encoded into ProsDS.

All the selected methods were introduced in the literature part. Inclination denotes the capability of the method in order to calculate pressure drop in the layout, which deviates from the horizontal plane. Beggs and Brill is the only method, which allows the inclination of the pipe. Three of the methods recognize some of the flow patterns. Some of the methods had their own friction factor correlation, but most of them did not. Two different friction factor correlations were used for the method of Lockhart-Martinelli in order to see the effect of friction factor on the pressure drop. Friction factor correlations Hagen-Poiseuille and Blasius were combined as a one correlation, where Hagen-Poiseuille was used for laminar flows when Reynolds number is below 2300. Otherwise, the correlation of Blasius was used. The Friction factor correlation of Churchill was also used for comparison. Selected friction factor correlations were also presented in the literature part.

Table 8. Selected pressure drop calculation methods.

Method	Friction factor correlations	Flow regimes	Inclination	Diabatic
Lockhart-Martinelli	Poiseuille-Blasius [PB] Churchill [Ch]	No	No	No
Friedel	Blasius	No	No	No
Müller-Steinhagen and Heck	Churchill	No	No	No
Beggs and Brill	Beggs and Brill	Yes	Yes	No
Bandel	Poiseuille-Blasius	Yes	No	No
Moreno-Quibén and Thome	Quiben-Blasius	Yes	No	Yes

6.2 Experimental data

6.2.1 **Database**

Three datasets of two-phase pressure drop measurements were presented in the literature. They contained total of 349 experimental data points. The pressure drop measurement techniques were excluded from this thesis and they were not analyzed. The pressure drop measurements were typically given in terms of superficial velocities for gas and liquid flows. The pressure drop range of the experimental data was from 10 $\frac{Pa}{m}$ to 3000 $\frac{Pa}{m}$. The liquid viscosities in the database varied from 0.001 Pa*s to 0.601 Pa*s. The database and the range of the operation conditions are presented in Table 9.

Table 9. Experimental database for two-phase pressure drops.

Dataset		**Badie**	**Andritsos**	**Gockal**	**Total**
Components		Air-Water Air-Oil	Air-Water Air-Glycerol	Air-Oil	
D [m]	Min	0.079	0.025	0.051	0.025
	Max		0.095		0.095
Data points		66	116	167	349
P [bar]	Min	1	1	7	1
	Max				7
T [K]	Min	293	288	294	288
	Max		300	482	482
η_L [Pa s]	Min	0.001	0.001	0.178	0.001
	Max	0.040	0.180	0.601	0.601
j_G [m/s]	Min	7.8	1.3	0.1	0.1
	Max	25.3	163.2	2.2	163.2
j_L [m/s]	Min	0.001	0.001	0.050	0.001
	Max	0.035	53.950	0.800	53.950
ΔP [Pa/m]	Min	20	2	124	2
	Max	380	26010	6742	26010
Pipe roughness		Smooth	Smooth	Smooth	
Measurement accuracy		± 5 Pa	-	1.4 %	
Reference		[94]	[95]	[96]	

6.2.2 **Physical properties**

Physical properties were not given in all of the datasets and therefore they had to be calculated. Physical properties, such as density and viscosity, needed correlations for calculations, because they are temperature dependent. Air density were calculated using an ideal gas law. The other correlations were generated using Microsoft Excel trend line for polynomial functions. The experimental values from the literature were used for generating the functions [27, 97, 98]. The used experimental values for physical properties are given in Appendix 2. The density and the generated viscosity functions for air are shown in the equations (85) and (86). In

similar manner, the generated functions for water are presented in the equations (87) and (88).

$$\rho_{air} = \frac{M * P}{R * T} \tag{85}$$

$$\eta_{air} = 4.600 * 10^{-8} * T + 4.580 * 10^{-6} \tag{86}$$

Where ρ_{air} Air density, kg m^{-3}

R Ideal gas constant for dry air, 8,3144621 J kg^{-1} K^{-1}

T Temperature, K

M Molar mass, mol/kg

η_{air} Air viscosity, Pa s

$$\rho_{water} = -0.00530 * \mathrm{T}^2 + 2.90369 * \mathrm{T} + 602.49497 \tag{87}$$

$$\eta_{water} = 4.0125 * 10^{-7} * \mathrm{T}^2 - 2.6092 * 10^{-4} * \mathrm{T} + 4.3015 * 10^{-2} \tag{88}$$

Where ρ_{water} Water density, kg m^{-3}

η_{water} Water viscosity, Pa s

6.3 Results of the calculations

Pressure drops were calculated for six two-phase pressure drop methods using given superficial velocities and physical properties from the experimental data. The results were compared against the database. An AAD percentage and the percentage of the calculated values that hit into the certain error range were used for the evaluation of the methods. The AAD as an evaluation method in the pressure drop values can be misleading, since the large errors might occur at small pressure drops even though the deviations between the calculated and

experimental values are only few Pascals per cubic meter. Therefore, the small pressure drops has larger impact on the overall AAD.

The experimental dataset of Badie contained compositions of air-water and air-oil. The AADs for the calculated values are shown in Table 10. The overall AADs for air-water dataset were high. Lockhart-Martinelli was the most accurate method. It predicted 64 % of the calculated values within ± 30 % of the experimental values. The method of Bandel was also accurate, but it generally underestimated the pressure drops for the dataset of Badie.

Table 10. Comparison of the calculated values with the experimental data of Badie.

Method	**AAD**			**In ±30 % range**		
	Air-water	Air-Oil	Total	Air-Water	Air-Oil	Total
Beggs and Brill	107 %	13 %	67 %	10 %	96 %	46 %
Friedel	98 %	19 %	65 %	31 %	75 %	49 %
Müller-Steinhagen-Heck	107 %	27 %	73 %	10 %	75 %	37 %
Lockhart-Martinelli-PB	43 %	17 %	32 %	49 %	86 %	64 %
Lockhart-Martinelli-Ch	41 %	17 %	31 %	54 %	86 %	67 %
Bandel	24 %	37 %	29 %	69 %	14 %	46 %
Quiben-Thome	32 %	63 %	45 %	44 %	11 %	31 %

The dataset of Andritsos was the most versatile including different flow patterns and components. The dataset also included single phase pressure drops, which helped to validate the calculations. Almost all of the methods predicted single phase pressure drop values within 30 % from the experimental data. The comparison of the calculated values with the experimental data of Andritsos is shown in

Table 11. However, the pressure drop calculations for the experimental data of Andritsos were inaccurate. The methods of Müller-Steinhagen-Heck and Bandel gave the most accurate results. The method of Beggs and Brill predicted all of the values within 60 %. Although, the AAD for the method of Beggs and Brill was high the precision of the predicted values was small.

Table 11. The calculation results for the experimental data of Andritsos.

Method	AAD			In ±30 % range		
	Air-water	Air-glycerol	Total	Air-water	Air-glycerol	Total
Beggs and Brill	73 %	67 %	69 %	19 %	36 %	31 %
Friedel	95 %	84 %	83 %	29 %	42 %	38 %
Müller-Steinhagen-Heck	66 %	53 %	57 %	32 %	52 %	46 %
Lockhart-Martinelli-PB	104 %	132 %	108 %	39 %	30 %	33 %
Lockhart-Martinelli-Ch	102 %	130 %	106 %	42 %	33 %	36 %
Bandel	44 %	45 %	42 %	45 %	46 %	46 %
Quiben-Thome	35 %	35 %	36 %	55 %	19 %	30 %

The experimental data of Gockal included air and high viscosity oil. The viscosity ratio between liquid and gas phase was around 2800, which can be considered as very high. The high viscosity ratio caused inaccurate results for some of the pressure drop methods. The data was very narrow containing only slug flow regime with low vapor qualities. All of the details and physical properties were given, which reduced the overall deviations between the calculations and experimental values. The results for the experimental data of Gockal are shown in Table 12. The overall AAD was low. The methods of Lockhart-Martinelli and Bandel had AAD below 10 %. The method of Müller-Steinhagen and Heck was very accurate since it predicted all of the values within 30 % and 92.8 % of the values within 20 %. The methods of Beggs and Brill and Friedel showed poor accuracy. The inaccuracy of the methods was probably caused by the high viscosity ratio between the liquid and gas phases.

Table 12. Comparison of the calculated values and the experimental data of Gockal.

Method	AAD	In ±30 % range	In ±20 % range
Beggs and Brill	63.9 %	3.0 %	0.0 %
Friedel	79.6 %	0.0 %	0.0 %
Müller-Steinhagen-Heck	11.9 %	100.0 %	92.8 %
Lockhart-Martinelli-PB	8.6 %	94.6 %	88.0 %
Lockhart-Martinelli-Ch	8.5 %	94.6 %	89.2 %
Bandel	7.5 %	98.8 %	97.0 %
Quiben-Thome	31.6 %	47.9 %	25.1 %

6.4 Analysis of the results

6.4.1 **Beggs and Brill**

The method of Beggs and Brill poorly correlated with the experimental data. The method had problems with predicting the viscosity of the two-phase flow with high vapor qualities when there were almost no liquid phase present. It was caused by the friction factor correlation, which uses logarithm function for liquid hold-up. There is a correction for single-phase gas and liquid pressure drops in the method. However, the transition from two-phase flow to single phase flow is discontinues. Single-phase correction takes the place when the superficial velocity for either the gas or the liquid phase approaches zero. Large errors occurred near the transition zone. In Figure 17 is demonstrated the deviations near the transition zone for the method of Beggs and Brill with and without the single-phase correction using air-water two-phase flow. From the figure can be seen that the change in the pressure drop near the transition zone is over 40 %. The used database contained plenty of values with high vapor qualities, which made the method of Beggs and Brill inaccurate. The same results were obtained using the Aspen Plus simulator. In addition, there was a warning in Aspen and it did not recommend to use the method with superficial gas velocities below 0.05 $\frac{\mathrm{m}}{\mathrm{s}}$ and superficial liquid velocities below 0.005 $\frac{\mathrm{m}}{\mathrm{s}}$.

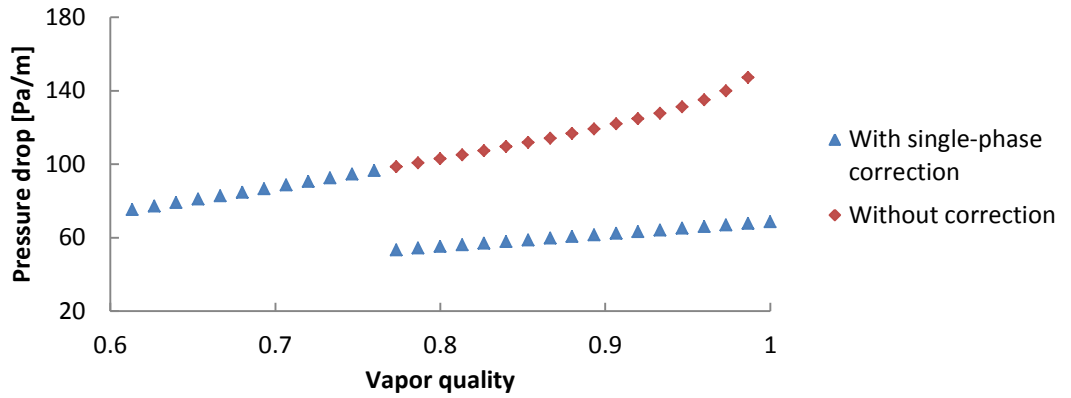

Figure 17. Pressure drop predictions of the method of Beggs and Brill with and without the single-phase correction for air-water two-phase flow in a horizontal pipe (D = 0.05 m) and massflux 20 $\frac{\text{kg}}{\text{m}^2\,\text{s}}$.

The method of Beggs and Brill predicted the air-oil data of Badie accurately with an AAD of 13 %. The experimental air-oil data of Gockal was predicted very poorly probably due to the very high viscosity of the oil, which was over ten times larger than the liquid viscosity in the experimental data of Badie. The overall AAD for the method of Beggs and Brill was high. In Figure 18 is shown the accuracy of the method.

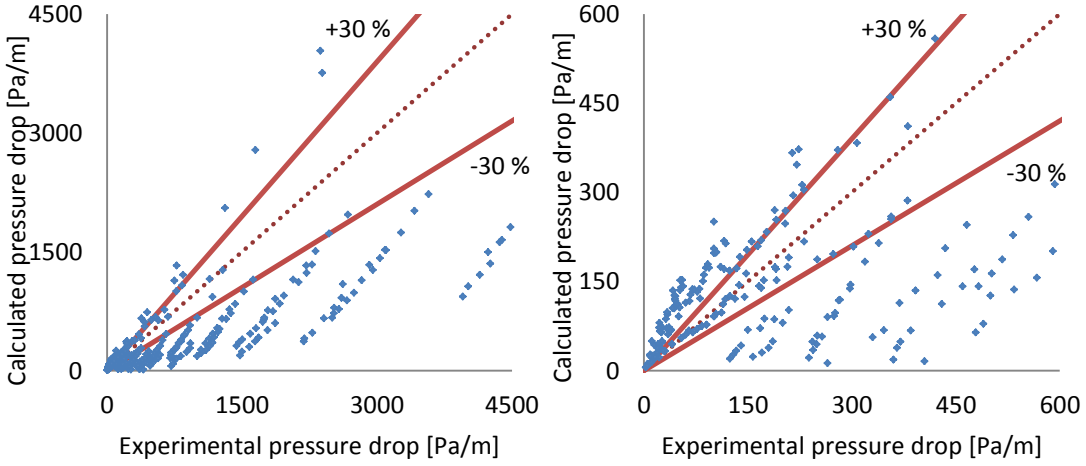

Figure 18. The calculations for the method of Beggs and Brill.

6.4.2 **Friedel**

The method of Friedel was used with the friction factor correlation of Blasius. It overestimated the low pressure drop air-water data of Badie. The method predicted the experimental data of Gockal very poorly, due to the high viscosity ratio between gas and liquid phases. The overall accuracy of the method was poor and it is shown in Figure 19.

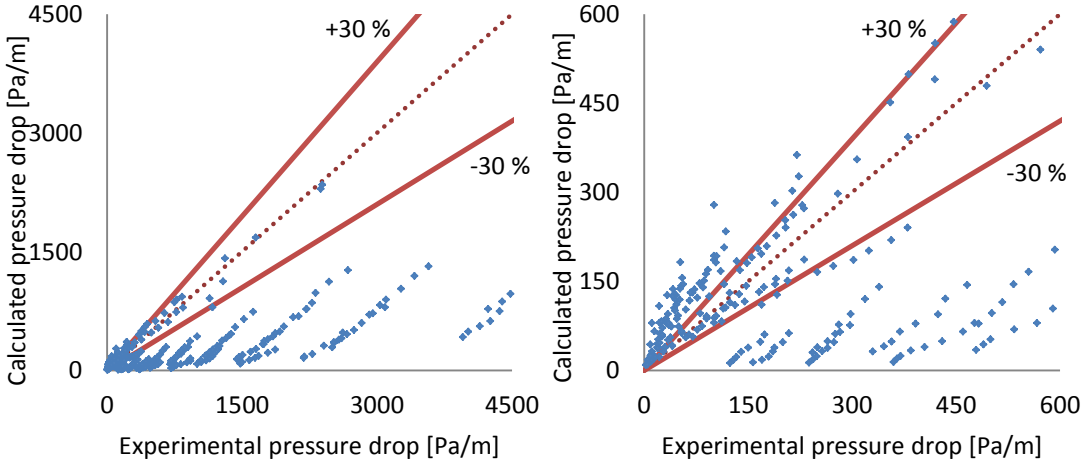

Figure 19. The calculations for the method of Friedel.

6.4.3 **Lockhart-Martinelli**

The method of Lockhart-Martinelli was used with two friction factor correlations: Poiseuille-Blasius and Churchill. There was dispersion in the results, but the overall performance of the method was good. The pipes of the experimental data were considered as smooth. Therefore, both of the friction factor correlations performed equally. However, Churchill has advantage to take into account the roughness of the pipe and it is continuous unlike Poiseuille-Blasius, where the friction factor correlation changes due to the Reynolds number. The accuracy of the method with the friction correlation of Churchill is shown in Figure 20.

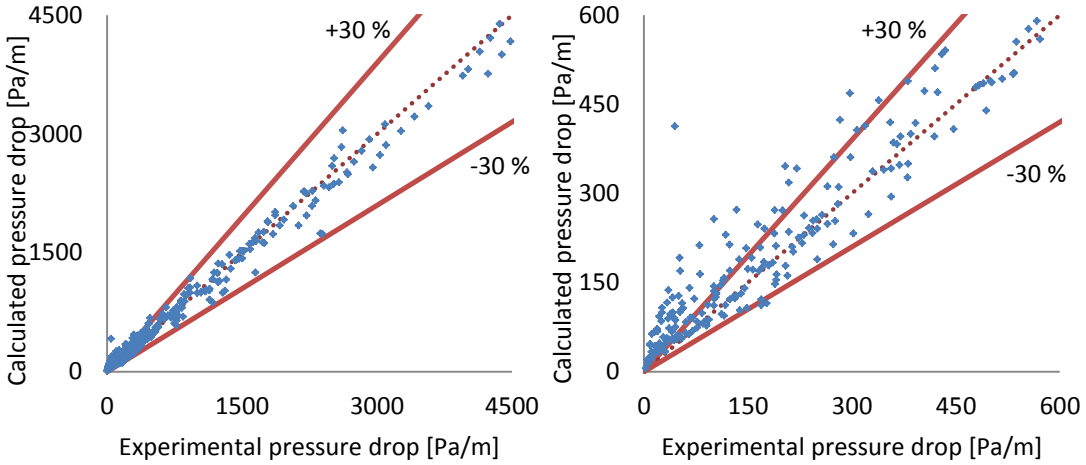

Figure 20. Calculations for the method of Lockhart-Martinelli with the friction factor correlation of Churchill.

6.4.4 **Müller-Steinhagen and Heck**

The method of Müller-Steinhagen and Heck had shown good results in the literature part. For the experimental data, it predicted the pressure drops accurately compared to the other methods. It was very good for high pressure drop air-oil data of Gockal. However, big errors occurred at small pressure drop values. The performance for the method Müller-Steinhagen and Heck is shown in Figure 21.

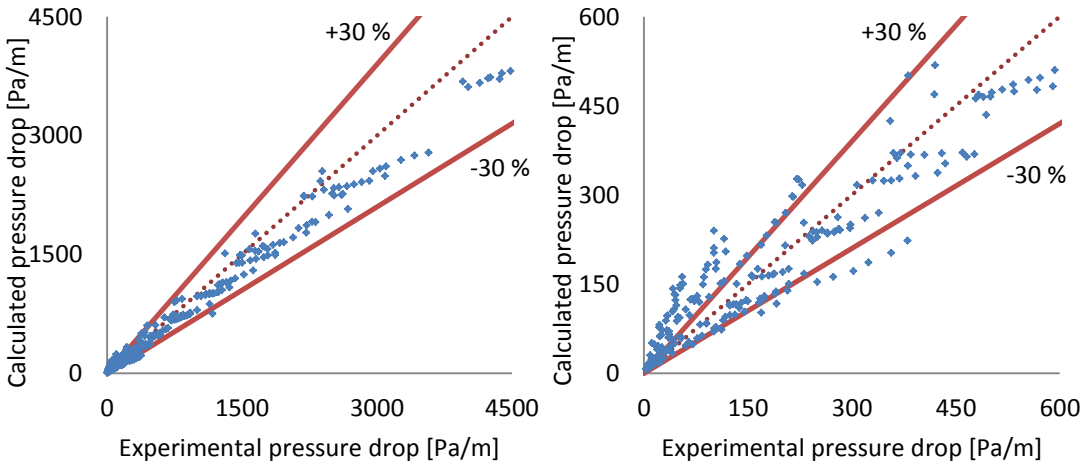

Figure 21. The pressure drop predictions for the method of Müller-Steinhagen and Heck.

6.4.5 **Bandel**

The method of Bandel recognizes three different flow regimes: annular stratified and transitional flows. Stratified flow was the most common flow regime among the calculations. The method predicted the pressure drops of the stratified flow regime accurately. The transitional flow regime was accurate for the data sets of Badie, but it did not predict the high viscosity data set of Gockal at all. Thus, there is probably a restriction for liquid-gas viscosity ratio in the transitional flow regime. The stratified flow regime predicted the pressure drops of the Gockal data most accurately, even though the data was predicted in the transitional flow regime. The annular flow regime was observed in the data set of Andritsos. The annular flow regime overestimated most of the calculated values. In addition, there was a high peak in pressure drop between stratified and annular flows. The method of Bandel was used only with stratified flow, because of the drawbacks with the two other flow regimes. In Figure 22 is shown the accuracy of the method. The method with only the stratified flow regime predicted pressure drops reasonably accurately for all of the three flow regimes. It slightly underestimated the values for other regimes, which can be seen from the figure at low pressure values. The method had the lowest AAD among all of the pressure drop methods. The overall accuracy of the method was the best with the method of Lockhart-Martinelli and Müller-Steinhagen and Heck. The scatter of the predicted values was also low.

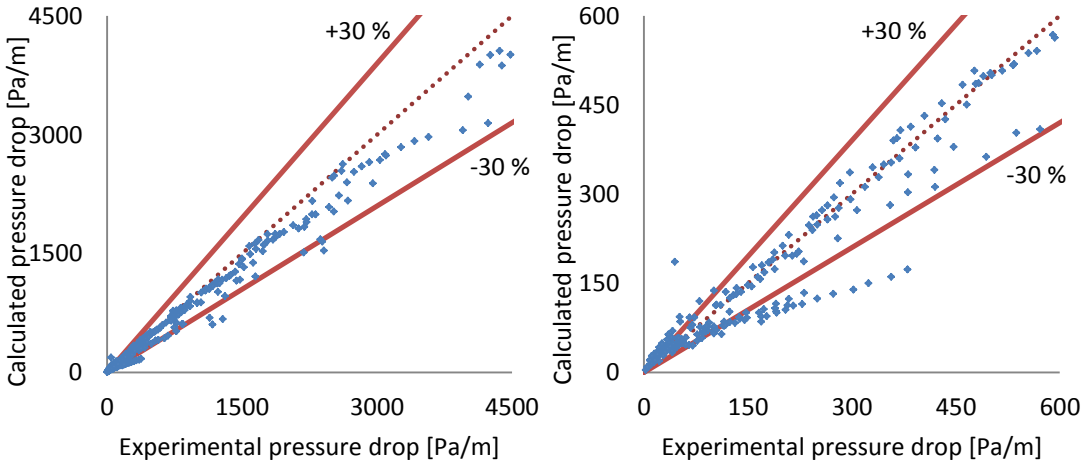

Figure 22. The pressure drop predictions for the method of Bandel.

6.4.6 **Quiben and Thome**

The method of Quiben and Thome includes the flowpattern map of Thome. The flow pattern map is designed for diabatic flows. It requires the latent heat and the heat flux for input values, which were not given in the experimental data. Therefore, the values had to be estimated. Stratified flow and slug-wavy were the most common flow regimes in the calculations. The method of Quiben and Thome did not predict the pressure drops well. It underestimated the pressure drops. Even though, the AAD for the air-water data of Badie was low, the method did not predict values well.

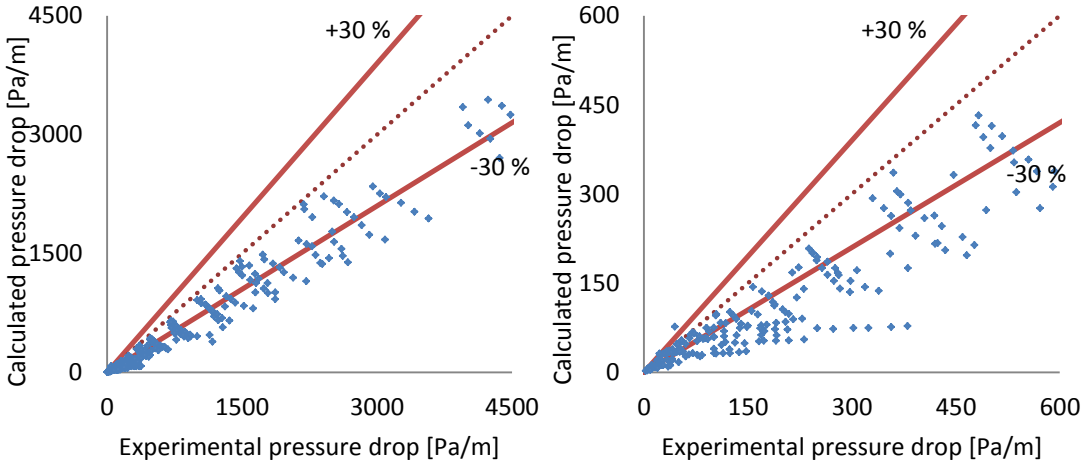

Figure 23. The pressure drop predictions for the method of Quiben and Thome.

6.5 ProsDS Implementation

The pressure drop methods of Lockhart-Martinelli, Müller-Steinhagen-Heck and Bandel were gave the most accurate results and they were chosen to be implemented into ProsDS. The selection of the pressure drop method wanted to be simple as possible. Therefore, the pressure drop methods together with friction factors can be chosen using one parameter only. The methods of Lockhart-Martinelli and Müller-Steinhagen-Heck can be used with both of the tested friction

factor correlations. The method of Bandel can be used with flow regimes or only with the stratified flow regime. The encoded methods and their variations are shown in Table 13.

Table 13. Implemented two-phase pressure drop methods.

Method	Friction factor	Details	Number
Lockhart-Martinelli	Poiseuille-Blasius	-	1
	Churhill	-	2
Müller-Steinhagen and Heck	Poiseuille-Blasius	-	3
	Churhill	-	4
Bandel	Poiseuille-Blasius	Flow regimes	5
		Stratified flow only	6

Block diagram for the method of Bandel is presented in Figure 24. In the method of Bandel, friction factor depends on the Reynolds number. The gas friction factor for annular region is calculated using vapor quality and it affects the flow pattern calculations. The flow pattern is determined using two iterations. After the first iteration, if the result meets the required criteria the flow pattern is recognized as an annular flow. The second iteration determines if the flow is stratified. If both of the iterations do not meet the required criteria, the flow is recognized as a transitional flow. Lastly, the roughness correction is applied.

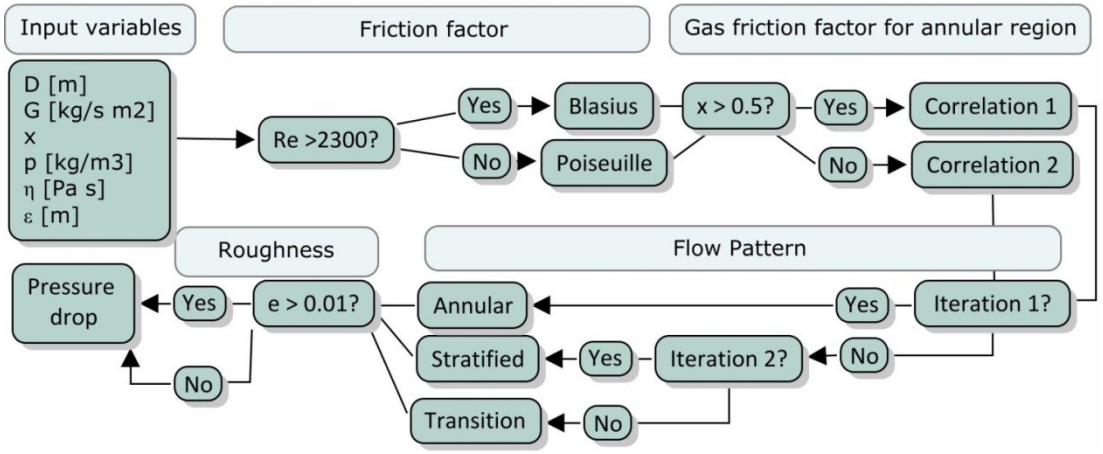

Figure 24. Block diagram for the method of Bandel.

From Figure 24 can be seen that there are three points which make the method of Bandel discontinuous: friction factor, gas friction factor for annular flow and the change in the flow regime. The discontinuity should be avoided in dynamic environment. Thus, both of the friction factor points were made smoother by calculating the average values in the change points. The flow pattern transitions may cause spikes in the pressure drop calculations.

The block diagram for the method of Lockhart-Martinelli is shown in Figure 25. From the figure can be seen that there are two discontinuity parts. The change in the friction factor correlation was made smoother similarly as in the method of Bandel. The method is Müller-Steinhagen-Heck is even simpler than the method of Lockhart-Martinelli, because it does not have the C-factor correlation. Therefore, there is less discontinuity in the method and it may be more stable in the changing dynamic environment.

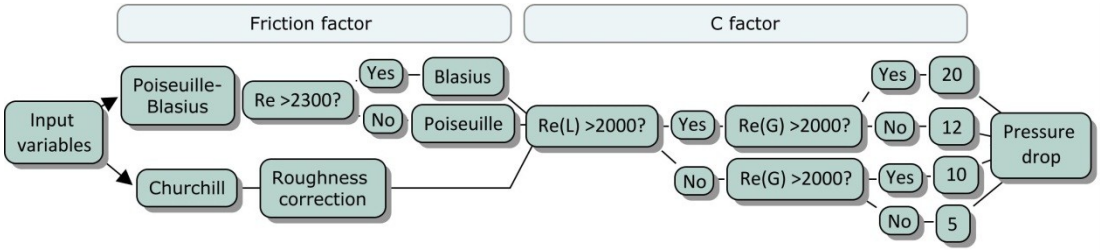

Figure 25. Block diagram for the method of Lockhart-Martinelli.

6.6 Case: Safety valve inlet piping

Three implemented two-phase pressure drop methods and the existing homogeneous two-phase model were tested by simulating a safety valve inlet piping case in ProsDS. The methods of Lockhart-Martinelli and Müller-Steinhagen-Heck were tested with both friction factor correlations: Poiseuille-Blasius (PB) and Churchill (Ch). The flow diagram of the case is presented in Figure 26. The mixture that consists of ethylene, propane and hydrogen, flows into a tank. The pressure in

the tank increases until the safety valve opens. Mixture from the tank flashes into an inlet pipe. The pressure drop in the inlet pipe is calculated using the two-phase pressure drop methods. After the pipe, the mixture flows into the safety valve. The details of the case are presented in Table 14. Slip ratio was assumed to be unity, in which case the true velocities for both phases were the same. Two different pipe diameters and roughness values were used in the case. The process was simulated for two hours.

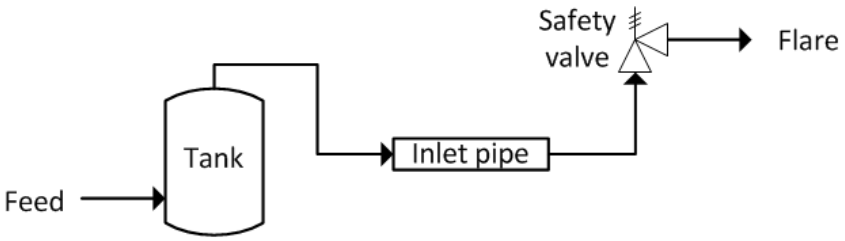

Figure 26. The flow diagram of the case.

Table 14. Details of the case.

Feed mass flow [kg/s]	160	Feed vapor fraction	0.24
Components	Ethylene Propane Hydrogen	Molar fractions	0.035 0.923 0.042
$T_{initial}$ [K]	326.7	$P_{initial}$ [kPa]	2580
ρ_L [kg/m^3]	419.0	ρ_G ρ_L [kg/m^3]	53.1
η_L [mPa s]	0.0106	η_G [mPa s]	0.002
Pipe diameter [m]	0.127, 0.152	Pipe length [m]	15
Pipe roughness [mm]	0.2, 0.001		

The simulation results for the case (D = 0.152, ϵ_r=0.2 mm) are shown in Figure 27. Results for the other configurations are shown in Appendix 3. It can be seen that the pressure drop and mass flow increased over the time. As shown in the figure, the method of Lockhart-Martinelli with the friction factor correlation of Churchill predicted significantly larger pressure drops compared to other methods. In addition, the case (D = 0.127, ϵ_r=0.2 mm) could not be simulated with the method,

because the predicted pressure drops of the inlet pipe were too high. As stated in the literature part, the pressure drop of the inlet pipe should not be greater than three percent of the set pressure of the safety valve. Even though the pressure loss in the inlet pipe was less than three percent of the set pressure of the safety valve, the safety valve calculations did not function and the predicted pressure drop started to oscillate. Other cases could be simulated using Lockhart-Martinelli with the friction factor correlation of Churchill, because the calculated pressure drops were lower.

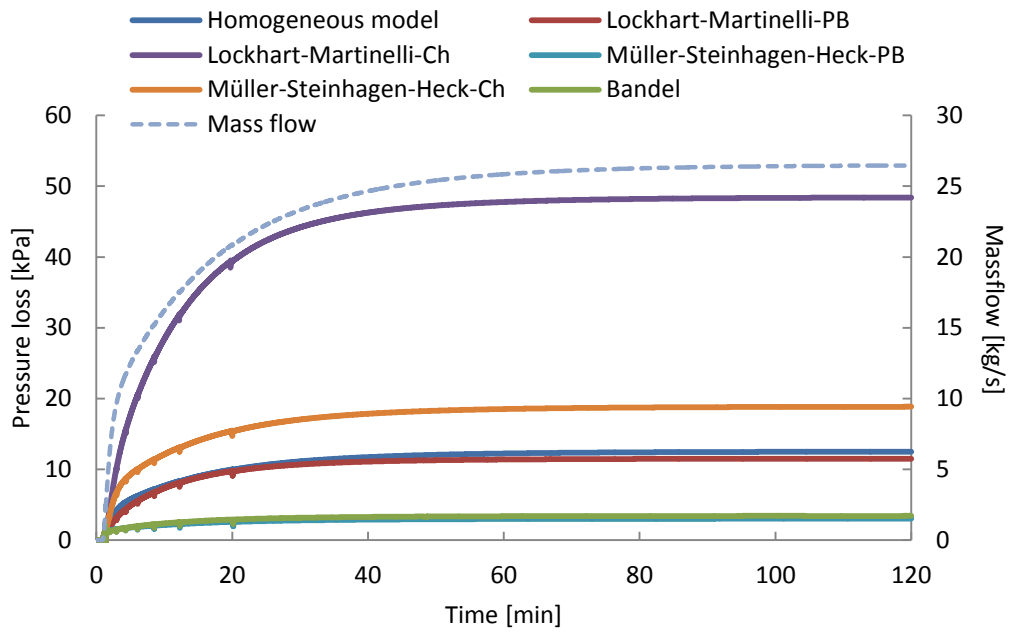

Figure 27. Simulation results for the case (D = 0.152, ϵ_r=0.2 mm).

The pressure drops had effect on the pressure of the tank. Higher pressure drop resulted in increased pressure inside the tank. The pressures of the tank for the case (D = 0.152, ϵ_r=0.2 mm) are presented in Figure 28. From Figures 27 and 28, it can be seen that differences in the pressures of the tank are equal to the calculated pressure drops.

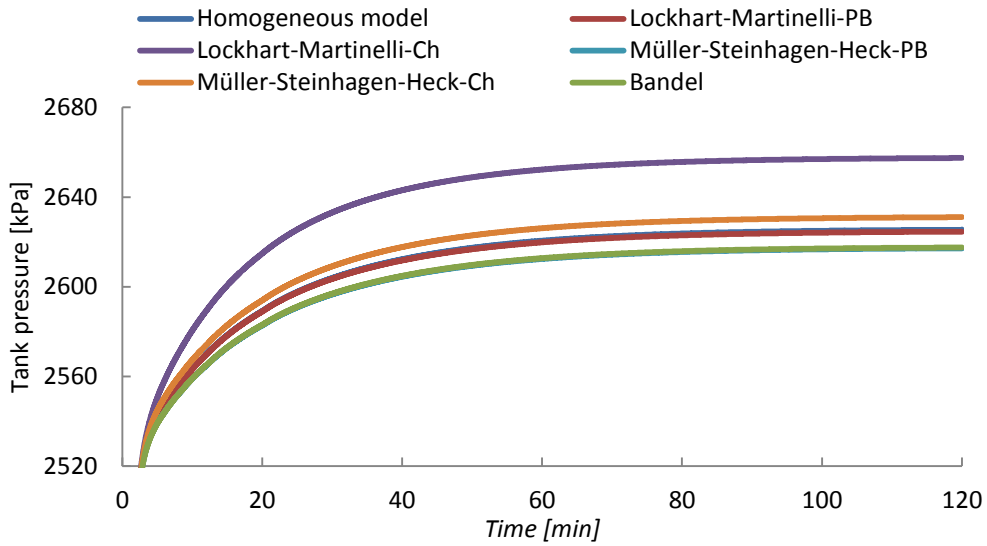

Figure 28. Pressures of the tank for the case (D = 0.152, ϵ_r=0.2 mm).

Velocities and vapor fractions in the inlet pipe for the case (D = 0.152, ϵ_r=0.2 mm) are presented in Figure 29. The velocities are lower for the methods with high pressure drops. Vapor fractions decreased with the time and they were the same for all of the methods.

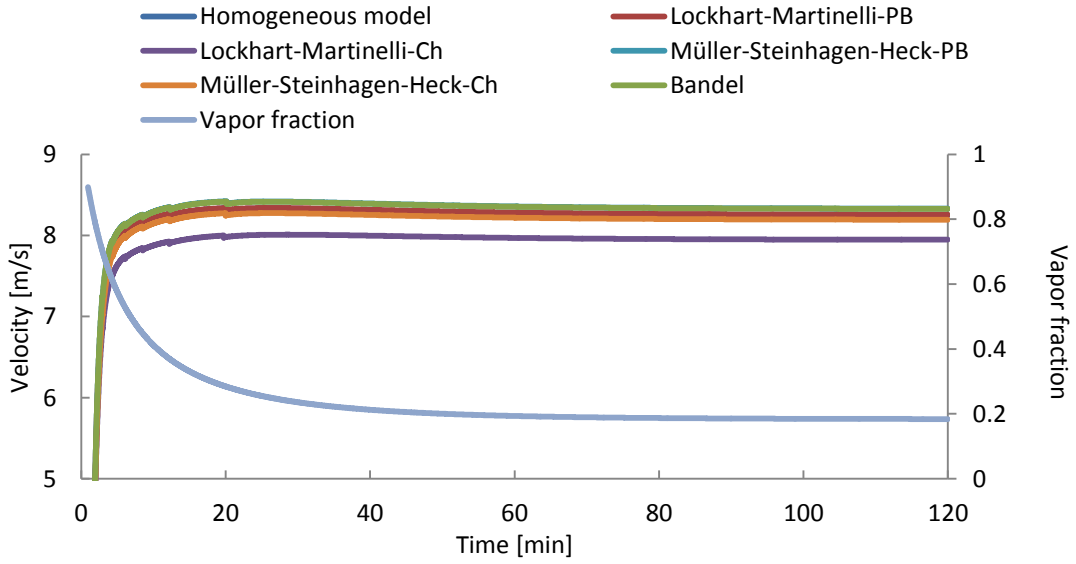

Figure 29. Velocities and vapor fractions of the inlet pipe for the case (D = 0.152, ϵ_r=0.2 mm).

The calculated pressure drops after two hour simulations are presented in Table 15. The calculated pressure drops differ from each other. The results indicate that the roughness has a large impact on the pressure drop. Friction factor correlation of Poiseuille-Blasius does not have roughness correction, which makes it invalid for rough pipes. The method of Bandel was simulated twice using flow pattern recognition and only with the stratified flow regime. The results were the same, because the flow regimes were identified as stratified flow. The method of Bandel underestimated the pressure drops for the rough pipes compared to the other methods, even though the method applies the roughness correction.

Table 15. Simulation results for the case of the relief valve inlet piping (t=2 hours).

Method	**Pressure drop [kPa]**			
D [m] ϵ_r[mm]	0.127 0.2	0.127 0.001	0.152 0.2	0.152 0.001
Homogenous model	32.3	17.1	12.5	6.7
Lockhart-Martinelli-Pb	27.2	27.2	11.5	11.5
Lockhart-Martinelli-Ch	-	65.8	48.4	48.4
Müller-Steinhagen-Heck-Pb	7.2	7.2	3.0	3.0
Müller-Steinhagen-Heck-Ch	48.2	25.7	18.8	10.1
Bandel	8.4	7.5	3.4	3.2

The method of Lockhart-Martinelli overestimated the pressure drops compared to others due to the high gas density. The effects of density on the method of Lockhart-Martinelli and others are shown in Figure 30. The calculations were made with Microsoft Excel using the values from the simulated case for smooth pipe (D = 0.152 m) with gas densities of 53 $\frac{kg}{m^3}$ and 5 $\frac{kg}{m^3}$. High gas density affected more to the pressure drop of the method of Lockhart-Martilli compared to the other methods. Method of Müller-Steinhagen and Heck with the friction correlation of Churchill performed well without having any problems. Overall, it is difficult to estimate the reliability and accuracy of the methods without experimental values.

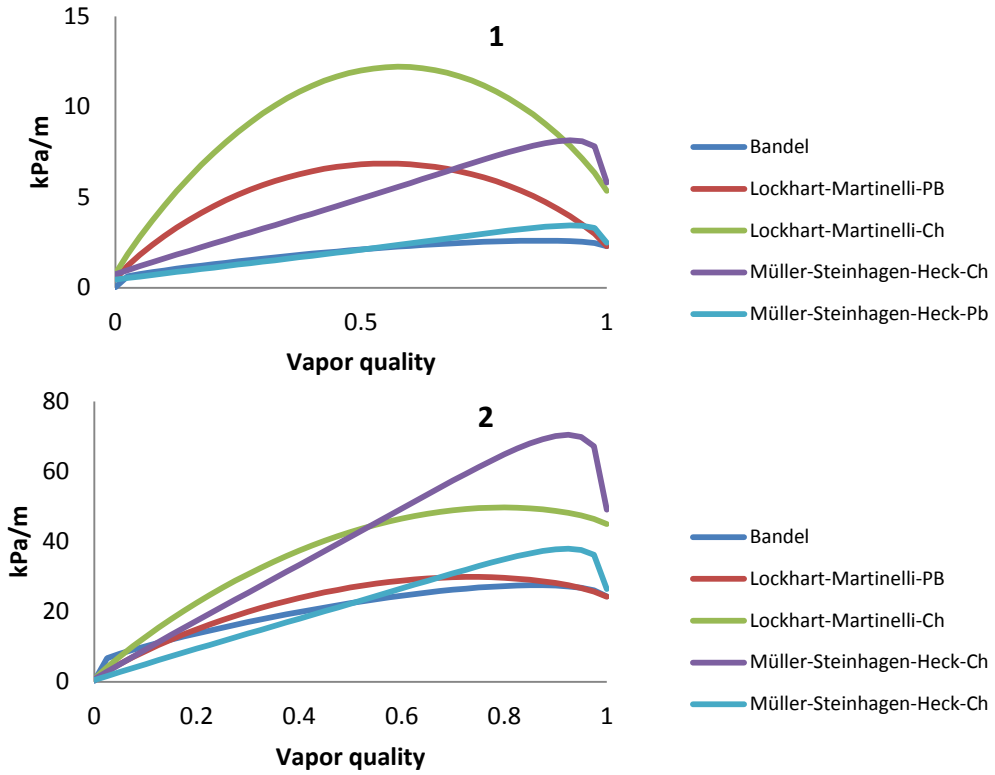

Figure 30. Effect of the density on the pressure drop methods using gas densities 1.) 53 $\frac{kg}{m^3}$ and 2.) 5 $\frac{kg}{m^3}$.

7 Further study

Viscosity can be calculated using various methods, but plenty of methods are needed. Two methods are required for both gas and liquid phases and two for their mixtures. In addition, the methods are valid only for a certain temperature range. Equation of state methods could be used for both phases and they have no temperature range limitations. They also work for mixtures. However, none of the methods discussed in this work serves as an all-around method, which would calculate the viscosity for all of the compounds. Equation of state methods should be studied more in order that they could be used to calculate viscosities for all of the compounds and be applied for a general use.

According to the applied part, most of the two-phase pressure drops can be predicted within ± 30 % using implemented methods. However, in certain situations the errors can be over 100 %. The database for the two-phase pressure drops used in this thesis was small. The largest deviations from the real values could be avoided by testing the methods using larger and more versatile database in order to see, which of the methods work best in each situation.

There are currently no two-phase pressure drop methods available, which would recognize every flow pattern and calculate the pressure drop of the two-phase flow accurately. Flow patterns and the effect of viscosity on it have a large impact on the two-phase flow and they should be involved in two-phase flow calculations. Therefore, further studies are required for developing new two-phase pressure drop methods, which would include flow pattern recognition.

8 Conclusions

The literature part was divided into two sections. First, the viscosity methods for both gas and liquid phases were reviewed. In addition, viscosity methods for different oil types were studied. Viscosity methods for pure compounds and non-polar mixtures can be predicted accurately. However, viscosities are difficult to predict for polar mixtures without knowing the interaction parameters for each substance. Viscosity methods for crude oils are often specified only for certain crude oil types making them impractical for a general use.

The second part focused on the gas-liquid two-phase flow. Two-phase pressure drop methods for horizontal pipes were reviewed and the effect of viscosity on the two-phase flow was studied. Two-phase pressure drops and flow patterns are difficult to predict. Less than thirty percent errors in the pressure drops are considered accurate.

The applied part was also divided into two sections. Firstly, the most practical and the best-performing viscosity methods from FLOWBAT according to the literature part were integrated into ProsDS. The methods were tested using the experimental data presented in the literature. The integrated viscosity methods are accurate for pure compounds and non-polar mixtures at different pressures.

Various two-phase pressure drop methods were compared in the second section of the applied part. Experimental data from the literature was used as reference values for the testing. The data consisted of gas-liquid mixtures with different viscosities. The methods of Bandel, Lockhart-Martilli and Müller-Steinhagen-Heck gave the most accurate results and they were encoded into ProsDS. The methods were tested with the existing homogeneous model in a safety valve inlet piping case. The results of the case differed significantly from each other. Thus, it is difficult to predict two-phase pressure drop reliably.

References

1. VISWANATH, D.S.Springer, 2007 *Viscosity of Liquids: Theory, Estimation, Experiment, and Data*, pp. 107-443.

2. ELSHARKAWY, A.M., HASSAN, S.A., HASHIM, Y.S.K. and FAHIM, M.A. New Compositional Models for Calculating the Viscosity of Crude Oils*. Industrial & Engineering Chemistry Research*, 08/01; 2013/08, 2003, vol. 42, no. 17. pp. 4132-4142 ISSN 0888-5885.

3. SMITH, D., BURGESS, J. and POWERS, C. Relief Device Inlet Piping: Beyond the 3 Percent Rule: With Careful Consideration, an Engineer can be Certain that an Installation Will Not Chatter*. Hydrocarbon Processing*, 2011, vol. 90, no. 11.

4. MATSUBARA, H. and NAITO, K. Effect of Liquid Viscosity on Flow Patterns of Gas–liquid Two-Phase Flow in a Horizontal Pipe*. International Journal of Multiphase Flow*, 12, 2011, vol. 37, no. 10. pp. 1277-1281 ISSN 0301-9322.

5. BRENNEN, C.E. *Fundamentals of Multiphase Flow.* Cambridge University Press, 2005.

6. BIRD, R.B., STEWART, W.E. and LIGHTFOOT, E.N.Wiley. com, 2007 *Transport Phenomena*, pp. 23-29.

7. POLING, B.E., PRAUSNITZ, J.M., JOHN PAUL, O. and REID, R.C.McGraw-Hill New York, 2001 *The Properties of Gases and Liquids*, pp. 9.1-9.2.

8. HIRSCHFELDER, J.O., BIRD, R.B. and CURTISS, C.F. *Molecular Theory of Gases and Liquids.* Chapman & Hall, 1954.

9. REID, R.C., PRAUSNITZ, J.M. and POLING, B.E. The Properties of Gases and Liquids, 1987.

10. NEUFELD, P.D., JANZEN, A. and AZIZ, R. Empirical Equations to Calculate 16 of the Transport Collision Integrals Ω for the Lennard-Jones (12–6) Potential*. The Journal of Chemical Physics*, 1972, vol. 57. pp. 1100.

11. KIM, S.K. and ROSS, J. On the Determination of Potential Parameters from Transport Coefficients*. The Journal of Chemical Physics*, 1967, vol. 46, no. 2. pp. 818-818.

12. MONNERY, W.D., SVRCEK, W.Y. and MEHROTRA, A.K. Viscosity: A Critical Review of Practical Predictive and Correlative Methods*. The Canadian Journal of Chemical Engineering*, 1995, vol. 73, no. 1. pp. 3-40.

13. CHUNG, T.H., LEE, L.L. and STARLING, K.E. Applications of Kinetic Gas Theories and Multiparameter Correlation for Prediction of Dilute Gas Viscosity and Thermal Conductivity. *Industrial & Engineering Chemistry Fundamentals*, 1984, vol. 23, no. 1. pp. 8-13.

14. CHUNG, T.H., AJLAN, M., LEE, L.L. and STARLING, K.E. Generalized Multiparameter Correlation for Nonpolar and Polar Fluid Transport Properties. *Industrial & Engineering Chemistry Research*, 1988, vol. 27, no. 4. pp. 671-679.

15. STIEL, L.I. and THODOS, G. The Viscosity of Nonpolar Gases at Normal Pressures. *AIChE Journal*, 1961, vol. 7, no. 4. pp. 611-615.

16. YOONM, P. and THODOS, G. Viscosity of Nonpolar Gaseous Mixtures at Normal Pressures. *AIChE Journal*, 1970, vol. 16, no. 2. pp. 300-304.

17. American Petroleum Institute. *API Technical Data Book 8th Edition.* New York: , 2006.

18. BROKAW, R.S. Predicting Transport Properties of Dilute Gases. *Industrial & Engineering Chemistry Process Design and Development*, 1969, vol. 8, no. 2. pp. 240-253.

19. WILKE, C. A Viscosity Equation for Gas Mixtures. *The Journal of Chemical Physics*, 1950, vol. 18. pp. 517.

20. HERNING, F. and ZIPPERER, L. Calculation of the Viscosity of Technical Gas Mixtures from the Viscosity of the Individual Gases. *Gas U.Wasserfach*, 1936, vol. 79. pp. 69-73.

21. RIAZI, M.R. *Characterization and Properties of Petroleum Fractions: (MNL 50).* ASTM International ISBN 978-0-8031-3361-7.

22. REICHENBERG, D. The Indeterminacy of the Values of Potential Parameters as Derived from Transport and Virial Coefficients. *AIChE Journal*, 1973, vol. 19, no. 4. pp. 854-856.

23. MEHROTRA, A.K., MONNERY, W.D. and SVRCEK, W.Y. A Review of Practical Calculation Methods for the Viscosity of Liquid Hydrocarbons and their Mixtures. *Fluid Phase Equilibria*, 1996, vol. 117, no. 1. pp. 344-355.

24. SHERWOOD, T.K., REID, R.C. and PRAUSNITZ, J. The Properties of Gases and Liquids. *Ref*, 1977, vol. 17. pp. 1-10.

25. JOSSI, J.A., STIEL, L.I. and THODOS, G. The Viscosity of Pure Substances in the Dense Gaseous and Liquid Phases. *AIChE Journal*, 1962, vol. 8, no. 1. pp. 59-63.

26. KNAPSTAD, B., SKJOELSVIK, P.A. and OEYE, H.A. Viscosity of Pure Hydrocarbons. *Journal of Chemical and Engineering Data*, 1989, vol. 34, no. 1. pp. 37-43.

27. SENGERS, J. and WATSON, J.T.R. *Improved International Formulations for the Viscosity and Thermal Conductivity of Water Substance.* American Chemical Society and the American Institute of Physics for the National Bureau of Standards, 1986.

28. KIRKWOOD, J.G. and BUFF, F.P. The Statistical Mechanical Theory of Surface Tension. *The Journal of Chemical Physics*, 1949, vol. 17. pp. 338.

29. ELY, J. Prediction of Dense Fluid Viscosities in Hydrocarbon Mixtures. *GPA Proc.of 61st Ann.Conv*, 1982. pp. 9-17.

30. HWANG, M.J. and WHITING, W.B. A Corresponding-States Treatment for the Viscosity of Polar Fluids. *Industrial & Engineering Chemistry Research*, 1987, vol. 26, no. 9. pp. 1758-1766.

31. LETSOU, A. and STIEL, L.I. Viscosity of Saturated Nonpolar Liquids at Elevated Pressures. *AIChE Journal*, 1973, vol. 19, no. 2. pp. 409-411.

32. TEJA, A. and RICE, P. Generalized Corresponding States Method for the Viscosities of Liquid Mixtures. *Industrial & Engineering Chemistry Fundamentals*, 1981, vol. 20, no. 1. pp. 77-81.

33. OKESON, K.J. and ROWLEY, R.L. A Four-Parameter Corresponding-States Method for Prediction of Newtonian, Pure-Component Viscosity. *International Journal of Thermophysics*, 01/01, 1991, vol. 12, no. 1. pp. 119-136 ISSN 0195-928X.

34. EYRING, H. Viscosity, Plasticity, and Diffusion as Examples of Absolute Reaction Rates. *The Journal of Chemical Physics*, 1936, vol. 4. pp. 283.

35. PRZEDZIECKI, J. and SRIDHAR, T. Prediction of Liquid Viscosities. *AIChE Journal*, 1985, vol. 31, no. 2. pp. 333-335.

36. ORBEY, H. and SANDLER, S.I. The Prediction of the Viscosity of Liquid Hydrocarbons and their Mixtures as a Function of Temperature and Pressure. *The Canadian Journal of Chemical Engineering*, 1993, vol. 71, no. 3. pp. 437-446 ISSN 1939-019X.

37. SASTRI, S. and RAO, K. A New Group Contribution Method for Predicting Viscosity of Organic Liquids. *The Chemical Engineering Journal*, 1992, vol. 50, no. 1. pp. 9-25.

38. MEHROTRA, A.K. Generalized One-Parameter Viscosity Equation for Light and Medium Liquid Hydrocarbons. *Industrial & Engineering Chemistry Research*, 1991, vol. 30, no. 6. pp. 1367-1372.

39. LAWAL, A. *Prediction of Vapor and Liquid Viscosities from the Lawal-Lake-Silberberg Equation of State.* , 1986.

40. HECKENBERGER, T. and STEPHAN, K. Cubic Equations of State for Transport Properties. *International Journal of Thermophysics*, 1991, vol. 12, no. 2. pp. 333-356.

41. QUIÑONES-CISNEROS, S.E., ZÉBERG-MIKKELSEN, C.K. and STENBY, E.H. The Friction Theory (F-Theory) for Viscosity Modeling. *Fluid Phase Equilibria*, 3/28, 2000, vol. 169, no. 2. pp. 249-276 ISSN 0378-3812.

42. QUIÑONES-CISNEROS, S.E., ZÉBERG-MIKKELSEN, C.K. and STENBY, E.H. One Parameter Friction Theory Models for Viscosity. *Fluid Phase Equilibria*, 3/1, 2001, vol. 178, no. 1–2. pp. 1-16 ISSN 0378-3812.

43. IRVING, J. *Viscosities of Binary Liquid Mixtures: The Effectiveness of Mixture Equations.* National Engineering Laboratory, 1977.

44. CAO, W., KNUDSEN, K., FREDENSLUND, A. and RASMUSSEN, P. Simultaneous Correlation of Viscosity and Vapor-Liquid Equilibrium Data. *Industrial & Engineering Chemistry Research*, 1993a, vol. 32, no. 9. pp. 2077-2087.

45. CAO, W., KNUDSEN, K., FREDENSLUND, A. and RASMUSSEN, P. Group-Contribution Viscosity Predictions of Liquid Mixtures using UNIFAC-VLE Parameters. *Industrial & Engineering Chemistry Research*, 1993b, vol. 32, no. 9. pp. 2088-2092.

46. AHMED, T. *Reservoir Engineering Handbook (4th Edition).* Elsevier ISBN 978-1-85617-803-7.

47. HEMMATI-SARAPARDEH, A., KHISHVAND, M., NASERI, A. and MOHAMMADI, A.H. Toward Reservoir Oil Viscosity Correlation. *Chemical Engineering Science*, 3/7, 2013, vol. 90, no. 0. pp. 53-68 ISSN 0009-2509.

48. BEGGS, H.D. and ROBINSON, J. Estimating the Viscosity of Crude Oil Systems. *Journal of Petroleum Technology*, 1975, vol. 27, no. 9. pp. 1140-1141.

49. BEAL, C. The Viscosity of Air, Water, Natural Gas, Crude Oil and its Associated Gases at Oil Field Temperatures and Pressures. *TP*, 1946, vol. 2018. pp. 94-115.

50. GLASO, O. Generalized Pressure-Volume-Temperature Correlations. *Journal of Petroleum Technology*, 1980, vol. 32, no. 5. pp. 785-795.

51. LABEDI, R. Improved Correlations for Predicting the Viscosity of Light Crudes. *Journal of Petroleum Science and Engineering*, 1992, vol. 8, no. 3. pp. 221-234.

52. EDREDER, E.A. and RAHUMA, K.M. TESTING THE PERFORMANCE OF SOME DEAD OIL VISCOSITY CORRELATIONS. *Petroleum & Coal*, 2012, vol. 54, no. 4. pp. 397-402.

53. MCCAIN, W.D., Jr. *Properties of Petroleum Fluids (2nd Edition).* PennWell ISBN 978-0-87814-335-1.

54. DUTT, N.V.K. A Simple Method of Estimating the Viscosity of Petroleum Crude Oil and Fractions*. The Chemical Engineering Journal*, 12, 1990, vol. 45, no. 2. pp. 83-86 ISSN 0300-9467.

55. ELSHARKAWY, A.M. and ALIKHAN, A.A. Models for Predicting the Viscosity of Middle East Crude Oils*. Fuel*, 6, 1999a, vol. 78, no. 8. pp. 891-903 ISSN 0016-2361.

56. ELSHARKAWY, A.M. and ALIKHAN, A.A. Models for Predicting the Viscosity of Middle East Crude Oils*. Fuel*, 6, 1999b, vol. 78, no. 8. pp. 891-903 ISSN 0016-2361.

57. BALTATU, M.E. Prediction of the Liquid Viscosity for Petroleum Fractions*. Industrial & Engineering Chemistry Process Design and Development*, 01/01; 2013/08, 1982, vol. 21, no. 1. pp. 192-195 ISSN 0196-4305.

58. PEDERSEN, K.S., FREDENSLUND, A., CHRISTENSEN, P.L. and THOMASSEN, P. Viscosity of Crude Oils*. Chemical Engineering Science*, 1984, vol. 39, no. 6. pp. 1011-1016 ISSN 0009-2509.

59. PEDERSEN, K.S. and FREDENSLUND, A. An Improved Corresponding States Model for the Prediction of Oil and Gas Viscosities and Thermal Conductivities*. Chemical Engineering Science*, 1987, vol. 42, no. 1. pp. 182-186 ISSN 0009-2509.

60. AASBERG-PETERSEN, K., KNUDSEN, K. and FREDENSLUND, A. Prediction of Viscosities of Hydrocarbon Mixtures*. Fluid Phase Equilibria*, 12/30, 1991, vol. 70, no. 2–3. pp. 293-308 ISSN 0378-3812.

61. GUO, X.-., WANG, L.-., RONG, S.-. and GUO, T.-. Viscosity Model Based on Equations of State for Hydrocarbon Liquids and Gases*. Fluid Phase Equilibria*, 12, 1997, vol. 139, no. 1–2. pp. 405-421 ISSN 0378-3812.

62. QUIBÉN, J.M. Experimental and Analytical Study of Two-Phase Pressure Drops during Evaporation in Horizontal Tubes*. Swiss Federal Institute of Technology, Lausanne, Switzerland*, 2005.

63. MANNAN, S. *Lees' Loss Prevention in the Process Industries, Volumes 1-3 - Hazard Identification, Assessment and Control (4th Edition).* Elsevier ISBN 978-0-12-397189-0.

64. THOME, J.R. Engineering Data Book III*. Wolverine Tube Inc*, 2004.

65. BRATLAND, O. Pipe Flow 2: Multi-Phase Flow Assurance*. Ove Bratland*, 2010.

66. CHENG, L., RIBATSKI, G. and THOME, J.R. Two-Phase Flow Patterns and Flow-Pattern Maps: Fundamentals and Applications. *Applied Mechanics Reviews*, 2008, vol. 61, no. 1-6. pp. 0508021-05080228 SCOPUS.

67. BAKER, O. *Design of Pipelines for the Simultaneous Flow of Oil and Gas.* , 1953.

68. ROUHANI, S.Z. and SOHAL, M.S. Two-Phase Flow Patterns: A Review of Research Results. *Progress in Nuclear Energy*, 1983, vol. 11, no. 3. pp. 219-259 ISSN 0149-1970.

69. MANDHANE, J., GREGORY, G. and AZIZ, K. A Flow Pattern Map for Gas—liquid Flow in Horizontal Pipes. *International Journal of Multiphase Flow*, 1974, vol. 1, no. 4. pp. 537-553.

70. TAITEL, Y., BORNEA, D. and DUKLER, A. Modelling Flow Pattern Transitions for Steady Upward Gas-liquid Flow in Vertical Tubes. *AIChE Journal*, 1980, vol. 26, no. 3. pp. 345-354.

71. KATTAN, N., THOME, J. and FAVRAT, D. Flow Boiling in Horizontal Tubes: Part 1: Development of a Diabatic Two-Phase Flow Pattern Map. *Journal of Heat Transfer*, 1998, vol. 120, no. 1. pp. 140-147.

72. THOME, J.R. and HAJAL, J.E. Two-Phase Flow Pattern Map for Evaporation in Horizontal Tubes: Latest Version. *Heat Transfer Engineering*, 2003, vol. 24, no. 6. pp. 3-10.

73. WOJTAN, L., URSENBACHER, T. and THOME, J.R. Investigation of Flow Boiling in Horizontal Tubes: Part I—A New Diabatic Two-Phase Flow Pattern Map. *International Journal of Heat and Mass Transfer*, 2005, vol. 48, no. 14. pp. 2955-2969.

74. HEWITT, G.F. and ROBERTS, D. Studies of Two-Phase Flow Patterns by Simultaneous X-Ray and Flash Photography, 1969.

75. MORENO QUIBÉN, J. and THOME, J.R. Flow Pattern Based Two-Phase Frictional Pressure Drop Model for Horizontal Tubes, Part II: New Phenomenological Model. *International Journal of Heat and Fluid Flow*, 10, 2007, vol. 28, no. 5. pp. 1060-1072 ISSN 0142-727X.

76. LOCKHART, R. and MARTINELLI, R. Proposed Correlation of Data for Isothermal Two-Phase, Two-Component Flow in Pipes. *Chem.Eng.Prog*, 1949, vol. 45, no. 1. pp. 39-48.

77. WHALLEY, P. Multiphase Flow and Pressure Drop. *Heat Exchanger Design Handbook*, 1980, vol. 2. pp. 2.3.

78. FRIEDEL, L. *Improved Friction Pressure Drop Correlations for Horizontal and Vertical Two-Phase Pipe Flow.* , 1979.

79. MÜLLER-STEINHAGEN, H. and HECK, K. A Simple Friction Pressure Drop Correlation for Two-Phase Flow in Pipes*. Chemical Engineering and Processing: Process Intensification*, 1986, vol. 20, no. 6. pp. 297-308.

80. BEGGS, D.H. and BRILL, J.P. A Study of Two-Phase Flow in Inclined Pipes*. Journal of Petroleum Technology*, 1973, vol. 25, no. 5. pp. 607-617.

81. BANDEL, J. *Druckverlust Und Wärmeübergang Bei Der Verdampfung Siedender Kältemittel Im Druchströmten Waagerechten Rohr*, 1973.

82. da Silva Lima, Ricardo J, et al. Ammonia Two-Phase Flow in a Horizontal Smooth Tube: Flow Pattern Observations, Diabatic and Adiabatic Frictional Pressure Drops and Assessment of Prediction Methods*. International Journal of Heat and Mass Transfer*, 2009, vol. 52, no. 9. pp. 2273-2288.

83. SHANNAK, B.A. Frictional Pressure Drop of Gas Liquid Two-Phase Flow in Pipes*. Nuclear Engineering and Design*, 12, 2008, vol. 238, no. 12. pp. 3277-3284 ISSN 0029-5493.

84. OULD DIDI, M.B., KATTAN, N. and THOME, J.R. Prediction of Two-Phase Pressure Gradients of Refrigerants in Horizontal Tubes. *International Journal of Refrigeration*, 11, 2002, vol. 25, no. 7. pp. 935-947 ISSN 0140-7007.

85. WEISMAN, J., DUNCAN, D., GIBSON, J. and CRAWFORD, T. Effects of Fluid Properties and Pipe Diameter on Two-Phase Flow Patterns in Horizontal Lines*. International Journal of Multiphase Flow*, 1979, vol. 5, no. 6. pp. 437-462.

86. FOLETTI, C., et al. Experimental Investigation on Two-Phase Air/High-Viscosity-Oil Flow in a Horizontal Pipe*. Chemical Engineering Science*, 12/1, 2011, vol. 66, no. 23. pp. 5968-5975 ISSN 0009-2509.

87. ZHAO, Y., et al. High Viscosity Effects on Characteristics of Oil and Gas Two-Phase Flow in Horizontal Pipes*. Chemical Engineering Science*, 5/24, 2013, vol. 95, no. 0. pp. 343-352 ISSN 0009-2509.

88. SZALINSKI, L., et al. Comparative Study of Gas–oil and Gas–water Two-Phase Flow in a Vertical Pipe*. Chemical Engineering Science*, 6/15, 2010, vol. 65, no. 12. pp. 3836-3848 ISSN 0009-2509.

89. DA HLAING, N., SIRIVAT, A., SIEMANOND, K. and WILKES, J.O. Vertical Two-Phase Flow Regimes and Pressure Gradients: Effect of Viscosity*. Experimental Thermal and Fluid Science*, 5, 2007, vol. 31, no. 6. pp. 567-577 ISSN 0894-1777.

90. VOGEL, E., KUECHENMEISTER, C., BICH, E. and LAESECKE, A. Reference Correlation of the Viscosity of Propane. *Journal of Physical and Chemical Reference Data*, 1998, vol. 27. pp. 947-970.

91. GIDDINGS, J.G., KAO, J.T. and KOBAYASHI, R. Development of a High-Pressure Capillary-Tube Viscometer and its Application to Methane, Propane, and their Mixtures in the Gaseous and Liquid Regions*. The Journal of Chemical Physics*, 1966, vol. 45. pp. 578.

92. BARRUFET, M.A., HALL, K.R., ESTRADA-BALTAZAR, A. and IGLESIAS-SILVA, G.A. Liquid Viscosity of Octane and Pentane Octane Mixtures from 298.15 K to 373.15 K Up to 25 MPa*. Journal of Chemical & Engineering Data*, 1999, vol. 44, no. 6. pp. 1310-1314.

93. IGLESIAS-SILVA, G.A., ESTRADA-BALTAZAR, A., HALL, K.R. and BARRUFET, M.A. Experimental Liquid Viscosity of Pentane Octane Decane Mixtures from 298.15 to 373.15 K Up to 25 MPa*. Journal of Chemical & Engineering Data*, 1999, vol. 44, no. 6. pp. 1304-1309.

94. BADIE, S., HALE, C.P., LAWRENCE, C.J. and HEWITT, G.F. Pressure Gradient and Holdup in Horizontal Two-Phase Gas–liquid Flows with Low Liquid Loading. *International Journal of Multiphase Flow*, 9/1, 2000, vol. 26, no. 9. pp. 1525-1543 ISSN 0301-9322.

95. ANDRITSOS, N. *EFFECT OF PIPE DIAMETER AND LIQUID VISCOSITY ON HORIZONTAL STRATIFIED FLOW (TWO-PHASE, WAVE GENERATION).* Ph.D. ed. United States -- Illinois: University of Illinois at Urbana-Champaign, 1986 ProQuest Dissertations & Theses Full Text.

96. GOKCAL, B. *An Experimental and Theoretical Investigation of Slug Flow for High Oil Viscosity in Horizontal Pipes.* , 2008.

97. STEPHAN, K. and LUCAS, K. *Viscosity of Dense Fluids.* Plenum Press New York, 1979.

98. HAAR, L., GALLAGHER, J.S. and KELL, G.S. *NBS-NRC Steam Tables: Thermodynamics Ans Transport Properties and Computer Programs for Vapor and Liquid States of Water in SI Units.* Taylor & Francis, 1984.

APPENDIX 1: Two-phase pressure drop method of Bandel

$$A = \frac{d^2\pi}{4}$$

$$Re_G = \frac{Gxd}{\eta_G};\ Re_L = \frac{G(1-x)D}{\eta_L}$$

$$f_G = \frac{0.3164}{\mathrm{Re_G}};\ f_L = \frac{0.3164}{\mathrm{Re_L}}$$

$$\Delta p_G = \frac{f_G x^2 G^2}{2D\rho_G};\ \Delta p_L = \frac{f_G (1-x)^2 G^2}{2D\rho_G}$$

$$f_{G,Ann} = 0.15\left(\frac{1-\mathrm{x}}{x}\right)^{0.5}\left(\frac{\eta_L}{\eta_G}\right)^{0.3} \quad if\ x \le 0.5$$

$$f_{L,Ann} = -0.31x^{0.1}$$

$$f_{G,Ann} = 0.16\left(\frac{1-\mathrm{x}}{x}\right)^{0.1}\left(\frac{\eta_L}{\eta_G}\right)^{0.3} \quad if\ x > 0.5$$

$$\Delta p_{Ann,min} = \frac{g\rho_L}{15\left(\frac{\eta_L}{\eta_G}\right)^{0.2}}$$

$$\Delta p_{Stra,max} = \frac{g\rho_L}{10x^{0.3}}$$

Annular flow iteration

$$V1_{Ann} = \frac{\Delta p_G}{\Delta p_L} * \frac{0.3164 + f_{G,Ann}}{0.3164 + f_{L,Ann}}$$

Initial values for iteration:

$$\varphi = \frac{1}{500} - \frac{1}{10};\quad B = \frac{1}{10}$$

$Start$: $\varphi = \varphi + B$

$$D_{G,Ann} = (1-\varphi)D; \quad D_{L,ann} = D - D_{G,Ann}$$

$$A_{G,Ann} = \frac{D_{G,Ann}^2 \pi}{4}; \quad A_{L,Ann} = A - A_{G,Ann}$$

$$IF \quad \frac{D_{L,ann}}{D} > 0.999 \rightarrow I$$

$$V2_{Ann} = \left(\frac{D_{G,Ann}}{D_{L,Ann}}\right)^{1.25} \left(\frac{A_{G,Ann}}{A_{L,Ann}}\right)^{1.75}$$

$$IF \quad \frac{V2_{Ann} - V1_{Ann}}{V1_{Ann}} \leq \frac{1}{100} \rightarrow End$$

$$IF \quad V2_{Ann} = V1_{Ann} \rightarrow End$$

$$IF \quad V2_{Ann} > V1_{Ann} \rightarrow Start$$

$$IF \quad V2_{Ann} < V1_{Ann} \rightarrow \ \varphi = \varphi - B; B = \frac{B}{2} \rightarrow Start$$

End:

$$CF_{Ann} = \left[1 + \left(\frac{f_{G,Ann}}{0.3164}\right)\left(\frac{D}{D_{G,Ann}}\right)^{1.25}\right]\left(\frac{A}{A_{G,Ann}}\right)^{1.75}$$

$$DP_{Ann} = \ \Delta p_G * CF_{Ann}$$

$$IF \quad DP_{Ann} \geq \Delta p_{G,Ann} \rightarrow \ \Delta p_{Two-phase} = DP_{Ann}$$

$$ELSE \rightarrow \ Stratified\ flow\ iteration$$

Stratified flow iteration

$$V1_{Stra} = \frac{\Delta p_G}{\Delta p_L}$$

$$\varphi = \frac{\pi}{1000} - \frac{\pi}{5}; \quad B = \frac{\pi}{5}$$

$Start$: $\varphi = \varphi + B$

$$A_{L,Stra} = \frac{D^2(\varphi - \sin\varphi)}{8}; \quad A_{G,Stra} = A - A_{G,Stra}$$

$$U_{L,Stra} = \frac{D\varphi}{2} + D\sin\frac{\varphi}{2}; \; U_{G,Stra} = D\left(\pi - \frac{\varphi}{2} + \sin\frac{\varphi}{2}\right)$$

$$D_{G,Stra} = 4\frac{A_{G,Stra}}{U_{G,Stra}}; \quad D_{L,Stra} = 4\frac{A_{L,Stra}}{U_{L,Stra}}$$

$$V2_{Ann} = \left(\frac{D_{G,Stra}}{D_{L,Stra}}\right)^{1.25}\left(\frac{A_{G,Stra}}{A_{L,Stra}}\right)^{1.75}$$

$$IF \quad \frac{V2_{Stra} - V1_{Stra}}{V1_{Stra}} \leq \frac{1}{100} \rightarrow End$$

$$IF \quad V2_{Stra} = V1_{Stra} \rightarrow End$$

$$IF \quad V2_{Stra} > V1_{Stra} \rightarrow Start$$

$$IF \quad V2_{Ann} < V1_{Ann} \rightarrow \; \varphi = \varphi - B; B = \frac{B}{2} \rightarrow Start$$

End:

$$CF_{Stra} = \left[1 + \left(\frac{D}{D_{G,Stra}}\right)^{1.25}\right]\left(\frac{A}{A_{G,Stra}}\right)^{1.75}$$

$$DP_{Ann} = \; \Delta p_G * CF_{Stra}$$

$$IF \quad DP_{Ann} \leq \Delta p_{Stra,max} \rightarrow \; \Delta p_{Two-phase} = DP_{Ann}$$

$$ELSE \rightarrow \; Transition\, region$$

Transition region

$$FH = \frac{0.3164x^{1.75}\eta_G^{0.25}}{2\rho_G D^{1.25}}$$

$$G_{Ann,min} = \left(\frac{\Delta p_{G,Ann}}{CF_{Ann}}\right)^{-1.75}$$

$$G_{Stra,max} = \left(\frac{\Delta p_{Stra,max}}{CF_{Stra}}\right)^{-1.75}$$

$$\Delta p_{Two-phase} = \Delta p_{Stra,max} * \exp\left(\frac{\ln\frac{G}{G_{Stra,max}}\ln\frac{\Delta p_{G,Ann}}{\Delta p_{Stra,max}}}{\ln\frac{G_{Ann,min}}{G_{Stra,max}}}\right)$$

Roughness correction

$$IF\ roughness\ \frac{\epsilon_r}{d}\ \geq 0.001$$

$$\Delta p_{Two-phase} = \Delta p_{Two-phase}\left(1000 * \frac{\epsilon_r}{d}\right)^{0.25}$$

APPENDIX 2: Physical properties

Table 1. Vicosity of air at atmospheric pressure. [97]

T [K]	η_{air} [Pa s]
260	0.0000165
280	0.0000175
300	0.0000184
320	0.0000193
340	0.0000202
360	0.0000211

Table 2. Density and viscosity of water at atmospheric pressure. [98]

T[K]	η_{water} [Pa s]
273.15	0.0017920
283.15	0.0013070
293.15	0.0010020
303.15	0.0007977
313.15	0.0006532
323.15	0.0005470
333.15	0.0004665
343.15	0.0004040
353.15	0.0003544
363.15	0.0003145

T[K]	ρ_{water} [kg/m3]
273.15	55.496
278.15	55.505
283.15	55.491
293.15	55.408
303.15	55.265
313.15	55.074
323.15	54.842
333.15	54.574
343.15	54.274
353.15	53.943
363.15	53.584

APPENDIX 3: Safety valve inlet piping

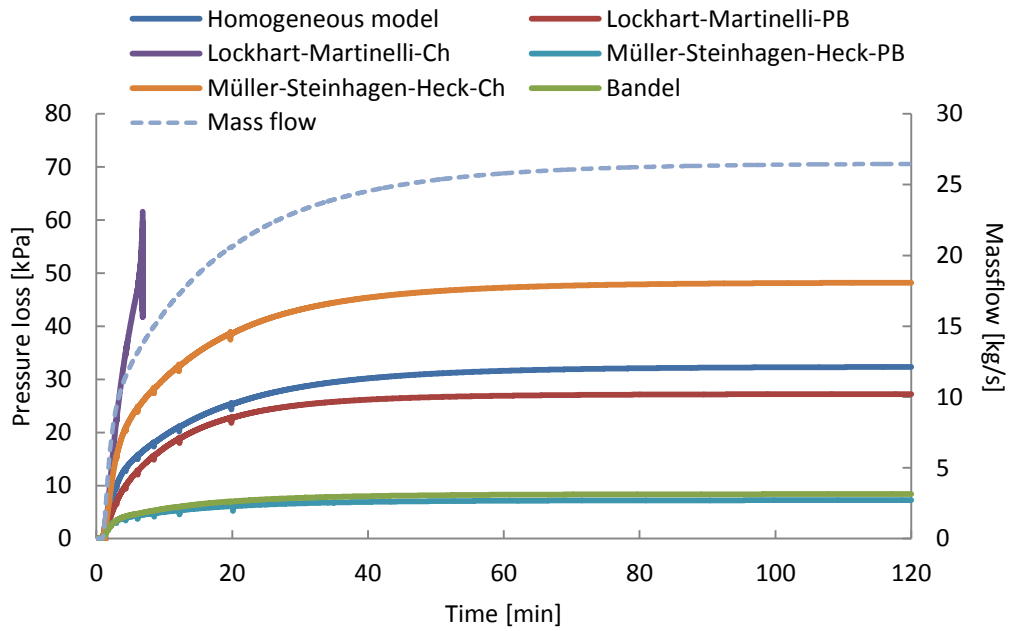

Figure 1. Simulation results for the case (D = 0.127, ϵ_r=0.2 mm).

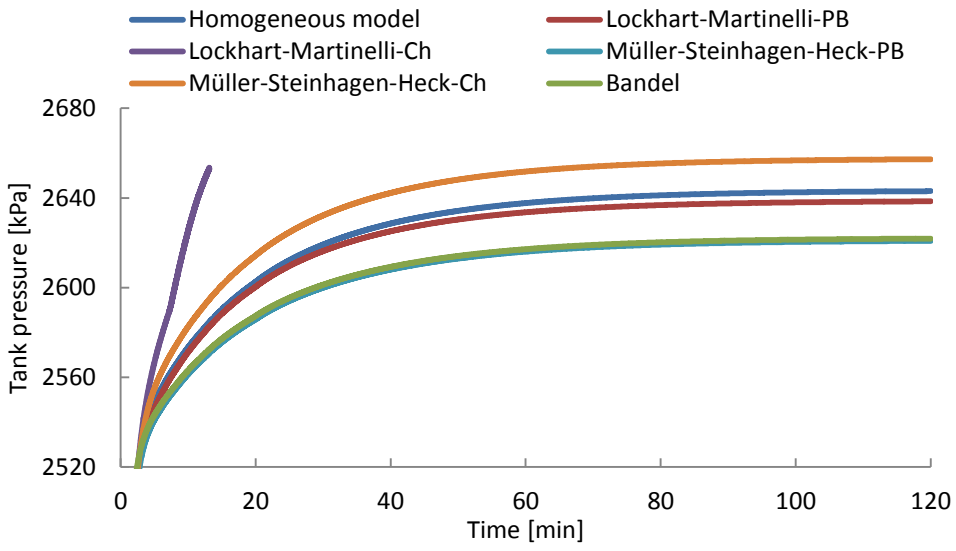

Figure 2. Tank pressure as a function of time for the case (D = 0.127, ϵ_r=0.2 mm).

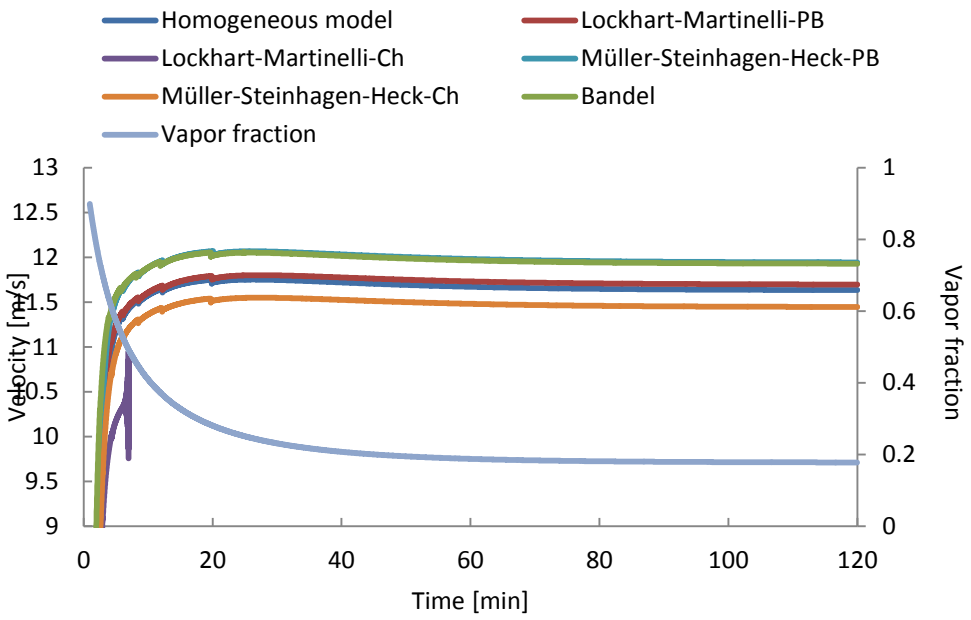

Figure 3. Velocities and vapor fractions for the case (D = 0.127, ϵ_r=0.2 mm).

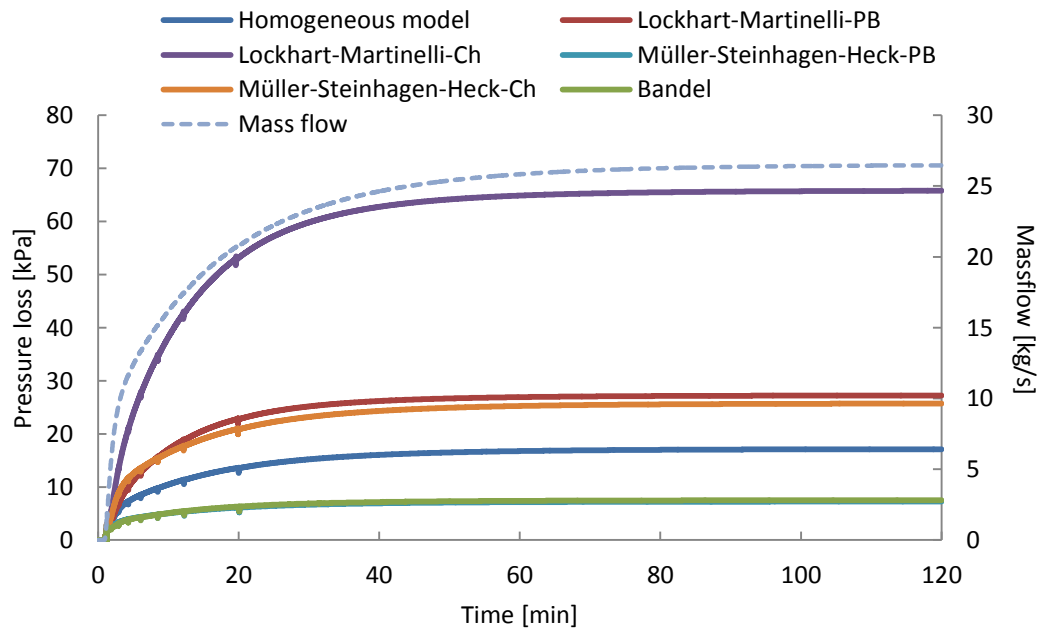

Figure 4. Simulation results for the case (D = 0.127, ϵ_r=0.001 mm).

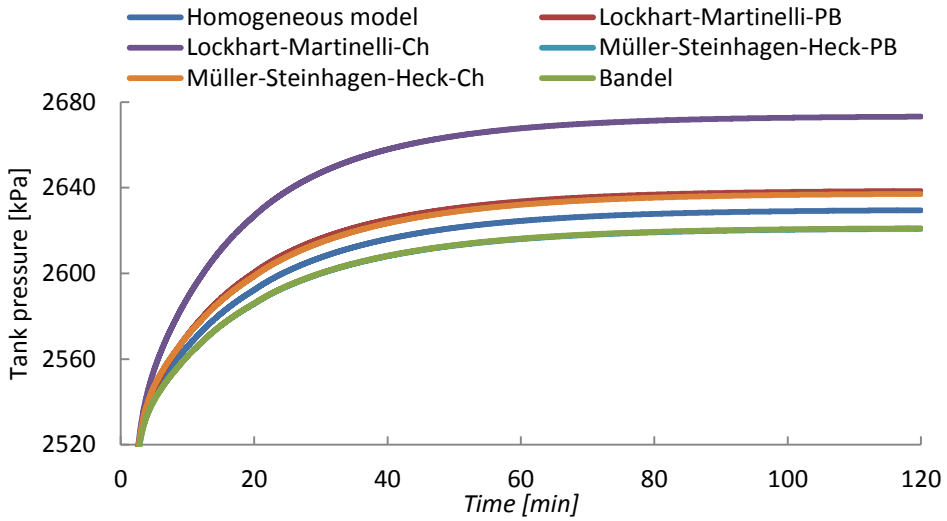

Figure 5. Tank pressure as a function of time for the case (D = 0.127, ϵ_r=0.001 mm).

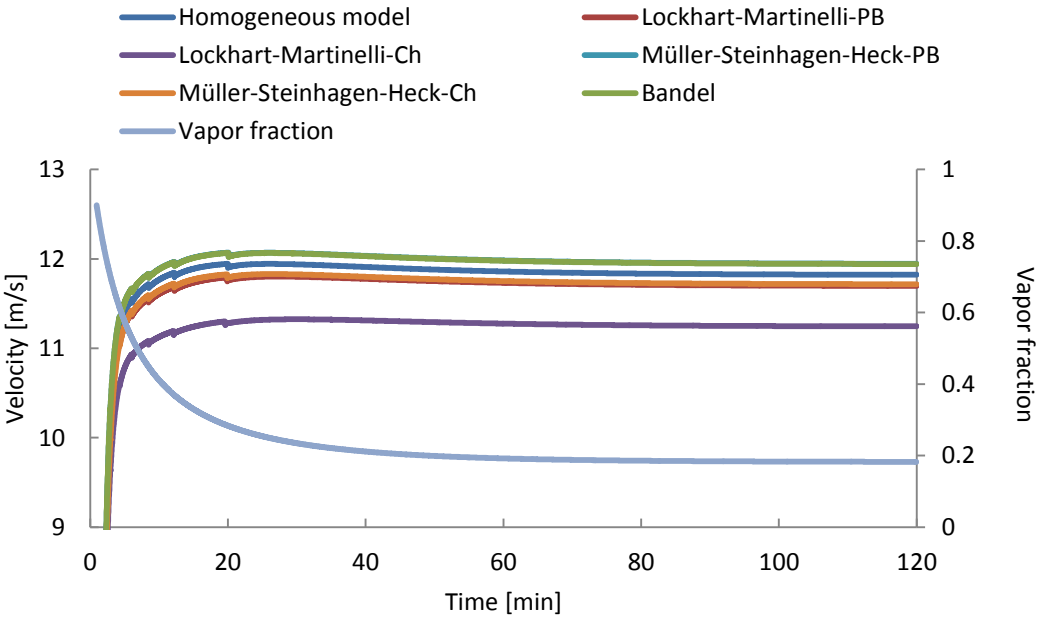

Figure 6. Velocities and vapor fractions for the case (D = 0.127, ϵ_r=0.001 mm).

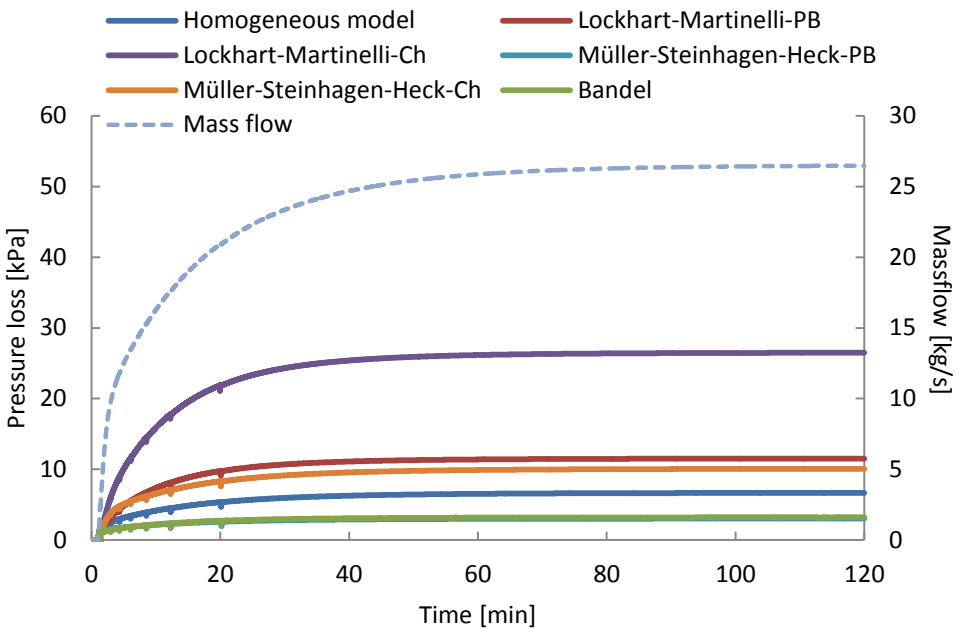

Figure 7. Simulation results for the case (D = 0.152, ϵ_r=0.001 mm).

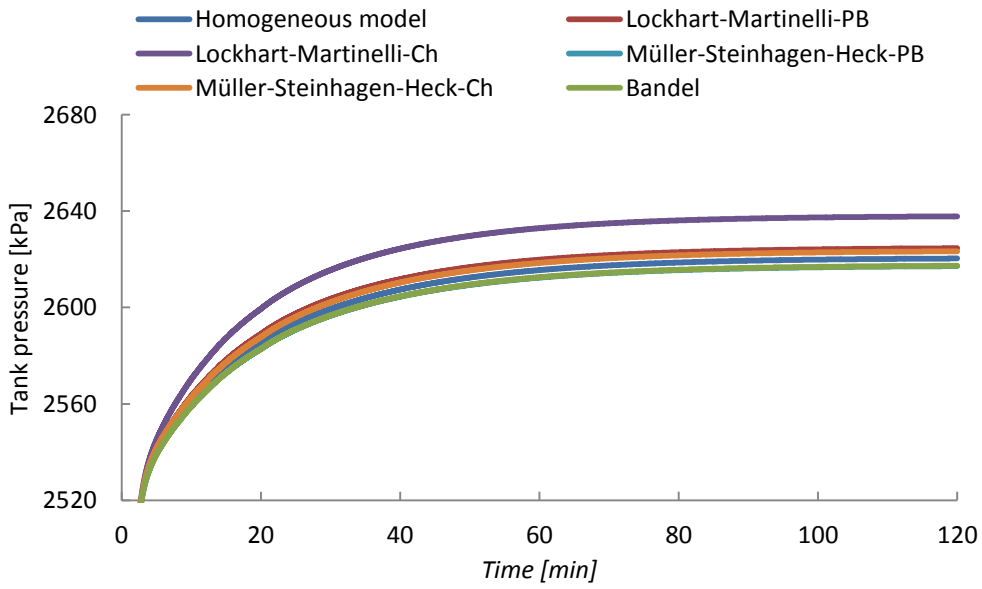

Figure 8. Tank pressure as a function of time for the case (D = 0.152, ϵ_r=0.001 mm).

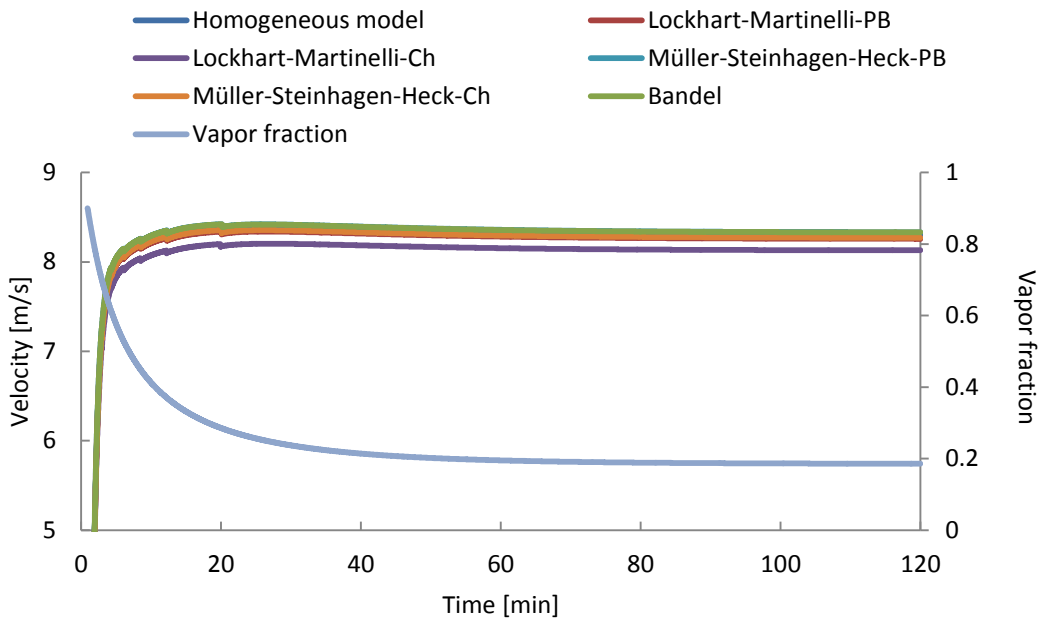

Figure 9. Velocities and vapor fractions for the case (D = 0.152, ϵ_r=0.001 mm).